WMA





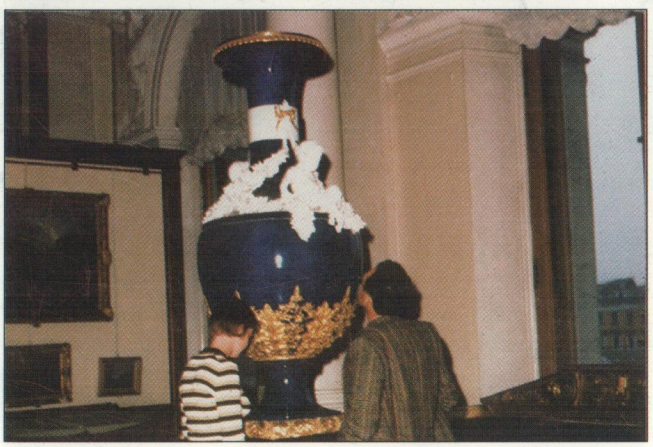


The Journal of Weather Modification

Volume 20 Number 1 *April 1988*

AVRAHAM GAGIN
(1933-1987)

This volume is "in memoriam" to Abe Gagin. Fifty-four years is too young for taking. He was a good friend and we all miss him a great deal.

Abe was a significant force at the international level and was liked by everyone. Adjectives seem inadequate but enthusiastic, dedicated, honest, faithful and generous are not overstatements. He had many marvelous facets; conversationalist, detente specialist, abundant humor, dedicated father, lover of country, serious worker. The cover photographs on this volume illustrate a few of these facets but they fall short of a complete picture. Abe will forgive this shortcoming.

It is fitting that a few colleagues have supplied a number of special thoughts about Abe for inclusion in this volume. Some remarks from Dr. K. Ruben Gabriel lead these thoughts. They were presented at the opening session of the Eleventh Conference on Weather Modification of the American Meteorological society, October 6, 1987 -- Edmonton, Alberta, Canada. Dr. Gabriel has kindly furnished these comments for publication. Additional thoughts have been provided by a few more of Abe's friends; Dr. Archie Kahan, Dr. William Woodley, Dr. Joanne Simpson, Mr. Stanley A. Changnon, and Mr. Lewis Grant. The volume could easily have been filled with personal feelings from other friends.

Our thoughts go out to Abe's family; Ilana, Udi, Ron.

PUBLISHED BY:

THE WEATHER MODIFICATION ASSOCIATION
P.O. BOX 8116
FRESNO, CALIFORNIA 93747 U.S.A.
PHONE: 209-291-5575

Cover photos: Tom Henderson

ISBN: 0739:1781

ADDITIONAL COPIES OF THE JOURNAL OF WEATHER MODIFICATION ARE AVAILABLE FOR U.S. $25.00 EACH (MEMBERS) AND U.S. $40.00 (NON-MEMBERS).

MEMBERSHIP INFORMATION IS AVAILABLE BY CONTACTING THE ASSOCIATION AT THE ABOVE ADDRESS.

- THE JOURNAL OF WEATHER MODIFICATION -

WEATHER MODIFICATION ASSOCIATION

VOLUME 20 NUMBER 1 APRIL 1988

TABLE OF CONTENTS: PAGE

- NON-REVIEWED SECTION -

"REVIEWED"

WINTERTIME CLOUD LIQUID WATER OBSERVATIONS OVER THE MOGOLLON RIM OF ARIZONA

Arlin B. Super and Bruce A. Boe
Bureau of Reclamation
Montrose, CO 81401

ABSTRACT

Liquid water, wind and other meteorological observations were made over the Mogollon Rim of Arizona from mid-January through mid-March 1987. A dual-channel microwave radiometer provided cloud liquid water (CLW) measurements. Winds were sampled by a variety of devices including a doppler acoustic sounder, tower-mounted anemometer and vane, rawinsondes and an aircraft equipped with an inertial navigation system. Temperature observations indicated that the bulk of the CLW was supercooled.

Distributions of vertically-integrated CLW are examined from the thirteen synoptic scale storms that occurred during the observational period. It is shown that most hourly means were less than 0.1 mm, implying limited liquid water contents. While some diurnal variation in CLW occurrence was found, the early morning maximum indicates it was not solar-forced and may have been the result of the random passage of storms. The durations of CLW episodes are shown to have varied from an hour to over a day.

The majority of CLW occurred with southwest winds although a secondary maximum was apparent with northeast flow. Both are upslope for the observing site.

The horizontal flux of CLW was estimated hourly over the crestline of the Rim, just upwind of the lee subsidence zone. Total flux per storm varied widely and three large storms produced three-quarters of the total (two month) flux. However, it is shown that the low hourly values of CLW produced much of the total flux because of their frequent occurrence. The cumulative frequency distribution of the 260 h with flux estimates is shown to be similar to that previously reported for the Grand Mesa, CO, 600 km to the north.

The total CLW flux for the two month sampling period is estimated to have been roughtly half the mean annual streamflow from the same area. This suggests that significant potential may exist for winter precipitation augmentation through cloud seeding on the Mogollon Rim.

1. Introduction

It has long been recognized that supercooled liquid water (SLW) is the required "raw material" for augmentation of precipitation by seeding winter clouds over mountain barriers (Ludlam, 1955). For detailed discussion of the processes involved see Dennis (1980). Some additional but limited potential may exist in conditions between ice and water saturation which will be ignored here. The amount of SLW that can be converted to snow on the ground will also not be considered in this paper. Here we are concerned with the frequency of occurrence of SLW and its magnitude and duration. Also, the flow or "flux" of SLW over the barrier will be estimated as this represents the absolute upper limit for precipitation augmentation potential.

It would be impractical for any cloud seeding program to convert all the seasonal SLW flux to snowfall because of constraints such as timely delivery of seeding agents to desired cloud regions, limited time available for ice crystal growth and fallout, possible suspension criteria imposed during wet periods, etc. However, if observations were to show the seasonal SLW flux to be only a very small fraction of natural annual streamflow from a region, the potential of seeding to augment the streamflow through increased snowfall would likewise be very limited on a percentage basis. Admittedly, even a small percentage increase in streamflow might represent a large volume of water in some drainages (e.g. the Sierra Nevada Mountains). However, small percentage increases are difficult to demonstrate with confidence.

On the other hand, if the SLW flux was found to be a large fraction of annual streamflow, this would suggest a possible large potential for cloud seeding. Estimation of the actual potential would involve consideration of the various constraints already noted, and a seeding program would be required to demonstrate the seasonal precipitation increase practical to achieve. However, observation of SLW and its flux over a barrier is clearly a very important first step toward estimating seeding potential.

While the importance of SLW flux has been recognized for many years, only recently has it been practical to routinely observe it. Development of the microwave radiometer (Hogg et al., 1983) has made possible continuous measurements of the integrated amount of liquid

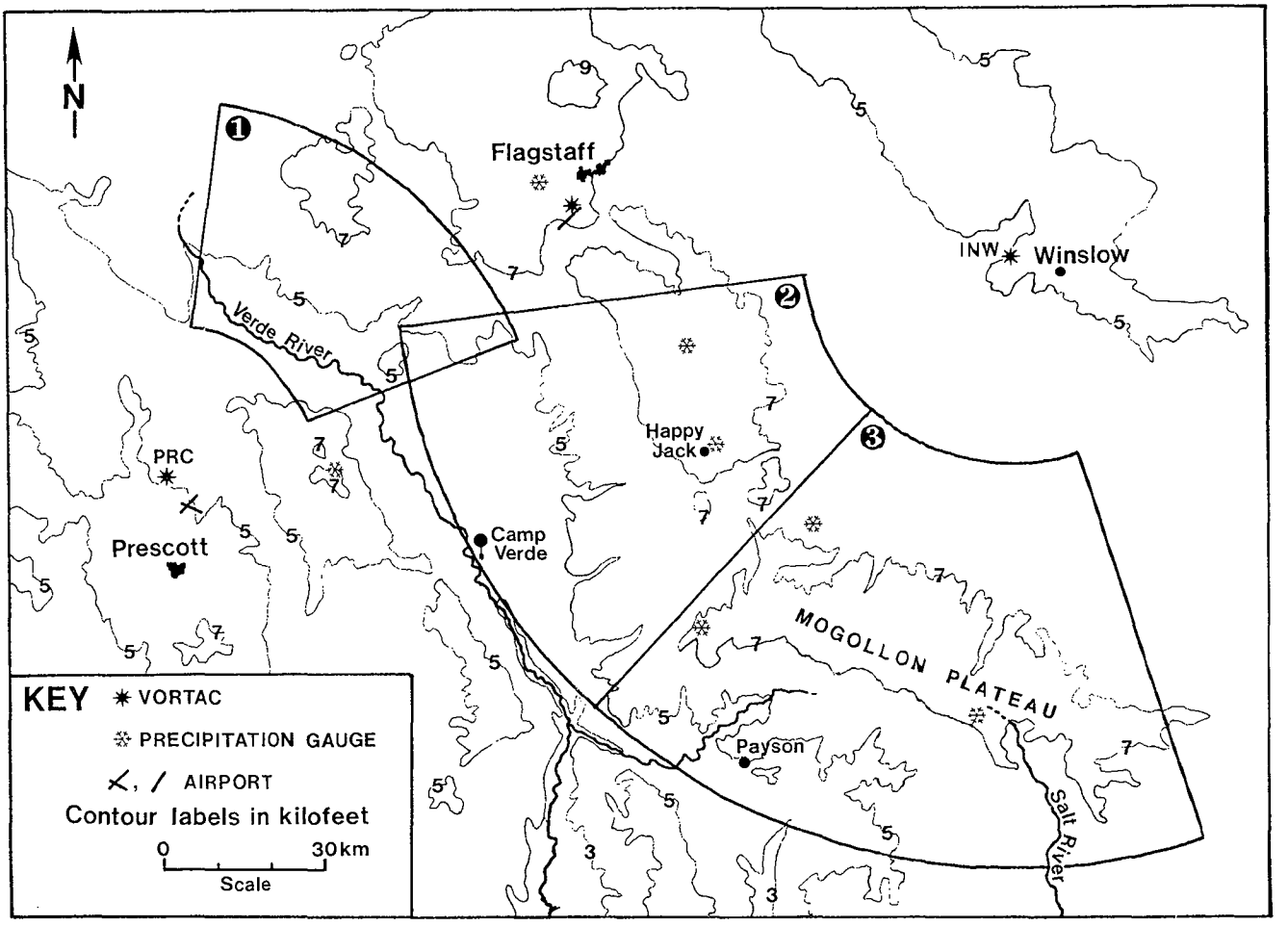

Fig. 1. Map of the Mogollon Rim project area in Arizona. Aircraft operations were concentrated in Area 2, especially near Happy Jack.

water above the instrument. When the liquid water is known to consist entirely of cloud droplets and not rain drops we will refer to it as cloud liquid water (CLW). When the CLW is supercooled, the radiometer measurements can be combined with wind speed and SLW flux estimates can be made as reported for the Grand Mesa, Colorado, by Boe and Super (1986), and Thompson and Super (1987).

2. Observations

A cooperative agreement between the U.S. Bureau of Reclamation (Bureau) and State of Arizona made possible initial observations and analyses of CLW over the Mogollon Rim. A field program was conducted from January 14 to March 17, 1987, at the Happy Jack Ranger Station, about 55 km south of Flagstaff, Arizona (Fig. 1). The Happy Jack (HJ) site was chosen primarily because of its location on the crestline of the Mogollon Rim, with electrical power availability and ease of access important secondary considerations. The site is at an elevation of 2290 m msl on a portion of the Rim that has its long axis extending NNW-SSE. The terrain gradually slopes toward the Verde River Valley to the SW and Little Colorado River Valley to the NE.

Bureau instrumentation operated at HJ included a microwave radiometer similar to that described by Hogg et al. (1983), a doppler acoustic sounder, a sensitive 5.4 cm radar (SWR-86, sensitivity -27 dBz at 3 km range), an aspirated Particle Measuring Systems (PMS) 2D-C probe, a high resolution precipitation gage and sensors for monitoring near surface air temperature, dewpoint temperature, wind vector and icing rate. The last three instruments were located about 30 m above the top of a small hill near HJ. In addition, two technicians lived at the site and made routine weather and pilot balloon (pibal) observations from about 0600-2400 (all times MST) each day.

The University of Wyoming King Air 200T cloud physics aircraft sampled several cloud systems during the field season in the HJ vicinity. Horizontal passes were typically flown at height intervals from cloud top or 5200 m (17,000 ft) msl, whichever was lowest, down to the lowest permissible flight altitude of 2930 m msl. Passes were generally parallel to the wind and directly over HJ. These observations showed the distribution of CLW, winds, and temperature, among other parameters.

The radar system was operated in an RHI mode and made one scan per 5 min from the zenith to 6 deg elevation angle toward the north. These observations showed the cloud (radar) top and top character, whether stratiform or convective.

The microwave radiometer (hereafter radiometer) was used in a vertically-pointing mode to provide the integrated amount of liquid water and water vapor passing directly above the unit. Radiometer data collected during cloud-free (and thus liquid

water-free) conditions were examined to determine the magnitude of the drift of the instrument. Much of the time baseline drift was sufficient to necessitate a correction of ±0.01 to 0.03 mm, but care was taken to maintain a zero or slightly negative baseline for liquid water. Thus, in all cases with positive readings, liquid water actually existed above the instrument.

It is noteworthy that the work of Heggli et al. (1987), partially based on the radiometer used in this study, indicated that radiometer-measured values of water vapor are very likely within 15% of actual values. Further, two similar radiometers operated near one another yielded very similar liquid and vapor values. The absolute accuracy of the liquid values is difficult to independently verify because of the lack of a suitable standard.

Other instruments provided wind measurements so that CLW flux could be estimated. These included tower-mounted sensors and a doppler acoustic sounder, all at HJ, rawinsonde observations from Camp Verde west of HJ (see Fig. 1), and aircraft-measured winds provided by the University of Wyoming King Air during some storms. Rawinsondes were released at normal synoptic times (1200 and 0000 GMT) on most days, with additional soundings at about 6 h intervals during periods of special interest. Since the observations were just upwind of the crestline in the prevailing southwesterly flow, the flux estimates approximate the amount of liquid water naturally available just prior to depletion in the lee subsidence zone. This can be thought of as nature's surplus water, not converted to precipitation due to the inefficiencies of the precipitation process in the winter clouds over the Mogollon Rim.

The radiometer does not respond to dry snow in the atmosphere or on the reflector, but wet snow on the reflector can cause serious overestimates of both liquid and vapor (Hogg et al., 1983). Both air temperature near the radiometer and the temperature of the reflector itself were monitored at 5 min intervals from January 29 to the end of the field season. Further, the type of snow and condition of the reflector were frequently noted during all storms, and the reflector was kept essentially clear of snow and water by a large blower and manual wiping when required. Even so, three brief periods with the wet snow problem existed during one storm. These three periods were obvious because of abrupt, several-fold increases in liquid and vapor values. Linear extrapolation from adjoining periods with valid data was used to estimate the CLW in these cases.

A more serious problem occurs when rain is present. While Hogg et al., (1983) used spraying tests to show a wet reflector has little effect on the readings, the presence of rain in the atmosphere above the unit can result in large increases in liquid water. The radiometer is unable to distinguish between that liquid water in the form of tiny cloud droplets (CLW of interest to cloud seeding potential) and that due to much larger rain drops. The mixed cloud droplet/rain drop condition was a problem during all or portions of only three storms as indicated by air and radiometer reflector temperatures above freezing, measured precipitation at HJ and/or observer notes of rain or melting ice hydrometers. The mixed cloud droplet/rain drop observations were excluded from the analysis to be presented. Section 3 will discuss the additional exclusion of a limited number of hours typed as mesoscale convective. A total of 260 h remained with CLW observations of which 225 h occurred after continuous temperature measurements started at HJ on January 29. (The earlier CLW data were supercooled according to National Weather Service hourly observations from Flagstaff or aircraft measurements).

Of the 225 h with temperature measurements at the radiometer site, 76% had mean temperatures from -7.4 to 0.0°C so the CLW was totally supercooled. The HJ site was rarely in cloud so CLW was above it and, therefore, almost always colder than the surface during storms.

Of the remaining 24% of the hours with the radiometer site warmer than 0°C, only 10 h were above 5.0°C. Assuming a typical lapse rate of 0.6°C per 100 m, the 0°C isotherm would be within 800 m of the radiometer with surface temperatures between 0.1 and 5.0°C. The vertical distribution of CLW was observed only when the aircraft was present and then only higher than 640 m above HJ. However, it appears reasonable to assume that at least some of the radiometer-observed CLW was supercooled in all but a small portion of the hours.

Happy Jack precipitation data and observer notes were examined for all hours with the radiometer site above 0°C when CLW was observed. Most of these hours had no observed precipitation. Those that did usually had very light precipitation. Frequent manual checks of the radiometer reflector kept it dry in such instances so the CLW observations to be discussed are believed to be valid; that is, not due to a wet reflector or rain. Virga may have been above the radiometer in some few cases but CLW observations accompanying surface temperatures above 1°C rarely exceeded 0.2 mm. Therefore, the large majority of CLW values are believed to be due to tiny cloud droplets, usually supercooled. Thus, while further discussion will usually refer to CLW, it can be considered a first approximation of SLW.

3. Storm Typing

A classification scheme was developed for the Arizona storms observed during mid-January to mid-March 1987. A storm episode was defined by the nearly continuous presence of CLW over HJ and/or hourly precipitation recorded by any gage in a seven gage network (see Fig. 1), having no interval >2 h during which neither SLW nor precipitation was observed. Precipitation gage resolution was 0.13 mm except at HJ where it was 0.05 mm. Some additional brief (<2 h) periods with CLW and/or precipitation were detected but were considered too insignificant to be classified as storms. These episodes were excluded from the analyses to be discussed.

Storm episodes were categorized by two characteristics, the scale of the storm and the presence or absence of convection. Convection was identified by examining the following: radar time-height and range-height indicator plots, the character of the liquid trace recorded by the

radiometer, aircraft observations, hourly weather reports from Flagstaff, time lapse movies taken from Payson (Fig. 1.), stability parameters derived from Camp Verde soundings, visual satellite imagery, and observations by the HJ crew. Those storms clearly associated with synoptic-scale features were so classified while the others were categorized as mesoscale. If an episode had convection present for half or more of its duration, it was classified as convective, otherwise it was termed stratiform.

Ten storm episodes were designated synoptic stratiform (SS), three were synoptic convective (SC) and three were mesoscale convective (MC). Mesoscale stratiform cases were not observed. The SS and SC cases will be considered together because of similar characteristics; they were generally stratiform clouds with some (usually weak) embedded convective elements in the SC cases. The SC cases contributed little to the overall population because only three episodes occurred and most of the hours from two of these were excluded because of rain-caused ambiguities in CLW values. It will be shown in Table 1 of Sec. 7 that the total horizontal flux of water from the two latter cases, including their likely predominate contribution from raindrops, was about 14% of the flux due to cloud droplets alone from the other storms observed.

The few MC cases were markedly different from the SS and SC storms. They were predominately convective with isolated or semi-isolated turrets, and were sometimes induced by solar heating. These cases contributed little to the seasonal precipitation and CLW flux, and they will be ignored in the discussion to follow.

4. Temporal Distribution of CLW

The frequency distribution of hourly mean amounts of vertically-integrated CLW is given in Fig. 2. For the 260 h with measured CLW, 66% had amounts less than 0.1 mm. Only 1 h exceeded 0.6 mm. This distribution is similar to the distribution of SLW reported by Super et al. (1986) for the Grand Mesa of west-central Colorado. To put these values into perspective, a cloud of 1 km vertical extent with uniform CLW content of 0.1 g m^{-3} would yield a vertically-intergrated liquid water amount of 0.1 mm. This suggests that most clouds over HJ had mean liquid water contents of no more than a few hundredths to one or two tenths gram per cubic meter of air. The King Air aircraft observations over HJ usually showed values in this range. Such values are typical of winter orographic clouds at a number of locations in the Rocky Mountain (Cooper and Marwitz, 1980; Rauber and Grant, 1986; Super and Heimbach, 1988).

The diurnal variation of CLW was examined by noting the number of times during the field program the hourly mean CLW amount exceeded zero for each of the 24 hours of the day. The range of occurrences was from 8 to 16. The period from 1700-2300 (all times MST) was a relative minimum with 8-9 occurrences per hour. While the maximum was 16 at 1100-1200, values of 10 existed only 2 h earlier and later. A broad general maximum was apparent from about 0300-0900, with 12-13 occurrences per hour. On average this maximum ws 46% greater than the evening minimum.

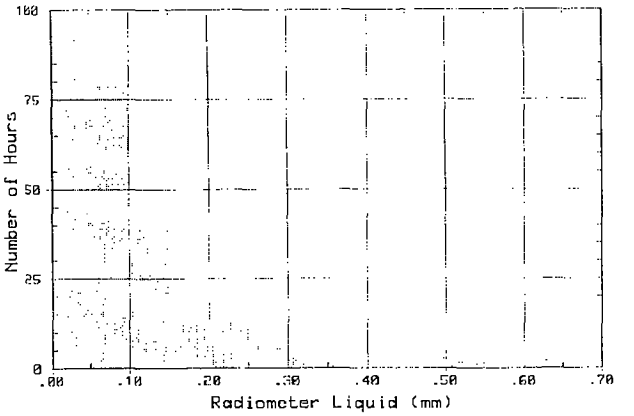

Fig. 2. Distribution of 1 h means of vertically-integrated cloud liquid water amounts.

It is not apparent whether the diurnal variation is significant, or simply the result of the random passage of synoptic scale weather disturbances during the limited two month observational period. Additional measurements would be needed to clarify this issue. At any rate, no pronounced afternoon maximum is apparent so solar heating was not a strong factor in CLW production. This adds credibility to the storm typing method as all these cases were classified as synoptically triggered.

A CLW (not storm) episode was defined, somewhat arbitrarily, by the near-continuous presence of CLW as indicated by the 1 h mean radiometer data. Periods up to 2 h without detectable CLW were allowed to occur within an episode. This definition resulted in 21 episodes from the 13 SS and SC storms.

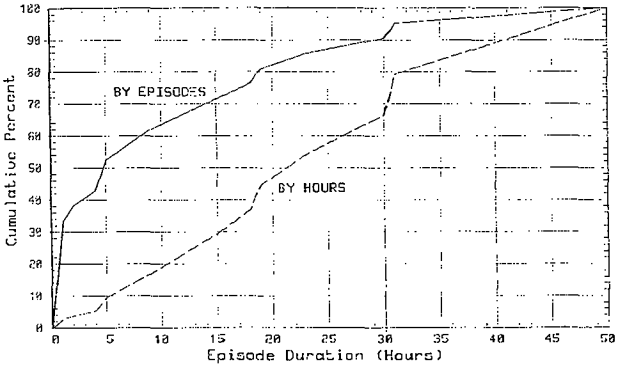

Fig. 3. Cumulative distributions of cloud liquid water (CLW) episodes (solid line) and hours with CLW (dashed line) as functions of episode duration.

The cumulative distributions of the 21 CLW episodes, and the hours with CLW present, are shown on Fig. 3 as functions of episode duration. Only 242 h of CLW observations are considered here, as opposed to 260 h in Fig. 2, because missing data prevented definition of episode durations in some cases. It is seen that about half the episodes were less than 5 h duration. Only 14% (3) of the episodes lasted over 24 h while 33% (7) lasted only 1 h. Over half of all hours with CLW were associated with the 4 episodes of duration $\geq$23 h. Conversely, the 11 shortest episodes, $\leq$5 h duration, yielded only 10% of all hours with CLW.

5. Relationships Between CLW and Wind Direction

Hourly mean wind directions were recorded at 30 m agl on a tower located atop a 70 m hill near HJ. These observations were not available until January 28 so only 233 h exist with both wind direction and detectable CLW data for SS and SC storms. These were used to construct Fig. 4 which shows the frequency distribution of occurrence of detectable CLW, whatever its magnitude, vs wind direction. Clearly most hours with CLW present were with SW winds, with 53% of all cases between 195-255° true. A secondary maximum existed for NE flow, with 24% of all cases having winds from 30-90°. Both SW and NE flows are approximately perpendicular to the axis of the Mogollon Rim in the HJ vicinity, so both represent upslope flow. Such flow should force orographic lifting and thereby enhance CLW production.

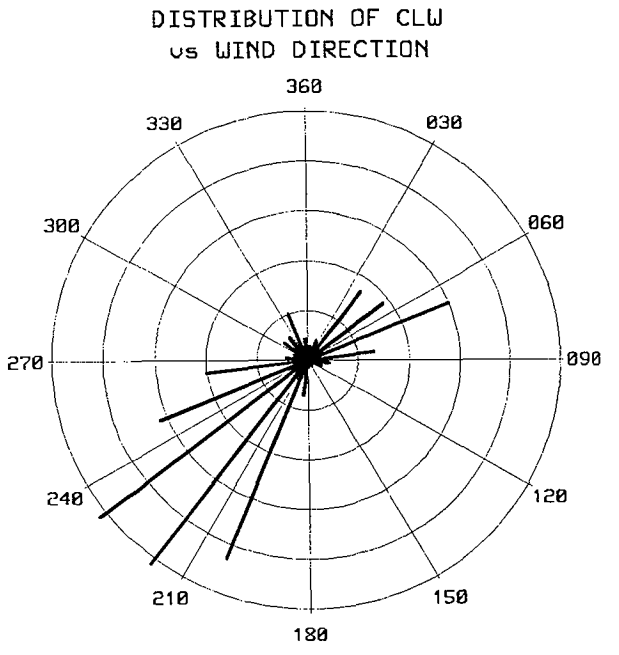

Fig. 4. Wind rose showing the distribution of hours with cloud liquid water vs wind direction in degrees true.

A plot like Fig. 4 (not shown) was constructed using winds observed by rawinsondes released at Campe Verde 42 km WSW of HJ. It showed a similar distribution for SW flow but only 8% of the CLW hours were associated with 700 mb winds from the 30-90° sector, far below the 24% shown for HJ tower winds in Fig. 4. This suggests the NE upslope cases are primarily a low-level, local phenomena over the Mogollon Rim, not usually observed near 3 km altitude over the Verde Valley to the west. The 700 mb distribution showed a secondary maximum of 15% of all cases from 285-300°, unlike the tower wind distribution.

6. CLW Flux Estimates

The horizontal flux of CLW has been estimated for each hour of the storm episodes observed during the 1987 winter field season. To convert measurements of integrated radiometer CLW to flux, it was necessary to make assumptions about both the vertical wind speed profile and the vertical distribution of the CLW.

A basic calculation of the volume flux VFz for any layer at mean height z having wind speed Vz and cross-sectional area Az can be given by

$$VFz = Az \times Vz \qquad (1)$$

(after Thompson and Super, 1987). The CLW flux CFz for each layer can then be calculated by

$$CFz = VFz \times CLWz \qquad (2)$$

where CLWz is the vertically integrated CLW for the layer. The total CLW flux is then the summation of the flux for all layers. Since one gram of CLW is equivalent to 1 cm^3 liquid water, Fg, the flux in g s^{-1} per meter crosswind, is

$$Fg = CLWz \times Vz \times 1000 \qquad (3)$$

where CLWz is in mm, and Vz is in m s^{-1}.

Neither the vertical distribution of the wind speed nor that of CLW were routinely measured throughout the entire cloud layer over HJ. Therefore, it was necessary to make some assumptions about these distributions which were based on periodic observations taken throughout the field season.

In the case of wind speed, the doppler acoustic sounder usually provided data in the lowest 570 m agl. An investigation using all available wind measurements indicated the highest level observed by the acoustic sounder was often representative of the mean wind speed in the lowest 1-2 km. Therefore, whenever acoustic sounder data near 570 m agl were available, they were assumed to represent the lowest 2 km layer above HJ with possible adjustment whenever aircraft winds were also observed in that layer.

All wind estimates above 2 km agl were based upon either upwind rawinsondes, or the preferred aircraft observations over the HJ vicinity when available. These two measurement systems also provided estimates for the lowest 2 km when acoustic sounder data were occasionally unavailable. Upwind rawinsonde winds were found to usually provide good to very good estimates of actual winds over HJ as measured by the aircraft.

Knowledge of the vertical distribution of CLW over HJ was obtained exclusively from aircraft sampling. For reasons of safety, the aircraft was not flown in cloud within 300 m (1000 ft) of the highest terrain, which resulted in a minimum flight altitude of 2930 m msl. Thus, the cloud layer in the lowest 640 m over HJ was not sampled by aircraft. However, many clouds were sampled at and above the minimum altitude, providing information of the CLW distribution further aloft.

The general indication from several storms was that the CLW tended to be concentrated in the lower portions of the clouds. (A similar distribution was found over the Grand Mesa, Colorado, see Holroyd and Super, 1984). For example, aircraft sampling of the Arizona synoptic scale storms generally revealed little CLW at

altitudes above 5 km msl (2.7 km agl). Also, CLW was sometimes detected by the radiometer in the lowest 640 m agl when the aircraft was observing exclusively ice crystal cloud at that altitude and above.

The method by which the hourly horizontal CLW flux was estimated was as follows: In the event that cloud tops were generally less than 2 km above HJ as observed by radar or aircraft, the CLW flux was calculated from Eq. (3) using the acoustic sounder speed measurement at 570 m agl and the total integrated CLW amount from the radiometer. If cloud depth consistently exceeded 2 km agl, a second layer was added. In that case, 50% of the integrated CLW was assumed to be in the lowest kilometer (2290-3290 m msl) and the speed for that layer was again considered to be that measured at 570 m agl by the acoustic sounder. The other 50% of the total CLW was assumed to lie above 1 km agl. The thickness of this designated upper layer was variable, depending upon overall cloud tops.

The mean wind speed for the upper layer was estimated using aircraft observations when available and otherwise rawinsonde data. Winds further aloft than 4.9 km (16,000 ft) msl were never used because CLW was infrequently detected that high.

7. Distributions of CLW Flux

Horizonal CLW flux estimates are tabulated in Table 1 for eleven storm episodes with valid data and two with some questionable data. Total flux per storm episode ranged from about 0.1 x 10^7 g to 42 x 10^7 g per meter of crosswind distance. The average hourly flux per storm ranged from 10 to 2710 g s^{-1} per meter of crosswind distance.

The character of the episodes varied greatly, from lengthy periods having significant CLW almost without interruption, to episodes with many hours of precipitation but little CLW. The three episodes with the highest total CLW fluxes also had measurable precipitation during more than 50% of the hours.

Table 1 shows that 75% of the total CLW flux for the two month field season (ignoring the two episodes with questionable values due to rain) occurred during only three storm periods which lasted a total of 156 h. Conversely, six of the eleven episodes with valid CLW estimates had a total of 167 h duration but contributed only 9% of the total flux. The three episodes which produced three-quarters of the total flux had SLW maxima associated with cold front passages, either pre- or post-frontal, or both. Secondary maxima were sometimes observed to be related to passage of a surface low or trough aloft.

The largest flux-producing storm, accounting for 35% of the seasonal total, occurred on February 23-26. This storm also produced considerable snowfall over a wide area. For example, the Prescott Airport was closed for a few days due to about 0.5 m of snow on the runways and insufficient equipment to remove it. Sections of Arizona interstate highways were closed for extended periods. The storm was locally reported as producing the heaviest snowfall in 20 years. It seems doubtful that any cloud seeding would be desired or allowed during such a storm.

Table 1. Summary of CLW flux estimates ranked by total flux per storm episode.

Date(s) (1987)	Total Flux*(x10^7 g)	Rank	Average Flux*(g s^{-1})	Rank	Episode Duration (h)	Percent of hours with CLW over HJ	Percent of hours with precipitation at HJ	Cummulative Total Flux * (x10^7 g)	(%)
Feb. 23-26	41.9	1	1455	3	80	73	69	41.9	35
Jan. 30-31	24.4	2	2710	1	26	96	85	66.3	56
Mar. 15-17	23.5	3	1305	4	50	96	78	89.8	75
Feb. 13-14**	9.2	4	1155	5	22	86	41	99.0	83
Feb. 19-21	5.3	5	305	7	48	58	46	104.3	87
Feb. 4	3.9	6	670	6	16	94	31	108.2	91
Jan. 15-17	3.4	7	150	10	64	33	59	111.6	93
Jan. 28	3.1	8	1730	2	5	100	0	114.7	96
Feb. 17-18	2.8	9	255	8	31	71	13	117.5	98
Feb. 15-16	1.8	10	200	9	25	60	0	119.3	100-
Jan. 19-20	0.1	11	10	11	26	12	69	119.4	100
The following fluxes were overestimated by unknown amounts due to rain above the radiometer									
Mar. 8-9**	13.1	--	1215	--	30	90	67	---	---
Mar. 6-7**	3.7	--	535	--	19	79	37	---	---

* per one meter crosswind distance
** SC type storms, all others were SS

Figure 5 shows the distribution of CLW flux plotted against hourly mean amounts of vertically integrated CLW. It is seen that the low values of CLW contributed much of the seasonal flux as previously found over the Grand Mesa, Colorado (Boe and Super, 1986). This is because of the much higher frequency of occurrence of CLW amounts less than 0.15 mm (Fig. 2). About 44% of the total flux was due to the 81% of all hours which had mean CLW amounts of 0.15 mm or less. Conversely, the 6% of all hours that had CLW amounts in excess of 0.35 mm yielded almost 30% of the total flux.

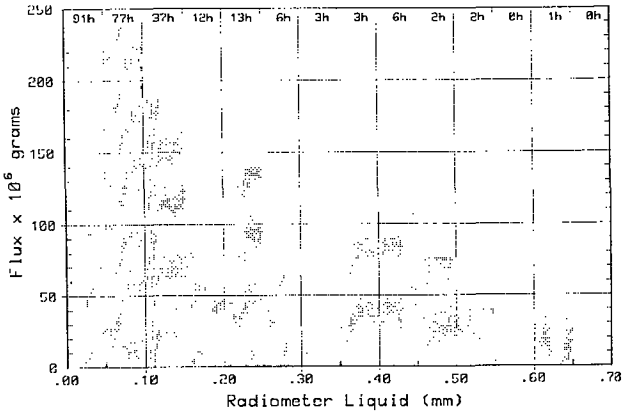

Fig. 5. Distribution of cloud liquid water (CLW) flux per meter crosswind vs vertically-integrated CLW amounts. The number of hours within each amount range are also noted.

It might appear attractive to limit seeding to the wetter (high CLW) periods in anticipation of high snowfall yields. However, the periods with low CLW amounts should not be discounted without further investigation. While their seeding potential may be low in terms of hourly snowfall rates, their seasonal contribution may be significant due to the higher frequency of opportunities. Ideally, both wetter and dryer CLW periods should be seeded if further study indicates both are seedable.

The cumulative frequency distribution of the 260 h with CLW flux estimates is shown in Table 2 along with the Grand Mesa, Colorado estimates of SLW, reported by Thompson and Super (1987). The Grand Mesa data were obtained with a microwave radiometer similar to that used at HJ, but the only wind speed measurement was from a 70 m tower atop the Mesa, while higher level winds tended to be somewhat stronger. Therefore, the Mesa flux observations are throught to be underestimated by perhaps 50-100% depending upon the depth of the CLW (known to be supercooled over the Mesa) and the vertical wind shear.

The Mesa estimates shown in Table 2 are significantly drier at the low end of the distribution where ratios are 2.5 or more, which suggests a higher frequency of clouds with very limited CLW. That might be expected since the Mesa is about 600 km NNE of HJ and 1000 m higher. However, the wetter hours yielded similar flux distributions at the two sites, with ratios less than 2.0. Such differences could be primarily due to the underestimated winds above the Mesa.

Table 2. Cumulative distributions of hourly mean values of CLW flux at Happy Jack, AZ and Grand Mesa, CO.

Percent of total hours	Happy Jack AZ flux ($g\ s^{-1}$)*	Grand Mesa CO flux ($g\ s^{-1}$)*	Ratio Happy Jack/Grand Mesa
5	100	20	5.0
10	140	40	3.5
20	200	80	2.5
30	315	145	2.2
40	435	200	2.2
50	630	295	2.1
60	845	470	1.8
70	1235	700	1.6
80	1750	1190	1.5
90	3035	2155	1.4
95	5250	3475	1.5
100	14,305	15,870	0.9
Total Hours/ Months of Data:	260/2	404/3	

* per one meter crosswind distance

One must be cautious in carrying the comparison too far because both data sets were of limited duration, being only 2 or 3 months long. Further, it is not known how representative these samples are of the normal CLW distributions. It may well be chance that both the mean number of hours with CLW per month, and the distributions shown in Table 2, were similar at the two sites. However, it is possible that the expected greater orographic contribution to CLW production over the steeper Mesa was largely balanced by synoptically-forced lifting of lower-based, hence warmer, and wetter clouds over Arizona.

Using the 260 h HJ data set it was found that about 50% of the total CLW flux occurred with only 12% of the total hours. Conversely, the 50% of the hours with lowest flux values contributed only 11% of the total seasonal flux. Similar distributions are common for mountain precipitation (e.g. Super et al., 1986) which is, of course, derived from SLW flux.

The 233 h with both valid CLW observations and HJ tower wind data were used to partition CLW flux by wind direction. It was found that 31% of the total flux occurred with SSW winds (195-210°). Fifty-five percent of the total flux was associated with wind directions from 195-240°, i.e., generally SW flow. The entire 0-90° quadrant contributed 17% of the total flux while the sector from 255-345° yielded 19% of the flux. Flux from the SE was negligible.

To put the CLW flux values into perspective, they will be compared with streamflow from the area of interest. The region immediately north of HJ is drained to the SW by Dry Beaver and Wet Beaver Creeks, which join the Verde River near McGuireville. Their combined mean annual runoff for the period 1966-1982 was 63,471 acre-ft. The crosswind extent of these watersheds, for SW flow, is about 31 km near the 2130 m (7000 ft) altitude contour. With a CLW flux of about 120 x 10^7 g per meter crosswind (Table 1), a total flux of approximately 3.7 x 10^{13} g results. Because one acre-ft is equivalent to 1.23 x 10^9 cm^3 (or grams) of water, the estimated two month flux across these drainages was near 30,000 acre-ft, or almost half the mean annual runoff from them. A significantly longer period of record would be required to test the representativeness of the mid-January to mid-March 1987 observations for typical Arizona winters. Further, determining what portion of the CLW flux can be converted to

snowfall is a different and complex subject. However, it is encouraging that a significant CLW flux was estimated during the initial Arizona field program. It is interesting to note that Rauber and Grant (1987) estimated the amount of SLW passing the crest of a mountain range in southern Utah for a single storm. The total flux for a 13 h period was 12.5 x 10^7 g per meter of crestline, equivalent to about 13% of the mean annual runoff from that target area. Only three storms in Table 1 had more CLW flux, and they were all of much longer duration.

8. Summary

Cloud liquid water (CLW) observations were obtained with a microwave radiometer atop the Mogollon Rim of Arizona from mid-January to mid-March 1987. Supporting wind observations allowed estimation of CLW flux over the barrier. Temperature measurements indicate that the large majority of the CLW was supercooled.

It was found that synoptic scale storms produced the bulk of the CLW. The airflow was usually from the southwest during CLW episodes, although northeasterly upslope flow was also an important contributor.

Vertically-integrated mean hourly amounts of CLW were less than 0.1 mm about two-thirds of the time that CLW was detectable. The highest value was under 0.7 mm, which suggests low liquid water contents were common and this was verified by aircraft observations. Nevertheless, more than 300 h with CLW were observed during the field season.

Durations of CLW episodes varied from 1 to 50 h, but the four episodes lasting 23 h or more accounted for over half the observed hours with CLW.

The total estimated CLW flux per storm also varied markedly from 0.1 x 10^7 to 42 x 10^7 g per meter of crosswind distance. About 75% of the total two month flux was due to only three storms. About 35% of the total flux was produced by a single 80 h episode, locally reported as the heaviest snowstorm in 20 years.

The distribution of hourly CLW flux plotted against the vertically-integrated CLW amount (Fig. 5), showed that most of the total flux was due to the many hours with light to moderate CLW amounts. While flux values were relatively low during these hours, their high frequency of occurrence suggests they should not be ruled out for possible cloud seeding potential.

The cumulative distributions of CLW flux from Happy Jack, Arizona and Grand Mesa, Colorado were compared, and found to be remarkably similar. Caution should be used in such comparisons because of the limited observational periods. However, based on the data sets available, the frequency of occurence, vertically-integrated amounts of CLW, and CLW fluxes all appeared similar at the two sites.

The two-month total estimated CLW flux over the Mogollon Rim was compared with mean annual streamflow from the same region, and the flux was found to be almost half the streamflow. This is an encouraging result, suggesting significant winter cloud seeding potential may exist over the Mogollon Rim of Arizona.

ACKNOWLEDGEMENTS

The authors are please to acknowledge the significant contributions to this research made by the following persons: Jack McPartland and Mike Collins of the Bureau of Reclamation, John Thompson, Bill Hauze, Richard Benner, George Wilkerson, and Marty Thorp of North American Weather Consultants, Jim Keller of the U.S. Forest Service, and Wayne Sand and George Bershinsky of the University of Wyoming are all acknowledged for their roles in the data collection program. The cooperation of the U.S. Forest Service in providing facilities at Happy Jack and Prescott, AZ was very important to the field program. Cindy Snook typed the several drafts of the manuscript.

This research was conducted under a cooperative program between the U.S. Bureau of Reclamation and the Department of Water Resources of the State of Arizona.

REFERENCES

Boe, B.A., and A.B. Super, 1986: Wintertime characteristics of supercooled liquid water over the Grand Mesa of western Colorado. J. Wea. Modif., 18, 102-107.

Cooper, W.A. and J.D. Marwitz, 1980: Winter storms over the San Juan Mountains, Part III: Seeding potential. J. Appl. Meteor., 19, 942-949.

Dennis, A.S., 1980: in Weather Modification by Cloud Seeding. 267 pp. Academic Press, New York.

Heggli, M., R.M. Rauber, and J.B. Snider, 1987: Field evaluation of a dual-channel microwave radiometer designed for measurements of integrated water vapor and cloud liquid water in the atmosphere. J. Atmos. Ocean. Tech., 4, 204-213.

Hogg, D.C., F. Guiraud, J. Snider, M. Decker, E. Westwater, 1983: A steerable dual-channel microwave radiometer for measurement of water vapor and liquid in the atmosphere. J. Clim. Appl. Meteor. 22, 789-806.

Holroyd, E., III, and A. Super, 1984: Winter spatial and temporal variations in supercooled liquid water over the Grand Mesa, Colorado. Preprints Ninth Conf. on Inadvertent and Planned Weather Modification, May 21-23, Park City UT, 59-60.

Ludlam, F.H., 1955: Artifical snowfall from mountain clouds. Tellus, 7, 277-290.

Rauber, R.M. and L. O. Grant, 1986: The characteristics and distribution of cloud water over the mountains of northern Colorado during wintertime storms. Part II: Spatial distribution and microphysical characteristics. J. Clim. Appl. Meteor. 25, 489-504.

Rauber, R.M. and L.O. Grant, 1987: Supercooled liquid water structure of a shallow orographic cloud system in southern Utah. J. Clim. Appl. Meteor., 26, 208-215.

Super, A.B., E.W. Holroyd, III, B.A. Boe, and J.T. McPartland, 1986: Colorado River Augmentation Demonstration Program Technical Report: January 1983-March 1985. U.S. Bureau of Reclamation, Division of Atmospheric Resources Research, Denver, CO, May, 1986. 42 pp.

Super, A.B. and J.A. Heimbach, 1988: Microphysical effects of wintertime cloud seeding with silver iodide over the Rocky Mountains. Part II: Observations over the Bridger Range, Montana. J. Appl. Meteor., accepted.

Thompson, J.R. and A.B. Super, 1987: Some estimates of supercooled liquid water flux in winter clouds over the Grand Mesa, Colorado. J. Wea. Modif., 18, 92-98.

GROUND-BASED SUPERCOOLED LIQUID WATER MEASUREMENTS IN WINTER OROGRAPHIC CLOUDS

Mark E. Solak, Rand B. Allan and Thomas J. Henderson
Atmospherics Incorporated
Fresno, CA 93727

ABSTRACT The use of ice detectors at mountain-top sites in winter orographic weather modification projects in the western U.S. is described. Refinements in data acquisition and interpretation are presented. The superiority of ice detector analog voltage records over deice signal-only data for determination of SLW characteristics is demonstrated. It is shown that ground-based ice detector and radiometer-derived supercooled liquid water (SLW) flux estimates exhibit reasonable correspondence. Ground-based SLW flux records are used with precipitation data to produce indications of precipitation efficiency, showing orderly transitions between periods of efficiency and inefficiency within storms. Ground-based SLW flux data suggest that, in some instances, increased precipitation rates alone do not necessarily signal diminished seeding opportunity.

1. INTRODUCTION

It has long been understood that a pivotal factor in any program designed to either apply or investigate winter orographic precipitation enhancement by use of freezing nuclei is the occurrence of supercooled liquid water (SLW) within cloud systems. In recent years the role and importance of low altitude SLW in winter orographic storms has been investigated with renewed vigor. This article provides an update on use of ground-based ice accretion measurements by Atmospherics Incorporated (AI) in the western U.S. Those measurements are used to investigate some aspects of winter orographic cloud systems relating to their precipitation enhancement potential.

Continuous measurements using ice detectors at mountain-top sites for the specific purpose of investigating low altitude supercooled liquid water for weather modification program design and decision making began in California with AI's observations on Squaw Peak near Lake Tahoe. That work was conducted as part of the Sierra Cooperative Pilot Project (SCPP), a winter precipitation enhancement research program funded by the Bureau of Reclamation. The initial methodology and findings have been reported in Henderson and Solak (1983) and Solak et al (1984). Those results, combined with microwave radiometer measurements in the same region (e.g., in Snider and Rottner, 1982), influenced a shift in the focus of SCPP research from primarily postfrontal convection to the more stratiform and widespread cloud types.

Earlier SCPP SLW investigations, based primarily on airborne observations and measurements, had suggested that very little SLW occurred in the stratiform cloud types. However, it became clear that the airborne investigations in stratiform situations were often severely limited by terrain-avoidance constraints on low altitude flight operations, yielding an incomplete assessment of SLW occurrence. In contrast, the mountain-top measurements supported earlier conventional wisdom and long-standing operational assumptions that significant amounts of SLW are commonly produced and often concentrated at low altitudes. That view arose from observations of significant rime ice accumulation on vegetation and structures in high terrain. It has been strengthened by seeding aircraft observations over other portions of the Sierra, and by airborne research measurements over and near the SCPP study area (Lamb et al, 1976).

Those early Sierra ground-level SLW studies highlighted the important practical factor of potential weather modification yield, which is affected by cloud coverage and type and has its upper limit defined by the magnitude of the SLW occurrence (i.e., the total mass of SLW potentially available for conversion and/or accretion, per storm or per unit time). In SCPP, although some cumuli were considered to present good seeding potential, their contribution to season total precipitation was recognized as being comparatively small. In contrast, the more widespread stratiform cloud systems were known to contribute a significant proportion of seasonal precipitation. The growing evidence in SCPP of substantial SLW occurring within those stratiform cloud systems made them increasingly attractive as potential seeding candidates.

Recent weather modification research, largely in the western states, has shed additional light on the occurrence and character of low altitude SLW, as well as at other levels, and its implications relative to weather modification potential, e.g., Sassen (1985) in Utah, Rauber et al (1986) in northern Colorado and Thompson and Super (1987) over Colorado's Grand Mesa. These and other recent findings have been based on measurements using research systems such as microwave radiometers, short wavelength radars and lidars. One of the goals of the work reported here is to demonstrate the utility of the comparatively simple mountain-top SLW measurement system to (1) provide useful operational seeding decision making guidance and (2) augment full cloud depth SLW measurements in research programs.

2. OBSERVATION SYSTEM

The prototype system used at the Squaw Peak site in California, described in detail in Henderson and Solak (1983), consisted basically of

an ice detector, heated cup and vane wind system, temperature sensor, back-up power system, and chart recorders. Some modifications were later incorporated, most notably inclusion of a heated orthogonal anemometer which provides high quality wind data with great reliability in icing environments. Since 1987 the SLW system has included onsite computerized data acquisition, producing high quality data at 5-min intervals, averaged from 5-sec sampling. The chart recorders have been retained to provide analog ice accretion records and to serve as backup to the computerized acquisition.

The key component of the SLW systems has been the Rosemount ice detector model 871FA, an electro-mechanical device which automatically deices and transmits a signal when a specified amount of ice has accreted onto its sensing element. After the deicing (heat) cycle, the detector cools and returns to sensing status in approximately 60 seconds. The model 871FA detector also provides a continuous analog output of the sensing probe oscillation frequency which corresponds to the instantaneous sensor ice load. Another model ice detector, the Rosemount 872B, has also been evaluated for possible incorporation into operational systems. The model 872B heats for 90 seconds, and requires approximately 4-5 minutes to cool sufficiently after each heat cycle to again accumulate rime ice. The 872B currently provides a deice signal only. Records from the ice detector(s) are used in conjunction with wind measurements to produce estimates of average SLW concentration at appropriate time intervals.

3. DATA ASPECTS

Our initial data interpretations, detailed in Henderson and Solak (1983), involved a "trip counting" method which is based on the ice detector's deice cycles. Note: the terms "trip" and "deice cycle" are used interchangeably, and refer to the point in time when the ice accumulation triggers the detector's heaters and a discrete deice signal is provided for the 6-7 second heat duration of the 871FA. Using each deice cycle to define an averaging interval, or by counting deice events within fixed time intervals, mean values of wind velocity were used with the cross-section area of the detector's sensing element to estimate sample volume (i.e., the volume swept out by the probe). The known ice mass (trip) accumulations and sample volume estimates were then used to produce crude estimates of SLW concentration in the air passing the measurement site. Only storms producing sufficient ice accretion on the probe to trigger its deicing heaters were analyzed. This method is still used by some investigators. Some important limitations of this basic method are described in part 4 of this article.

Onsite observations of the ice detector's performance in a variety of icing conditions have led to adjustments to our data reduction and SLW parameter calculation methods. For example, observations of the detector's very low sensing threshold, combined with its ability to accurately indicate small scale variability during ice accretion events, has enabled a shift from the deice signal-only data to the oscillation frequency analog output for accurate determination of ice accretion values. Further, the effects of residual melt (not totally shed after deicing) which can occur in light wind situations are now eliminated during data reduction. These adjustments have improved the accuracy and utility of the observations. The key refinements and additions in data reduction and SLW calculations are listed below.

- Analog ice detector oscillation frequency records from the model 871FA are manually reduced to determine ice accretion mass values. This allows identification and analysis of rime ice accumulation periods of "sub-trip" magnitude which are not documented in "trip-only" output. The data reduction interval can then be tailored to specific project requirements. Part 4 of this article describes the output differences in more detail.
- Effects of residual melt drops on sensing element downward operations (after heat cycles) are identified in analog traces and excluded from calculations.
- Ice detector model 871FA 60 sec off-duty (heat, cooldown) periods are eliminated from in sample volume estimates.
- First-order adjustments for estimated droplet collection efficiency are applied to accumulation amounts, based on laminar flow equations originally develop by Ranz and Wong (1952).
- SLW flux estimates are routinely developed for assessing event magnitude and comparison with other SLW observations.

4. ICE DETECTOR OUTPUT COMPARISONS AND USES

Our investigations have involved the Rosemount model 871FA and 872B ice detectors. Both employ the same operating principle and sensing element configuration. However, having been designed for distinctly different uses, their standard outputs differ. The model 871FA was developed for the aviation industry and provides an analog output corresponding to rime loading on its sensing element, as well as a 6-7 sec deice signal when a preset rime load threshold has accumulated and the instrument's deicing heater is triggered. Thus, it senses and indicates. In contrast, the more recent model 872B was designed for use as a warning device for fixed structures and produces only a deice signal after significant atmospheric icing has occurred. Those output differences must be carefully considered when using the data to assess atmospheric conditions.

Our initial data interpretations were based on the "trip counting" (deice signal) method used in recent years by a few investigators. But, field observations and data comparisons (detailed below) have provided convincing evidence that using the analog (sensing) output is superior for research applications. Consequently, all results in this article are based on manually reduced analog records of ice accretion.

To illustrate the differences between the two probe models' output, a simulated chart section is shown in Figure 1. It depicts the combined analog and trip signal provided by the 871FA detector as

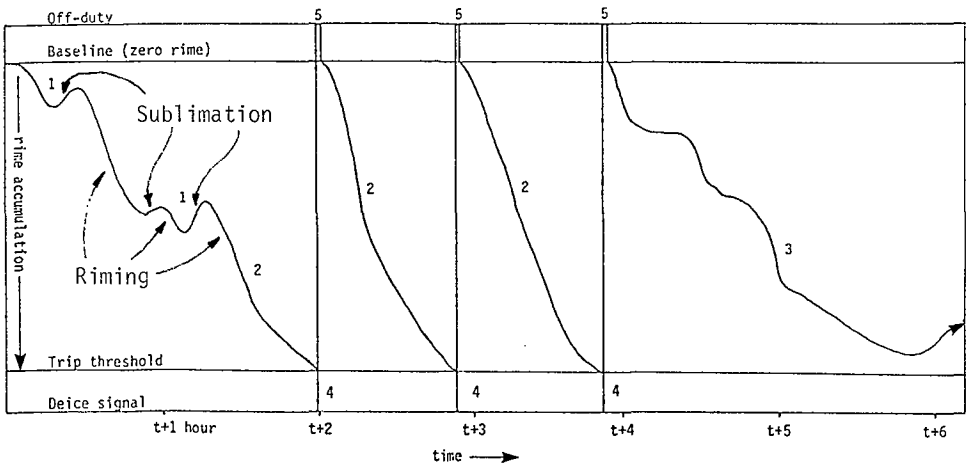

Figure 1. Example chart record of combined analog sensing (rime ice load) and deice "trip" signal output from the model 871FA ice detectors used in ground-based investigations. The trace segments are numbered for reference to text discussion.

routinely used in our field work. The 872B probe output, in its currently available configuration, would consist of the three deice trips only, with no indication of accretion rates or character. Features commonly seen in analog traces from ground-based observations are shown in Figure 1.

During storm onset the initial accumulation of rime ice on the sensor commonly occurs over a period of 2-3 or more hours before the first instrument deice cycle. The duration of this initial accumulation period is influenced by the LWC and wind velocity (i.e., the SLW flux), the preset trip threshold value and the continuity of the initial probe riming during storm onset. Interspersed riming and sublimation periods are commonly noted in analog traces prior to the first detector deicing cycle because cloud conditions fluctuate during storm onset. Prior to the first deice event in Figure 1 (chart section 4 at t+2h), 20% more actual accretion occurred than the "trip-only" output would have indicated. Rime accumulation leading to the next two trips (near t+3 and t+4), is much more uniform. No significant interspersed sublimation is indicated in the chart sections labeled "2" between t+2 and t+4, and each trip represents a true ice accumulation. However, after the third trip (near t+4) chart section 3 shows additional accretion from t+4 through t+6 that would not be indicated in the trip-only output because the deice threshold was not reached. This additional accretion, not documented in the "trip only" records, constitutes nearly 25% of the total occurring in the overall example.

In viewing the analog trace example, several drawbacks to using trip-only (standard 872B) output become apparent.

1)The 872B cannot accurately indicate the start or end of probe riming events. In contrast, the 871FA continuous analog output provides those times unambiguously.

2) The 872B cannot indicate accumulations of rime ice less than its deice threshold value. Many ice accretion events are simply not documented in trip-only data.

3) The 872B cannot accurately indicate rime accumulations when interspersed sublimation/riming periods occur.

4) The fact that the 872B data consist of "trip" points only, with no indication of the character of the ice accumulation period, forces an analyst to assume uniform conditions between instrument deicing cycles. The elapsed time between trips can vary widely, and during low magnitude icing occurrences the resultant averaging periods can be unacceptably long. The 871FA analog records capture fine-scale ice accretion rate variability and allow data reduction at uniform intervals tailored to the specific application.

5. FINDINGS

Strategically sited ground-based SLW observations can be used to address a number of practical questions related to project design and operations. Data obtained within the Utah/NOAA cooperative weather modification research program are used to address the factors of (a) accurately identifying the start and end of SLW occurrences at low altitudes, (b) determining the storm-by-storm contribution to seasonal low altitude SLW flux, (c) characterizing site winds during SLW occurrences, (d) determining temperature characteristics during those occurrences, (e) investigating relationships between SLW and precipitation and (f) assessing detector and radiometer data relationships.

The SLW system in Utah was located on an exposed ridge at 2978 m (9768') elevation approximately 3 km west of the crest of the Tushar Range in southwestern Utah (see Figure 2). The Tushars are oriented primarily north-south, rising from an 1800 m valley floor about 4 km east of Beaver to a ridgeline ranging from 3000-3700 m elevation about 20 km east. Near the SLW site the crestline averages about 3400 m. In 1987 the Utah/NOAA field operations documented 11 storms during the six-week period of 01 February through 15 March. Those 11 storms are listed in Table 1.

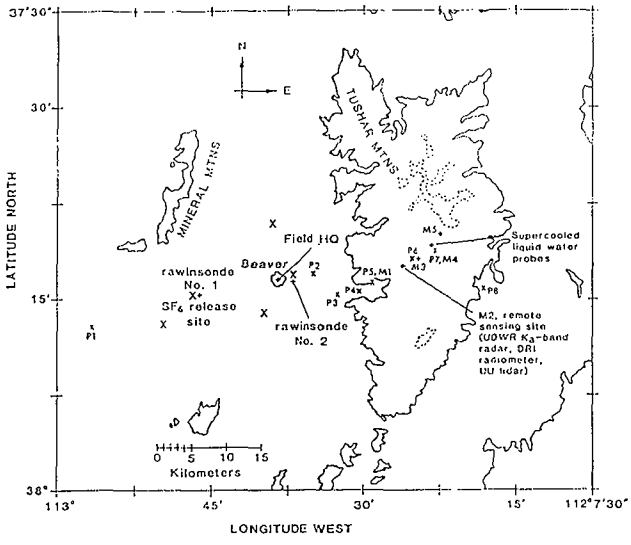

Figure 2. Locations of the instrumentation in the 1987 Utah/NOAA field research program. Symbols P1, P2, . . . indicate sites of surface precipitation gages. Symbols M1, M2, . . . indicate sites of surface precipitation microphysics observations. Large unlabeled symbols X show sites of mechanical weather stations. Contours of terrain are at 2438 m MSL (solid line) and at 3353 m MSL (dashed line).

TABLE 1. Utah/NOAA 1987 STORM periods

STORM	Date	Start Time (MST)	Date	End Time (MST)	Dur(h)
1	03 Feb 87	1300	04 Feb 87	0300	14.0
2	10 Feb 87	0730	10 Feb 87	1700	9.5
3	11 Feb 87	1500	12 Feb 87	1300	22.0
4	13 Feb 87	1500	14 Feb 87	1100	20.0
5	15 Feb 87	1600	16 Feb 87	1400	22.0
6	18 Feb 87	1400	18 Feb 87	1940	5.7
7	23 Feb 87	1000	25 Feb 87	2300	61.0
8	07 Mar 87	0800	07 Mar 87	2000	12.0
9	08 Mar 87	0500	08 Mar 87	2400	19.0
10	13 Mar 87	1330	13 Mar 87	1800	4.5
11	14 Mar 87	2300	15 Mar 87	2120	22.3
				Total:	212.0

A. Ice Detector (Model) Comparisons

Documentation of the true onset, end and character of SLW occurrences is of obvious value in operations and research applications. The Utah observations in 1987 marked our first comparisons of model 872B (trip-only) and model 871FA (analog) output from collocated detectors under field conditions. Those field comparisons, using 871FA data as a standard because of its analog output, confirmed the significant differences illustrated in the example (Figure 1) presented earlier in this article. Onsite observer's notes have verified the 871FA's low sensing threshold and the ability of its analog output to document small-scale variability. Table 2 presents the durations and magnitudes of atmospheric icing events as indicated by the two detector models during the Utah study. Durations for the 872B represent the full elapsed time between the first and last instrument trips, whereas the 871FA durations are sums of non-zero 5-minute icing periods. The SLW mass values in Table 2 were determined using the detector total ice accretion mass measurements. Those measured ice accretion amounts have been extrapolated to represent the mass of SLW passing through a window 1 meter square to facilitate comparison with other systems' data.

TABLE 2. Comparison of 871FA and 872B icing probes using 1987 season Utah/NOAA riming data

STORM	Hrs of indicated riming 872B	Hrs of indicated riming 871FA	Total ice mass ($kg\ m^{-2}$) 872B	Total ice mass ($kg\ m^{-2}$) 871FA
1	0	4.3	0	0.676
2	0	0.9	0	0.446
3	4.8	4.6	2.232	2.827
4	4.8	11.9	13.950	15.755
5	0	0.7	0	0.050
6	0	1.0	0	0.081
7	0	4.5	0	0.595
8	0	0.9	0	0.136
9	1.4	3.6	1.674	1.978
10	0	0.3	0	0.019
11	0	2.3	0	0.453
	11.0	35.0	17.856	23.016

As shown in Table 2, the 872B output indicated the presence of SLW in only three storms, although some SLW was measured in all eleven storms by the collocated 871FA. During those three storms, the 872B reported 55% of the cumulative duration and 87% of the total ice mass measured by the 871FA. Over the full season, the 872B reported 31% of the cumulative riming duration and 78% of the total ice mass. Further, STORM 3 illustrates a duration-related problem inherent in the assumptions required when using trip-only output. In that case the 872B duration is greater than that reported by the 871FA.

B. Storm Contribution to Season Total SLW Mass

SLW mass and its flux are measurements that can be used in a basic way to estimate the upper limits of seeding potential in precipitation augmentation efforts. This practical concept is important, even if used only as a coarse indicator as input to a number of weather modification considerations, such as:

- assessment of overall augmentation potential during project design,
- determination of the distribution of SLW occurrences and their relative magnitudes over a measurement period,
- developing subsequent engineers' estimates of operational levels of effort and attendant costs, and
- day-to-day operations seeding decision making, if available real-time

Using Utah/NOAA ice detector data, total SLW mass values for each of the 11 STORMS (STORMS = broadly inclusive analysis periods which encompass the early onset through dissipation phases of precipitation events) investigated during that project's 1987 field period were calculated using ground-based ice accretion data. Those values are presented in Figure 3 as a ranked cumulative distribution.

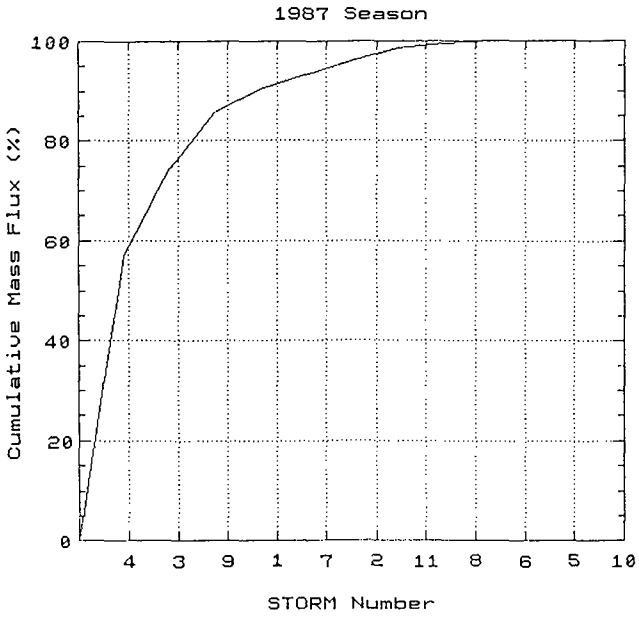

Figure 3. Cumulative SLW mass flux, 1987 season, by STORM.

It can be seen in Figure 3 that although some SLW was detected during each STORM, a small number of events contributed a large proportion of the season total amount. For example, STORMS 4, 3 and 9 produced over 85% of the total ice mass measured at the ground-based site. However, their combined duration occupied only 29% of the total season STORM duration. As an extreme example, STORM 4 alone produced well over half the season total, most of which occurred during a 7 hour period. This characteristic is consistent with indications in radiometer data from the 1985 season in Utah; Rogers et al (1986) reported that two STORMS had produced approximately 70% of the season's total liquid water flux, and that one 30 hour period had contributed nearly 50% of the season's total.

The information shown in Figure 3 and the earlier findings of Rogers et al (1986) indicate the importance of continuously monitoring the magnitude of SLW and its flux. It appears that effective precipitation enhancement research and operations must be able to identify, assess and properly respond to the comparatively few dominant events which contain the large quantities of SLW. This would be of increased importance if resources were limited.

C. SLW Versus Site Wind Characteristics

1987 Utah data during probe riming events were assessed to characterize site wind relationships with SLW content and flux. Figure 4 compares all full season non-zero SLW content and flux occurrences with wind direction at 5-min intervals.

Unadjusted SLW content is estimated using the simple expression,

$$LWC = M_t/V_s$$

where M_t is the measured ice mass (g) and V_s, the volume of air swept out by the probe, is the product of the mean wind velocity (m s^{-1}), the duration of the detector on-line period (s) and the probe cross-section (m^2). Those values are then adjusted for estimated probe collection efficiency using equations adapted from Ranz and Wong (1952). The now-computerized calculations account for the inverse relationship of collection efficiency to sensor diameter and temperature, and its direct relationship with droplet size and velocity. Average values of wind velocity and temperature are input, along with the probe diameter and, in the absence of measured droplet size spectra, an assumed 12 micron median droplet diameter. Using the indicated collection efficiency, the appropriate adjustment is then applied to each SLW value. The adjusted values are used in this article. SLW flux per unit time, in this case expressed as g m^{-2} s^{-1}, is obtained using,

$$Flux = M_t/(C*D_s)$$

where C is the probe cross-section (m^{-2}) and D_s is the sample duration in seconds.

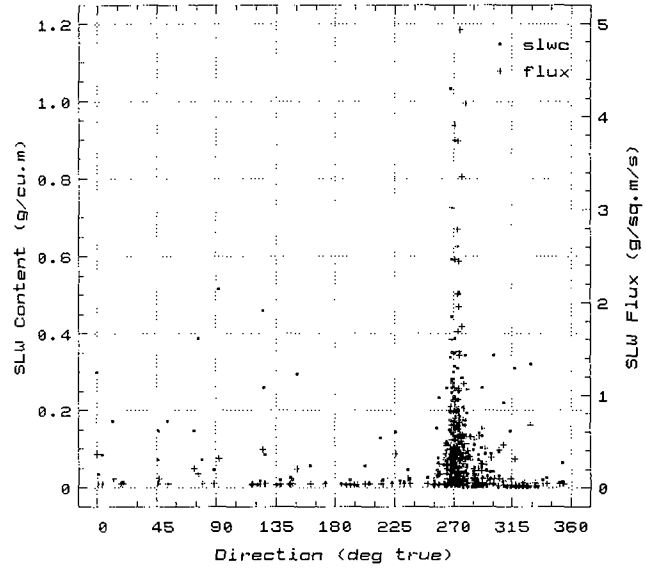

Figure 4. SLW content and flux vs. wind direction during 1987 full season combined probe riming events, 5-min averages.

The prominence of near-surface flow in the sector 260-290 during probe riming occurrences is clearly seen in Figure 4, and reflects terrain effects to a degree. However, although SLW content is seen to be somewhat a function of wind direction, SLW flux shows a much stronger wind direction dependence. Westerly flow is essentially barrier-normal to the Tushar Range which is oriented basically north-south. These data suggest that orographic lift is important in production of SLW at low altitudes.

Figure 5 compares 5-min interval SLW content and flux with wind velocity, and sheds additional light on the wind regimes which produce and enhance SLW of potential weather modification significance (i.e., comparatively large amounts for conversion to ice crystals). A weak inverse relationship (r = -.21) between SLW content and

velocity can be seen. However, SLW flux exhibits a positive and somewhat stronger relationship (r = .36), providing additional evidence of the importance of flow with a strong orographic component in SLW production.

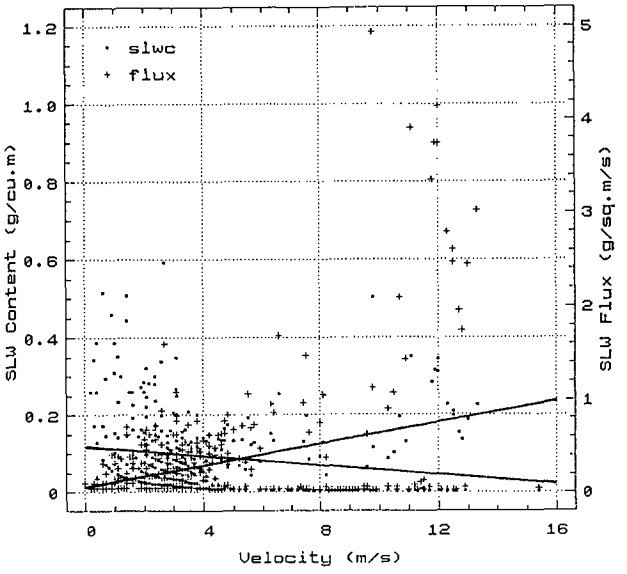

Figure 5. Regression of SLW content and flux with site wind velocity during 1987 full season combined probe riming events, 5-min averages.

D. SLW Versus Temperature

Full season SLW content and flux values, averaged for 5-min intervals, were compared with temperature data at the SLW site. Those data are shown in Figure 6. SLW was observed at temperatures as cold as -13C. Two distinct maxima in SLW content were found, from -2 to -3C and from -7 to -8C. The flux data show the same maxima, but only weakly from -7 to -8C. Inverse relationships between SLW content and site temperature were found; i.e., lower SLW content and flux values occurred generally at colder temperatures. The SLW content indication is consistent with the hypothesis put forward by Grant and Kahan (1974), that warmer orographic clouds should exhibit higher LWC values than colder orographic clouds. They reason that the higher LWC values are to be expected due to fewer snow crystals to utilize the SLW, and the greater water vapor holding capacity of warmer air. A similar inverse relationship between SLW content and temperature was shown in mountain top measurements in Colorado by Hindman (1986). The large flux values from -2 to -3C reflect the dominance of STORM 87-4 which produced over half the total season SLW mass at the detector site.

E. Relationship Between SLW and Precipitation

The relationship between supercooled liquid water and precipitation has important weather modification implications, and was also investigated in the Utah data. A project Belfort weighing gage (P6), located in the upper watershed at 2609 m elevation 3.7 km southwest of the ice detector site, was chosen for this comparison because of the completeness of its record and its relatively high data quality (locations shown in Figure 2).

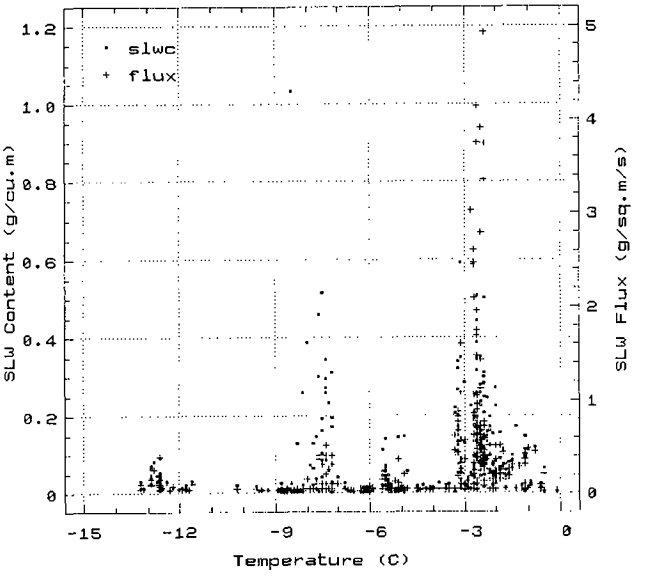

Figure 6. SLW content and flux vs. temperature during 1987 full season combined probe riming events, 5-min averages.

The SLW and precipitation data were analyzed in the following manner. A lag time of 15 minutes was employed in the riming data to attempt to relate conditions at the gage site to those at the icing station. The 15-minute lag time approximates the seasonal average wind speed of 4.5 m s^{-1}. For the full 1987 eleven-STORM sample, probe riming occurred during approximately half the 30-minute periods of measurable precipitation. Thirty-minute accumulations of precipitation and probe rime ice for each of the eleven STORM periods were compared using a linear regression analysis.

Since the Utah/NOAA project definition of a STORM includes a period of minimal activity prior to the onset of precipitation or riming, and generally continues beyond the end of any significant precipitation, a new unit of analysis called a **storm** (lower-case letters) was adopted here. In this study the **storm** is defined as the period between the first incidence of either precipitation at gage P6 or probe riming and the last incidence of either precipitation or riming. When regression analysis was performed on each **storm**, (see Table 3) an interesting pattern is observed:

-For the three **storms** (4, 3 and 9) that comprised 86% of the total seasonal SLW mass accumulation at the detector site, positive correlations of .17 to .53 were noted between precipitation amount and probe rime accumulation.

-The remaining **storms** exhibited weak negative correlations ranging from 0 to -.22, excepting overall STORM 7 which yielded: a=.39, b=-.13 and c= no precipitation at P6 for the three distinct cloud systems within STORM 7's overall duration.

TABLE 3. Correlation Coefficients of Probe Riming Rate to Precipitation Rate at Merchant Creek, Within 11 STORMS Ranked by SLW Mass Accumulation

	correl. coeff., 30 min. intervals		
STORM	STORM[1]		storm[2]
87- 4*	+0.48		+0.46
3*	+0.65		+0.53
9	+0.37		+0.17
1	-0.13		-0.17
7*#	+0.18		+0.16
		(a)	+0.39
		(b)	-0.13
		(c)	NP
2	-0.12		-0.22
11	-0.13		-0.14
8	NP		NP
6	NP		NP
5*	-0.13		-0.13
10	+0.22		0.00

1 standard project definition
2 defined as the period between the first and last occurrence of either precip at P6 or probe riming at the ice detector site
* project priority analysis cases
\# STORM 7 contains three distinct cloudy periods, labeled a, b and c
NP no measurable precipitation

Major **storms**, exemplified by numbers 4 and 3 (which produced approximately 74% of the season total probe rime mass in 1987) produced large quantities of supercooled liquid water in conjunction with precipitation rate increases. However, for the remaining 1987 **storms**, when the mid and upper barrier precipitation rate increased, the low altitude supercooled liquid water supply did not show a corresponding increase. These initial storm-scale findings challenge the notion that high precipitation rates alone necessarily signal decreased seeding opportunity because we report instances of concurrent high precipitation rates and high SLW production.

Because we have shown that both SLW production and precipitation rates vary widely between and within the various phases of significant precipitation events, it may be more instructive to assess and compare those factors at shorter (operationally meaningful) time intervals. To that end SLW flux data and precipitation rates were compared to provide indications of trends in relative precipitation efficiency. Following a comparison procedure applied by Rogers et al (1986) which used radiometer data, ice detector accretion records and precipitation data were used to develop similar relative efficiency indications for two major Utah STORMs, 85-9 and 87-4. In both cases 30-min interval data were used, matching the basic temporal resolution of the precipitation data. The ice detector accretion amounts were sums of 5-min values.

SLW flux past the ground-based detector site was calculated from the ice mass collected by the detector and adjusted for estimated collection efficiency, as described earlier. The values were expressed in kg m^{-2} h^{-1}. In these studies, precipitation rates were determined for the western slope of the Tushar Range along a 20km barrier transect from approximately 1875m elevation in the upper foothills to over 2900m in the upper watershed near the ice detector site. Thirty-minute averages of six gages (P2-P7) in 1985 and five gages (P2-P6) in 1987 were used. The gage data were converted from inches per half hour to mm h^{-1}.

The STORM 85-9 data are presented in Figures 7a and 7b. In (7a) two distinct periods of high SLW flux are clearly seen, from 1700-2200 and from 0500-0800. The earlier period of high SLW flux is not accompanied by high precipitation rates, so comparative precipitation inefficiency is inferred. In contrast, the latter period of high SLW is followed soon thereafter by a significant precipitation rate increase, so higher storm precipitation efficiency is indicated during most of that phase.

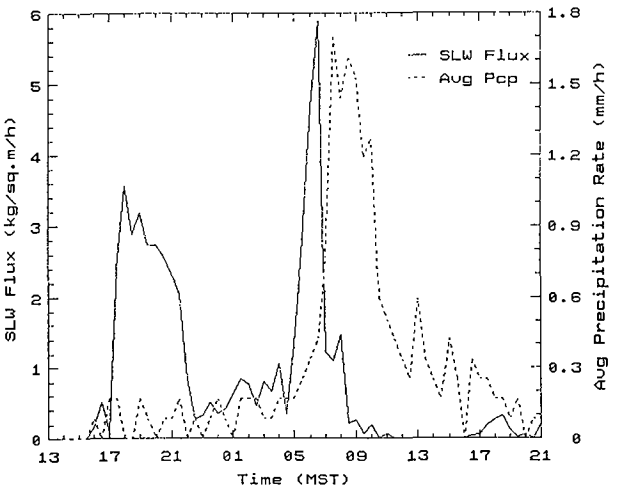

Figure 7a. Time series of 30-min Mt. Holly SLW flux and multi-gage average precipitation rate, STORM 85-9: 08-09 February 1985.

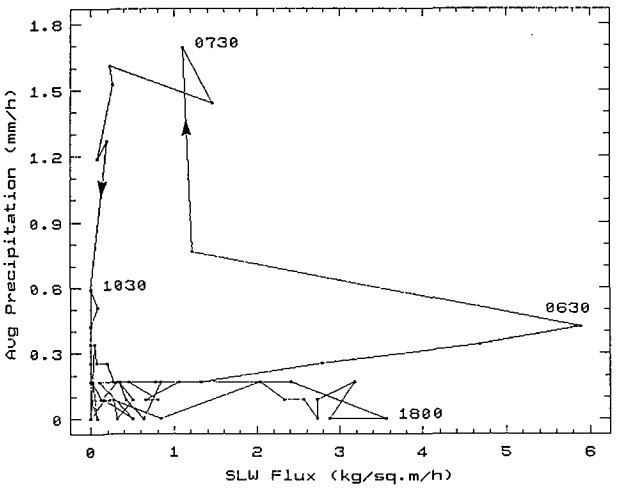

Figure 7b. Scatterplot of 30-min Mt. Holly site SLW flux and average precipitation rate, STORM 85-9: 08-09 February 1985. The points are connected to show changes in relative precipitation efficiency with time.

In (7b) the same data are presented, but as a scatterplot. When the points are connected chronologically, the plot serves to indicate trends in comparative storm efficiency and inefficiency. Our simple conceptual model of storm efficiency follows a spectrum from very high to very low precipitation efficiency. High efficiency would be characterized by high precipitation rates in conjunction with low SLW flux. Periods of low precipitation efficiency would exhibit low precipitation rates and high SLW flux. Consideration of other factors affecting precipitation enhancement potential is beyond the scope of this article. The two high SLW flux periods can be seen. The first, bracketing the label at 1800 centered in the lower portion of the plot area, shows a cluster of several half-hour periods with high SLW and low precipitation rates (inefficient precipitation production). The second high SLW flux period is initially dramatic (0630), but the points very soon migrate to the upper left portion of the plot as the precipitation increases and the SLW flux decreases, indicating a period of more efficient precipitation. Analysis of radiometer data for this storm shown in Rogers et al (1986) show the same periods of "efficiency" and "inefficiency". An important characteristic in Figure 7b is the reasonably orderly transitions between "efficient" and "inefficient" storm segments of a few hours' duration. This tendency for well-sustained temporal trends in indicated storm efficiency suggests that adequate time for recognition and assessment of potentially seedable periods exists in certain storms. This is of further significance when recalling that the storm described in Figure 7b dominated the SLW flux for the 1985 season in both the radiometer and ice detector records, producing approximately half the seasonal totals for both observation systems.

The same analysis method was applied to STORM 87-4, a well organized frontal system, which was dominant in the seasonal SLW flux data at the ice detector site. The only difference from the 85-9 study was that in 87-4 study data from the highest elevation gage (P7) were not available. In this case distinct and sustained efficient and inefficient periods were also found. The data are shown in Figures 8a and 8b. In contrast to STORM 85-9 which exhibited two SLW surges, only one dramatic period of high SLW occurred in STORM 87-4. Its onset brought modest SLW at the detector site, but precipitation across the western slope of the Tushars occurred at significant rates. After about 4 hours of relatively high precipitation rates (with average half-hourly precipitation rates peaking over 4 mm h^{-1}), dramatic prefrontal SLW increases occurred. The SLW flux peaked immediately prior to the frontal passage to nearly 15 kg m^{-2} h^{-1}, more than twice the peak value for STORM 85-9. The massive SLW flux was due to strong acceleration of the barrier component flow ahead of the surface cold front, combined with elevated SLW content. As the SLW flux was increasing, the precipitation rates trended lower than the earlier period, resulting in a 3h period of storm inefficiency representing a significant potential seeding opportunity.

Following the cold frontal passage, which was marked by thunderstorms, rapid clearing was observed across the study area. About an hour after the frontal passage, precipitation began again and was accompanied by low magnitude SLW at the detector site. This period of high precipitation efficiency lasted for about 7 hours.

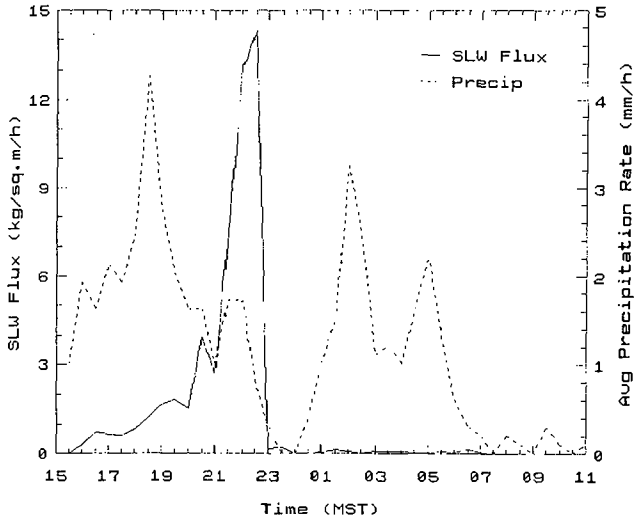

Figure 8a. Time series of 30-min Mt. Holly site SLW flux and multi-gage average precipitation rate, STORM 87-4: 13-14 February 1987.

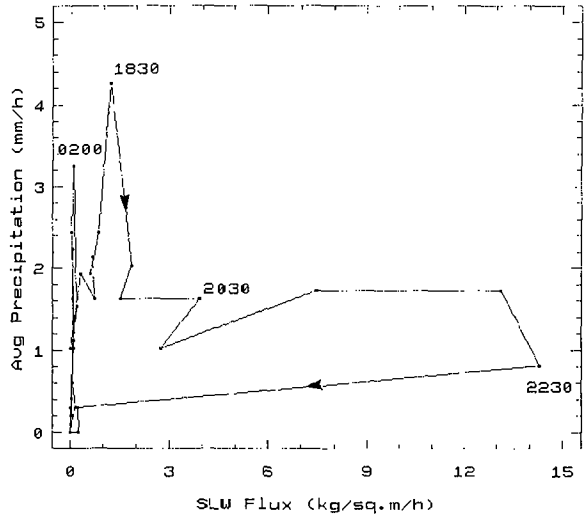

Figure 8b. Scatterplot of 30-min Mt. Holly site SLW flux and average precipitation rate, STORM 87-4: 13-14 February 1987. The points are connected to show changes in relative precipitation efficiency with time.

F. Ice Detector/Radiometer SLW Flux Comparisons

Ground-based SLW measurements in Utah and elsewhere have played a useful role in weather modification research, documenting the magnitude and frequency of low altitude SLW over mountainous terrain at altitudes where airborne measurements are not permitted. It is desirable to relate these point measurements to SLW measurements documenting the full cloud depth.

Consequently, a few preliminary comparisons between ice detector and radiometer-derived SLW flux estimates were made using Utah data. These comparisons involved the 1985 "priority analysis" cases at the STORM scale and the STORM 85-9 case at intervals as short as 30 minutes.

When STORM total SLW flux from the ice detector site was compared to the radiometer-derived estimates of full depth, barrier-wide liquid flux, the two independent systems ranked the STORMs identically. Table 4 shows the ranked totals; the dominance of STORM 85-9 is again apparent. The values are well correlated. Percentages pertain to the four-STORM sample.

TABLE 4. Ice Detector/Radiometer Flux Comparisons, STORM Scale

STORM	Ice Det Flux kg m^{-2} h^{-1}	Radiometer Flux[1] AF, 50 km width
85-9	35.44 (94.5%)	6235 (83.7%)
85-13	1.08 (2.9%)	861 (11.6%)
85-8	.86 (2.3%)	252 (3.4%)
85-11	.12 (.3%)	97 (1.3%)

[1] Corrected liquid water (AF = Acre Feet), Table III, Rogers et al. (1986)

The STORM 85-9 case was assessed at finer time intervals. Three-hour, barrier wide, (50km) radiometer liquid water volume values, calculated by Rogers et al. (1986) using 700mb rawinsonde winds, were compared with ice detector-derived flux values for corresponding time blocks. The comparison is shown in Table 5. At 3h intervals reasonable correspondence is seen, but with some apparent offsets in peak values. Those are due to the 3h averaging, especially when a dominant short-term maximum occurs near a break between intervals, but may also reflect real differences due to the altitude(s) at which the SLW was occurring. Simple correlation coefficients between the two systems' flux values are shown for 3h and 6h blocks. Improved correspondence between the two systems' data is seen at 6h, but the sample is very small.

TABLE 5. Ice Detector/Radiometer Flux Comparisons, STORM 85-9, 3 and 6-hr Scale

Rawinsonde Time (GMT)	3h avg radiom. liquid water depth (mm)	Radiom. liquid water vol (AF/50 km)		Ice det. SLW Flux (kg m^{-2} h^{-1})	
12	0.000	0.0		0.000	
15	0.000	0.0		0.000	
00 (17L)	0.273	1190.1		5.618	
			2052.6		12.921
03 (20L)	0.236	862.5		7.303	
06 (23L)	0.052	247.4		1.261	
			1513.2		3.286
09 (02L)	0.227	1265.8		2.025	
12 (05L)	0.232	1150.5		7.641	
			2345.7		10.433
15 (08L)	0.275	1195.2		2.792	
18 (11L)	0.206	312.9		0.077	
			329.6		0.542
00 (17L)	0.010	16.7		0.465	
03 (20L)	0.000	0.0		0.263	

Detector Flux vs Radiometer Volume: at 3h, r = .69, n=9
at 6h, r = .88, n=4

Comparisons were also made at 30-min intervals through the full duration of STORM 85-9, and for each of its four phases. Scatterplots of SLW flux and precipitation, drawn from the ice detector system (as shown in Figure 7b) and using radiometer data (plot not shown here) show many similarities in their respective indicated periods of precipitation inefficiency and efficiency. A more direct comparison of flux estimates involved a time series of STORM 85-9 30-min flux values from the two measurement systems through the storm, presented in Figure 9 with the four STORM phases indicated. The storm phases are described in Table 6 which appears below. The ice detector-derived values in this plot were not adjusted to account for its position downwind of the radiometer, partly because the radiometer data were obtained in varying proportions of zenith and azimuth scanning modes. Good correspondence is seen in the SLW maxima in phase I and bracketing 0600 in phase III. Poor correspondence can also be seen from mid-phase II to early phase III, and from mid-phase III through phase IV, indicating periods when the SLW was occurring above the ice detector's elevation.

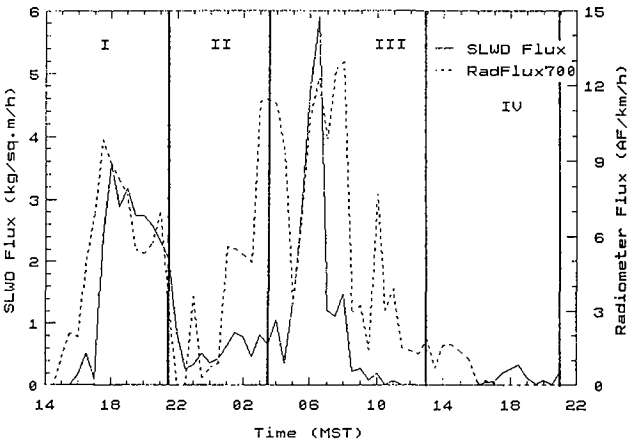

Figure 9. Time series of Mt. Holly ice detector and Merchant Valley radiometer-derived SLW flux. The project STORM phases are indicated; times are in MST.

Simple (linear) regressions were run for each of the four phases, without any time lag and with a 30-min lag applied to the detector data to account for the distance between the measurement sites. A summary is shown in Table 6. Each storm phase is described. The degree of correspondence between the mountain-top and full-depth (radiometer) flux estimates, as well as the effect of the fixed lag for advection, varies among the STORM phases. Thirty-minute data within the various phases (i.e., cloud types and synoptic patterns) show correspondence ranging from excellent (r = .91 in orographically induced altocumulus) to poor (r <.5 in shallow, dissipating layers and isolated cap clouds).

TABLE 6. Ice Detector/Radiometer SLW Flux Estimates Compared by STORM Phase, 85-9

Phase	Times (MST)	Correlation No Lag	30min Lag	Description
I	1400-2130	.771	.906	Orogr.induced/ enhanced alto cumulus layer
II	2130-0330	.490	.768	Altocu layer with embedded conv.elements
III	0330-1300	.613	.352	Immed. pre and postfrontal; synoptic scale disturbance produced meso-scale bands
IV	1300-2100	-.543	-.582	Dissip stage, decreasing precip from shallowing clouds
STORM	1400 8FEB 2100 9FEB	.636	.552	

6. CONCLUSIONS

Refinements in the ground-based supercooled liquid water system sensors, data acquisition methods and data interpretation have produced highly useful information regarding SLW characteristics for winter orographic weather modification research and operations.

Ice detector accretion data in analog form is far superior to "trip-only" records, especially for research applications. Care must be exercised in drawing conclusions from trip-only data pertaining to icing occurrence and duration, as well as in estimating SLW concentration and flux.

Comparisons of ice detector and radiometer-derived SLW flux estimates show good correspondence in many instances and informative differences in others.

Estimates of "relative precipitation efficiency" using SLW flux derived from ground-based ice detector measurements show orderly transitions between comparatively efficient and inefficient storm periods of a few hours duration. This result suggests adequate continuity for real-time recognition of, and response to, potential seeding opportunities (inefficient storm periods).

Comparisons of low-altitude SLW flux values and precipitation rates suggest that increased precipitation alone does not necessarily signal diminished augmentation potential. This suggestion must be further investigated, taking into account other factors to more objectively determine seedability.

Acknowledgements

This work was performed as one of several contracts between the State of Utah (Division of Water Resources) and a number of federal,state, university and private sector groups. In turn, the overall activities are supported by the Department of Commerce within the Utah/NOAA Cooperative Weather Modification Research Program. We are grateful for the collaboration of the many dedicated investigators within the program and the team spirit so necessary in field research programs of this type.

7. REFERENCES

Grant, L. O., and A. M. Kahan, 1974: Weather Modification for augmenting orographic precipitation. Weather and Climate Modification, Hess, Ed., 282-317.

Henderson, T.J. and M. E. Solak, 1983: Supercooled liquid water concentrations in winter orographic clouds from ground-based ice accretion measurements. J. Wea. Modif., 15, 64-70.

Hindman, E.E., 1986: Characteristics of supercooled liquid water in clouds at mountaintop sites in the Colorado Rockies. J. Climate and Appl. Meteor., 25, 1271-1279.

Lamb, D., K.W. Nielsen, H.E. Klieforth and J. Hallet, 1976: Measurement of liquid water content in winter cloud systems over the Sierra Nevada. J. Appl. Meteor., 15, 763-775.

Ranz, W. E. and J. B. Wong, 1952: Impaction of dust and smoke particles on surface and body collectors. Industrial and Engineering Chemistry, 44, 1372-1381.

Rauber, R.M. and L.O. Grant, 1986: The characteristics and distribution of cloud water over the mountains of northern Colorado during wintertime storms. Part II: spatial distribution and microphysical characteristics. J. Clim. and Appl. Meteor., 25, 489-504.

Rogers, D.C., R.M. Rauber, L.O. Grant, 1986: Studies of wintertime storms over the Tushar Mountains of Utah. Report by Colo. State Univ. Ft. Collins to Utah Division of Water Resources, 50 pp.

Sassen, K., 1985: Supercooled liquid water in winter storms, 1985. Preliminary climatology from remote sensing observation. J. Wea. Modif., 17, 30-35.

Snider, J.B. and D. Rottner, 1982: The use of microwave radiometry to determine a cloud seeding opportunity. J. Appl. Meteor., 21, 1286-1291.

Solak, M.E., T.J. Henderson and R.B. Allan, 1984: Final report - data collection and analysis, volume three - ground based measurement systems, SCPP. Report by Atmospherics Inc. submitted to Bureau of Reclam., 70 pp.

Thompson, J.P. and A.B. Super, 1987: Wintertime supercooled liquid water flux over the Grand Mesa, Colorado. J. Wea. Modif., 19, 92-98.

THE BRIDGER RANGE, MONTANA, 1986-1987 SNOW PACK AUGMENTATION PROGRAM

James A. Heimbach, Jr.[1]
Montana State University
Bozeman, MT 59717

and

Arlin B. Super
Bureau of Reclamation
Montrose, CO 81401

Abstract

A winter orographic snow pack augmentation program was conducted for the benefit of a ski resort near Bozeman, Montana, during the winter of 1986-87. The operational goals were to help ensure a timely opening of the resort and to increase the snow pack, especially for the Christmas-New Year's holiday season. Seeding was from a single surface-based AgI generator located well up the west slope of the Main Bridger Ridge. Three hundred and eighty five hours were seeded during the period of 11 Nov. to the end of Feb. A research program was "piggy-backed" upon the operations to test the targeting effectiveness, to document the existence of supercooled liquid water, to examine the microphysical aspects of the seeding and to determine if the seeding increased the seasonal snow pack. Supercooled liquid water was documented and AgI was verified as crossing the Main Ridge by an acoustical ice nucleus detector. Analysis of sedimentation plate images suggested that aggregation and riming were important contributors to the rapid growth of crystals falling on the ski resort, the center of which was 4 km SE of the generator. Target-control analysis of snow course data suggested 35 to 50% additional seasonal snow pack within the target.

1. INTRODUCTION

The winters of 1984-85 and 1985-86 had low snow pack accumulations at the Bridger Bowl ski resort near Bozeman, Montana (MT). At the request of the local non-profit ski area, Montana State University planned and implemented a snow pack enhancement project using cloud seeding during the winter of 1986-87. The project's goal was to increase the snow pack, especially early in the winter to provide a timely opening of the ski area, and to have abundant snow for the Christmas-New Year's holiday season. The operations were based on research done in the same area from 1968 through 1972 during the randomized exploratory Bridger Range Experiment (Super and Heimbach, 1983, hereafter SH), and again in 1985 when physical experiments were conducted (Super and Heimbach, 1988).

SH found strong statistical evidence of a seeding signal over the Bangtail Ridge target area (see Fig. 1) for 700 mb and ridge top temperatures $\leq$-9C. Super (1986), in further a posteriori analyses of the Bridger Range Experiment data, found the largest seeding signals occurred in the 700 mb wind range of 240-300 deg. Precipitation data were not collected in support of the Bridger Range Experiment within the ski resort boundary; however, target-control analysis of independently collected snow course data indicated anomalously high snow water equivalents in the ski area at the end of the two winters the northern seeding site was operated.

During Jan. 1985 airborne measurements of microphysical parameters were made in seeded storms over the Bangtail Ridge to test hypotheses previously unaddressable due to budget and technical constraints (Super and Heimbach, 1988). Seeding in 1985 was from the southern of two sites used in the earlier experiment. Measurements confirmed targeting of the silver iodide (AgI) ice nuclei, and indicated increased ice crystal concentrations with greater estimated precipitation rates within seeded portions of some storms which had supercooled liquid water present.

[1]Currently at the University of North Carolina at Asheville.

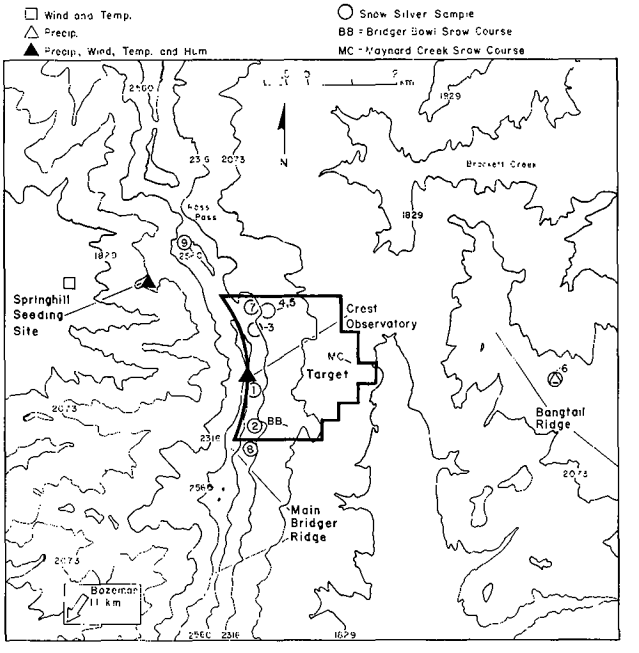

Fig. 1. Operations area for the 1986-87 Bridger Range winter orographic weather modification project. Elevations are in meters MSL.

2. OPERATIONS

Seeding during the 1986-87 winter was done with a single ground-based modified Skyfire generator burning a mixture of 3% by weight AgI complexed with NH_4I-acetone-water in a propane flame. About thirty grams of AgI were burned per hour. At -10C, a common temperature at the Main Ridge, the efficiency of the aerosol was found by Garvey (1975) to be 6×10^{13} ice nuclei g^{-1} AgI. The complex and generator were identical to those used in the Bridger Range Experiment and the 1985 experiment. The seeding site was the northern of two sites used in the earlier experiment and is labeled "Springhill Seeding Site" in Fig. 1. It was well up the west slope of the Main Ridge at an

elevation of 2121 m. The seeding generator was manually operated, requiring an operator on site 24 hours per day during any potentially seedable conditions.

The seeding criteria used during 1986-87 were:

1. Winds from 240-300 deg. true as measured at the Crest Observatory (Fig. 1), by pilot balloons released from the seeding site, or from observing the cloud base motion.

2. The Main Ridge Crestline had to be obscured in cloud.

3. After 1 Jan. the seeding site temperature had to be below -5C.

The first criterion was determined to be the optimal wind direction range for seeding from the 1970-72 randomized experiment. The second criterion assumed that supercooled liquid water would most likely be present when cloud base was below the crestline. The third criterion assumed that the utilized AgI complex becomes active in significant concentrations at or below -9C at crestline elevations as suggested by SH. Under average conditions this would correspond to below -5C at the seeding site elevation.

Seeding operations commenced on 11 Nov. 1986 and ceased 28 Feb. 1987, with the last seeded day being 24 Feb. To ensure the public welfare was maintained, suspension criteria were imposed. Seeding would have stopped if the Bridger Bowl snow course (see Fig. 1) showed 200% or more of normal snow pack (normal plus 100%) during Nov. and Dec. 1986, 125% in Jan. and normal in Feb. 1987. These criteria were not invoked due to the unusually low frequency of storms during the winter.

For the months Nov. through Feb. 94, 84, 99, and 107 h were seeded, respectively. November and the first ten days of Dec. had frequent storm conditions. From 10 Dec. to the end of that month precipitation events were limited. January and Feb. produced far less than the normal snow pack over the area. Fifteen days in Jan. had measurable precipitation at the seeding site, but many of these events could not be seeded due to inappropriate winds. February was dry until the thirteenth, and thereafter several good seeding periods occurred. By 1 Mar., Snow Survey measurements showed the snow water equivalent of several snow courses in southwestern Montana as low as 50% of normal.

3. ASSOCIATED RESEARCH PROGRAM

Four goals were addressed by an adjunct research program.

1. Test whether the resort area was targeted with AgI.

2. Document the occurrence of supercooled liquid water above the Main Bridger Ridge just upwind (west) of the ski area.

3. Examine the near-source microphysical characteristics of seeding.

4. Determine any departure from normal in the ski area snow water equivalent.

Because of the limited resources available for the research program, only surface observations were made, and some of these were limited to several storms in Jan. and Feb. Instrumentation at the Crest Observatory, located on the crestline forming the west boundary of the target area, consisted of the following:

(1) A National Center for Atmospheric Research (NCAR) acoustical ice nucleus counter (Langer, 1973) was used to monitor ice nuclei at -20C. Because background concentrations were consistently 0-1 L^{-1}, the acoustical counter was essentially an AgI detector.

(2) A Rosemount 871CB1 icing rate meter was mounted 8 m above the crestline. This device had a 0.64 cm diameter probe of 1.75 cm^2 cross-sectional area. An accumulation of 0.07 g ice (derived through wind tunnel tests) on this probe triggered a melting cycle which was logged on a strip chart. These icing events and the wind speed were used to estimate supercooled liquid water content, assuming unity collection efficiency. Because the actual collection efficiency will be less than unity for small cloud droplets and light winds, some underestimation of supercooled liquid water content can be expected.

(3) Wind speed and direction were measured at 10 m above the crestline by an anemometer and vane defrosted by heat lamps.

(4) Vertical ice particle flux was measured by a device described by Langer (1970). Ice particles were drawn isokinetically down a 3 mm capillary tube from a 2.5 cm diameter intake. The particles (or sometimes clumps of particles) were counted and continuously recorded in the manner of the acoustical ice nucleus counter.

(5) For selected storms, a photographic device produced 35 mm slides of ice particles collected on glass sedimentation plates exposed for known time intervals. Crystal images were manually sized and assigned habits. Contributions of the various habits to crystal concentrations and estimated precipitation rates were derived following the procedures of Holroyd (1987). The minimum discernable size was 0.12 mm. Smaller particles could be confused with dust and they contributed negligibly to the estimated precipitation.

(6) Air temperature and humidity were measured by a hygrothermograph in a weather shelter.

Besides the Crest Observatory measurements, ambient temperature and humidity, precipitation, surface wind, and winds aloft (from pilot balloons) were observed at the seeding site. The silver content of the snow pack was sampled soon after the seeding program terminated (see Sec. 6).

4. CASE STUDIES OF NEAR-SOURCE MICROPHYSICAL EFFECTS

Portions or all of ten seeded storms were sampled at the Crest Observatory during Jan.-Feb. Two case studies will be presented in detail to examine the presence of AgI, supercooled liquid water and microphysical (ice particle) characteristics. Microphysical characteristics are of particular interest because of concerns about limited time for ice particle nucleation, growth and fallout since the center of the intended target area was only about 4 km southwest of the seeding site (Fig. 1). The snow course analysis of SH strongly suggested that prior seeding from that site significantly increased snowfall in the ski area. However, the physical mechanisms involved were not well understood.

Recent work by Finnegan and Pitter (1987) indicates that ice nucleation can sometimes commence immediately downwind of the AgI generator at temperatures below -6C due to supersaturation produced by combustion of acetone and propane. Conditions required for this rapid nucleation often existed at the Springhill seeding site so high concentrations of tiny ice crystals may have formed essentially at the seeding site. Further, Takahashi et al. (1986) suggest that aggregation of small crystals could provide precipitable particles within several minutes.

4.1 13-14 February 1987

On 13 Feb. a storm started at approximately 1430 (all times Mountain Standard) and lasted until 0600 on the 14th. During its course, nine of the Crest Observatory hourly averaged wind directions were classed as variable ($\geq$180 deg. range over the hour). The other hours had averaged wind directions which ranged from 277 to 282 deg. true. The supercooled liquid water content could not be estimated because the anemometer cups were rimed during most of the storm in spite of the heat lamps focused upon them. However, the icing rate meter cycled more frequently between 0200 and 0300 than during any other hour sampled throughout the winter. The winds at the seeding site were variable or southeasterly, and 0 to 2 m s^{-1} during this storm.

The top portion of Fig. 2 shows a plot of ice nucleus concentrations derived from the acoustical counter and the seeded period for this case. The calculated concentrations (effective at -20C) include a x10 multiplication suggested by Langer (1973) to account for crystal losses in the cloud chamber. The peak concentrations reached $5x10^3$ L^{-1}. The jagged appearance of this plot is due to the logarithmic ordinate exaggerating the low concentrations. The discrete appearance over most of the plot corresponds to one count per minute, the digitizing interval, which converts to slightly over one ice nucleus L^{-1}. On this plot a concentration of zero corresponds to "0.3" L^{-1}. A total filter was put on the intake at 1940 and again at 2007 to insure the counter was working properly, i.e., not generating false counts. It was removed after a significant drop in ice nucleus detection rate was observed.

It is noteworthy that AgI was clearly detected at the Crest Observatory less than 4 h during the approximate 16 h seeded period. It was typical of the storms sampled that AgI was clearly at the Observatory only a fraction of the seeded period. Of course, the AgI plume may have been above or to either side of the single observing point when AgI was not being monitored. A much more elaborate sampling program would be required to test this supposition.

The bottom portion of Fig. 2 shows the vertical ice particle flux data which does not show a close correlation with the ice nucleus trace. This is likely because supercooled liquid water, which is believed necessary for the seeding to be effective, was not present until after 2000. Thereafter there is some correspondence with high ice nucleus concentrations although high vertical ice particle flux continued after the ice nucleus concentration decreased to background levels. It is unknown whether AgI existed at levels above the Crest Observatory after about 2220 or the high flux was a natural phenomenon. Unfortunately, vertical flux data are missing for the AgI plume registered between 1830 and 1900. The high ice nucleus concentrations corresponded with winds slightly north of west.

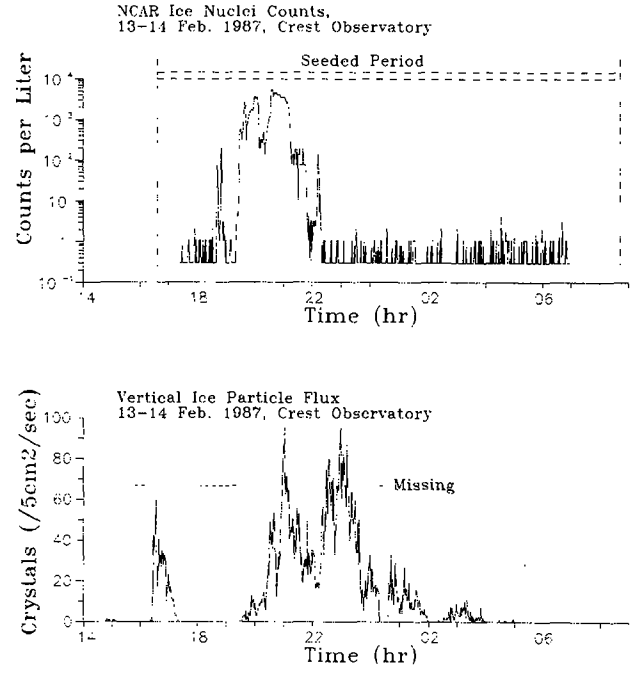

Fig. 2. Ice nucleus and vertical ice particle flux measurements for case of 13-14 Feb. 1987.

Figure 3 shows the results of analyzing the photographed sedimentation plates. The photography did not start until 1853 because warm temperatures during the earlier portion of the storm caused melting of the crystals on the plates. "Compact/hex" particles (plates) had the highest concentrations as would be expected from the ambient temperatures, which ranged from -2, at the start of the storm, to -7C on the Crest Observatory. It should be noted that previous airborne plume tracing over the Main Ridge Crest (Super, 1974) indicated that AgI often reached about 400-500 m above the crestline, where temperatures should be about 3C colder than at the Crest Observatory. One would expect plates and/or needles in this regime (Magono and Lee, 1966), and

during portions of this relatively warm storm higher concentrations of linear crystals were seen than in any other storm sampled. Aggregates contributed most of the precipitation (see bottom of Fig. 3). These aggregates were made up of plates and linear particles, with aggregates of the latter being observed in the later portions of the storm.

Although the Crest Observatory was successfully targeted for part of this storm, the AgI may not have been highly effective for two reasons. First, supercooled liquid water was not evident during much of the plume impactμ and second, the temperatures were warmer than considered optimum for ice nucleation with the AgI complex used. Aggregation of small particles was observed during AgI plume detection, giving greater terminal velocities. This aggregation supports the concept of a near-source seeding signal.

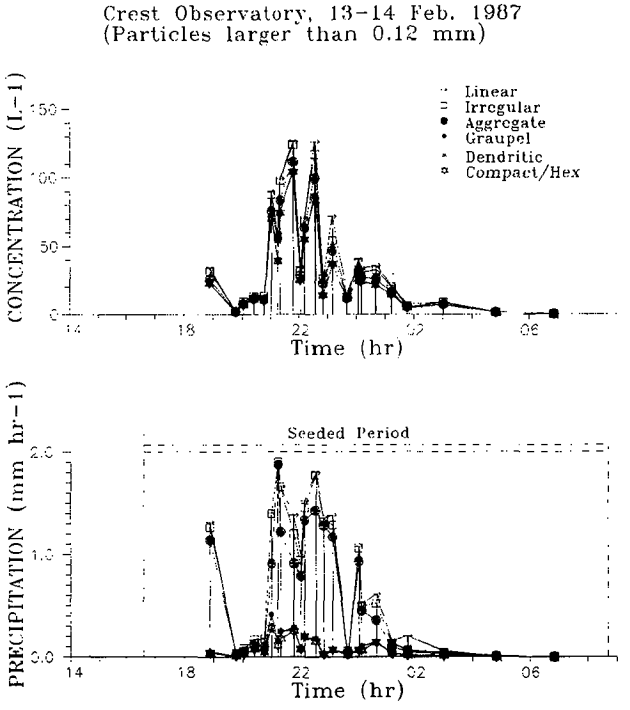

Fig. 3. Ice crystal concentrations and estimated precipitation contributions from six habit classes for 13-14 Feb. 1987.

4.2 22 February 1987

A storm which was observed at the Crest Observatory during its entire lifetime started in the early morning of 22 Feb. Associated with this storm was northwesterly flow aloft which steered a weak frontal system over Montana. Four hours had variable winds at the Crest Observatory, and the remainder were west to west-northwesterly. The hourly speeds ranged from 4 to 9 m s^{-1}, lower than typical. Very high ice nucleus concentrations were detected for over an hour. Figure 4 shows a time plot of ice nuclei and the seeded period. After the time of highest concentrations, there was a lingering period of relatively high ice nucleus counts which could represent a residual or a limited transport from the generator.

Supercooled liquid water was observed from approximately 0830 to 1200. The peak hourly liquid water content according to the Rosemount device was 0.04 g m^{-3} between 0900-1000. Two Rotorod samples (see Rogers et al., 1983) gave contents of 0.07 and 0.06 at 0910 and 1016 respectively. Rimed particles were seen prior to 0830, indicating supercooled liquid water existed above the Crest Observatory.

Figure 4 also shows the vertical ice particle flux trend during the storm. The flux was variable as was characteristic of all the storms sampled. In spite of this variability, some covariability with ice nuclei is apparent, with the highest flux corresponding to the period of AgI plume detection.

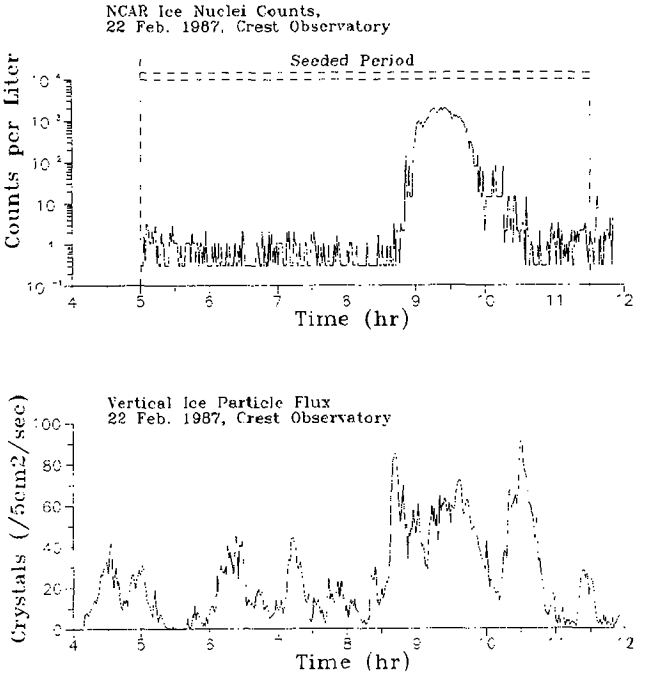

Fig. 4. Ice nucleus concentrations effective at -20C and vertical ice particle flux for 22 Feb. 1987.

Figure 5 shows the concentrations and estimated precipitation rates derived from the 14 photographs taken during the course of the storm. Both plots show an apparent response to the seeding although there is some natural variability. The highest ice particle concentrations and precipitation rates occurred between 0830-1030, in close agreement with the elevated ice nucleus counts of Fig. 4. The Crest Observatory temperature averaged -10C during the seeded period which would be in the plate growth zone (Magono and Lee, 1966). The greatest concentrations were in the "compact/hex" category meeting the expectation that the ice particles grew at temperatures near those observed. During the period when high ice nucleus concentrations were detected, higher plate concentrations were found, and though not evident from Fig. 5, the aggregates contributing most of the precipitation were made up mainly of plates and irregular crystals.

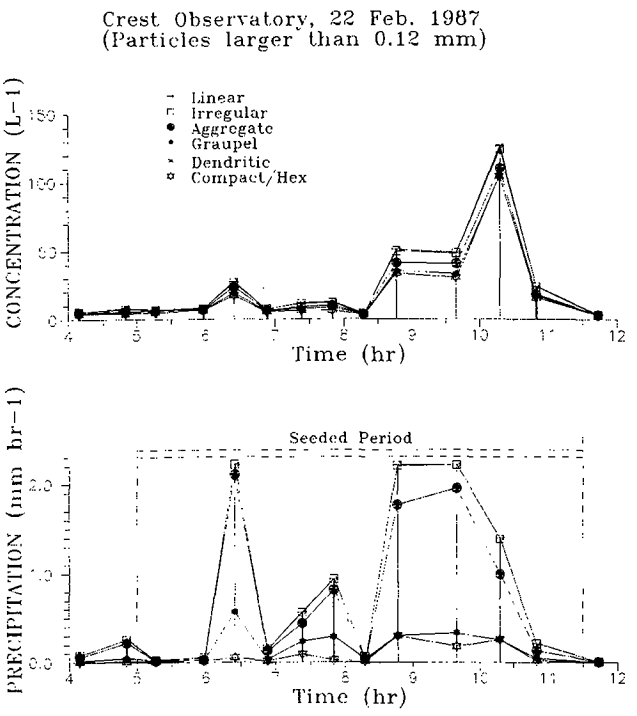

Fig. 5. Ice crystal concentrations and estimated precipitation contributions from six habit classes for 22 Feb. 1987.

4.3 Summary of Microphysical Observations

For a majority of the cases sampled at the Crest Observatory, temperatures were in the range which would produce plates or needles, i.e. -4 to -12C (ibid.). Targeting of the AgI at the Crest Observatory was not always successful, but in those cases when it was, increased ice particle fluxes were often associated with the AgI plumes. Photographic evidence showed increases in plates and/or tiny (<0.3 mm) particles. There were not enough needles or columns observed to give any conclusions regarding their production by AgI. In some instances there were increases in the number of aggregates associated with the AgI plume, and these had a high proportion of plates.

The two microphysical hypotheses for increasing precipitation over the target area were: 1) more ice particles would be generated, and 2) though not necessarily large enough to fall out individually, aggregation of these crystals would produce particles large enough to fall within the target area. The hypotheses appear to have been borne out for at least some of the seeded periods. Photography showed that during periods of significant snowfall rates, there was riming of the crystals, indicating that even with seeding, not all the available supercooled liquid water was being processed and some accretional growth was helping the precipitation process. Accretional growth was not anticipated as being significant, however in one case, 16 Feb., precipitable particles were associated with the production of many small graupel-like particles (0.5-1.5 mm). Above background ice nucleus concentrations were detected on the 16th with the highest concentration occurring during the initial portions of the storm.

5. SUMMARY OF SEASONAL SUPERCOOLED LIQUID WATER CHARACTERISTICS

Out of a total of 2310 hours sampled by the Rosemount device from 21 Nov. through 28 Feb., 155 hrs or 6.7% had supercooled liquid water detected. One hundred and nine hours, or 70% of the hours having liquid water, had ridge top winds between 240-300 deg. true, which was the range of winds specified for seeding. Twenty-seven hours, or 17%, had winds with an easterly component. Reference to Fig. 1 shows that upward motion and associated liquid water production might be expected for both easterly and westerly flow over the Main Ridge. Eighteen hours, or 12% of the hours having supercooled liquid water, had variable winds at the Crest Observatory.

Most hourly mean values of supercooled liquid water content at the Crest Observatory were 0.05 g m^{-3} or less with occasional values up to 0.10 g m^{-3}. As previously noted these are believed to be underestimates due to the assumed unity collection efficiency for the Rosemount probe. Also, one might expect larger contents at higher elevations since the lower levels could be affected by riming on surface features. Such a vertical gradient was suggested in computer simulations for the Park Range of Colorado (Rauber and Grant, 1981).

6. SAMPLING OF SNOW SILVER CONTENT

Nine snow samples were taken from eight snow pits during 6 to 12 March 1987, soon after seeding terminated. Trace silver analysis was done by the Desert Research Institute, Reno, Nevada. Table 1 lists the results in the order of collection, with the locations keyed on Fig. 1. Background from Table 1 is about 10^{-11} g Ag mL^{-1} which is similar to that found earlier in the Bridger Range Randomized Experiment. Samples 4 and 5 corresponded to snow layers that fell during Nov.-Dec. and Jan.-Feb., respectively, as identified by a snow and avalanche expert who monitored the ski area snow pack throughout the winter.

Table 1. Results of snow silver analyses (10^{-12} g Ag mL^{-1}).

Sample	Silver Content	pH	Elev. (m)	Remarks
1	19.4	4.9	2451	
2	40.4	4.9	2393	
3	91.3	4.6	2323	
4	78.8	4.9	2265	Nov.-Dec. layer
5	69.0	4.2	2265	Jan.-Feb. layer
6	48.9	4.9	2216	
7	41.3	5.1	2423	
8	13.0	4.9	2438	Detection limit
9	13.0	4.7	2423	Detection limit

Reference to Fig. 1 shows that the lowest (detection limit) values occurred on the ends of the N-S sampling line. The highest values were essentially ESE-SE of the seeding site, but even sample 2 in the southern portion of the target was well above background as was the single sample on the Bangtail Ridge. The relatively low value of sample 1, taken just below the Crest Observatory, is puzzling. However, it should be noted that this snow pit was on a very steep slope, sheltered

by trees upslope and to the south. The other pits were in areas having less slope and were more exposed.

7. TARGET-CONTROL ANALYSIS OF SNOW COURSE DATA

Two snow courses are maintained by the Soil Conservation Service Snow Survey in the ski resort target area. These were used in the analysis presented by SH. One is named Bridger Bowl, indicated as "BB" in Fig. 1, with an elevation of 2210 m MSL. Unfortunately, in 1986, extensive logging was carried out to the edge of this course. There was visible evidence of snow scouring and deposition on the course during early 1987 due to the increased exposure. Analysis of the 1 March point-by-point variability of the ten sampling point course revealed that in 1987 individual sampling points had much greater departures from the course mean than ever observed since the snow course was first sampled in 1965. Accordingly, in the authors' opinion, the Bridger Bowl snow course is no longer suitable for evaluation of cloud seeding. The other snow course within the target is Maynard Creek ("MC" in Fig. 1), located at 1893 m MSL. This site has been sampled since 1968 but was moved prior to the winter of 1974-75. Only post-1974 measurements are used in the analysis to follow to avoid the uncertainties of adjusted data.

The target-control analysis used arithmetic mean snow water equivalent data from groups of snow courses outside the range of seeding influence to predict that of Maynard Creek. Linear least-squares fits, and correlation coefficients between target and control data were derived using nonseeded winters. Estimates of what would have occurred naturally over the target were derived from the regression line. Table 2 summarizes the target-control analysis for the 1 Mar. measurements, the first made following the last day of seeding, 24 Feb.

Table 2. Highlights of 1 Mar. Maynard Creek target-control analysis. Control years are 1975-86.

Control Course(s)	Correlation Coefficient	Residual Inches SWE	Residual %
1,2,3,4	0.927	1.9	35.4
1	0.958	2.1	40.9
1,4,5,6	0.987	2.4	50.2

1. Sacajawea 3. New World 5. Four Mile
2. Shower Falls 4. S. Fork Shields 6. Grasshopper

Three sets of control courses are shown. Sacajawea alone and the means of the combined group Sacajawea, Shower Falls, New World and South Fork Shields are presented because these same courses were used in the analysis of SH. Figure 6 shows the results of the analysis using Sacajawea as the sole control. This suggests an additional 40.9% snow water equivalent due to seeding. This is the largest residual in Fig. 6 and amounts to an additional 2.1 inches snow water equivalent. Sacajawea, the nearest available control course, is approximately 6.2 km NNW of Maynard Creek. Both of these courses are on the east slope of the Main Bridger Ridge and are about the same altitude: 1996 m MSL for Sacajawea and 1893 m MSL for Maynard Creek.

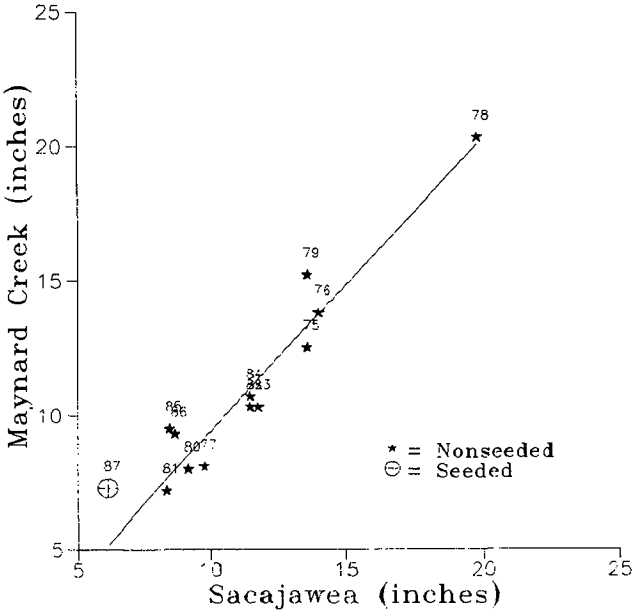

Fig. 6. Maynard Creek versus Sacajawea snow course snow water equivalent accumulations for 1 Mar., 1975-87.

Figure 7 shows a target-control analysis for 1 Mar. using the group of controls whose average snow water equivalent was best correlated with Maynard Creek out of all possible combinations of snow courses within 100 km. There is less scatter than in Fig. 6 indicating a better predictability as quantified by the correlation coefficients in Table 2. Figure 7 suggests a 50.2% snow water equivalent increase due to seeding, corresponding to 2.44 inches additional snow water equivalent.

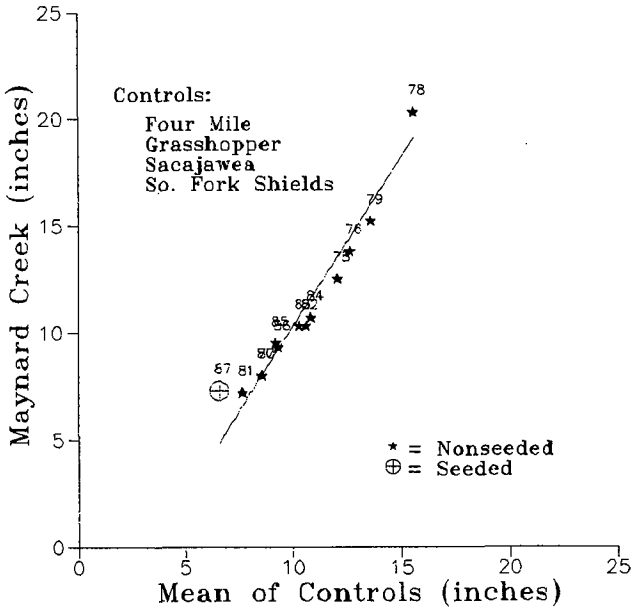

Fig. 7. Maynard Creek snow course snow water equivalent accumulations of 1 Mar. 1975-87 versus the average of Sacajawea, South Fork Shields, Four Mile, and Grasshopper.

It is noteworthy that 1 Mar. 1986 had the second lowest snow pack recorded at Maynard Creek. A number of snow courses in the area had the lowest snow pack of record. The suggested increase associated with the 1986-87 winter seeding is particularly encouraging in view of the exceptionally dry winter.

8. DISCUSSION

The 1986-87 seeding operation attempted to target the Bridger Bowl ski resort which was limited in size, existing on parts of four sections. It's center was only 4 km SE of the seeding site. Previous research detected a strong seeding signal further downwind over the Bangtail Ridge 5 to 20 km E of the Main Ridge. Analysis of snow course data from the period of randomized seeding strongly suggested a seeding signal was also present in the ski resort for the two winters an AgI generator was operated from the same site used during the 1986-87 winter.

Although previous research gave reason for optimism regarding the potential success of the 1986-87 operations, there were questions concerning the targeting of the resort, the frequency of seedable conditions, and how ice particles resulting from seeding could grow to precipitable sizes so close to the seeding site. Measurements made during the 1986-87 winter documented targeting of the AgI and the existence of supercooled liquid water above the Crest. Evidence was found of small seeding-induced particles aggregating to larger particles. Also, it was observed that particles sometimes became rimed enough to enhance their fall speed.

The winter of 1986-87 produced anomalously low snow packs over all of Montana, and several snow courses had record lows late in the winter despite good accumulations in Nov. and Dec. In view of the regionally low snow water equivalent, the increase suggested at the Maynard Creek snow course within the target area is very encouraging. Unfortunately, the logging next to the Bridger Bowl snow course rendered that site unsuitable for a historical target-control analysis. The use of Sacajawea, the nearest snow course, as a control suggested about a 40% increase at Maynard Creek due to seeding. This indicated percentage increase is approximately double that found in the Bridger Range Experiment which employed 50:50 randomization.

Targeting of the AgI was shown to be effective for at least part of the operations by the ice nucleus detector. The snow silver analyses indicated silver concentrations well above background in the ski area and at the single point sampled downwind. The snow silver samples showed a pronounced north-south gradient with the highest silver contents being east-southeast to southeast of the generator. Increased silver content doesn't prove that the seeding modified snowfall as scavenging of AgI by natural snowfall can enhance the snow silver content. However, lack of enhanced silver levels in the target area would indicate failure to target the seeding material.

The periods with highest ice nucleus concentrations detected at the Crest Observatory were associated with some northerly wind component or variable directions. West through west-southwest winds were often found to have several ice nuclei per liter effective at -20C, well above background levels which ranged from 0 to 1 L^{-1}. The elevated ice nucleus concentrations could have been from limited transport from the generator, or residuals from previous seeding. This made control periods difficult to define. Targeting assumed low-level terrain forcing unless northwesterly winds were present. During several experiments, the time from generator start to first detection of ice nuclei at the Crest Observatory, just 3 km from the seeding site, was found to be 15 to 25 min.

The photography of 22 Feb. suggests that an abundance of plates was associated with AgI seeding with a Main Ridge temperature of -10C, a typical value during winter storms. Aggregates of these plates provided a large proportion of the estimated precipitation accumulation. On 13-14 Feb. a similar aggregation of plates was associated with high ice nucleus concentrations. Later in this case the aggregates were of linear particles. Another mechanism which could allow seeding to provide precipitable ice particles within a few kilometers of the generator could be growth by riming. This mechanism was observed on 16 Feb. when many small graupel-like particles with diameters from 0.5 to 1.5 mm were collected on the sedimentation plates.

In summary, the limited research program yielded several indications supportive of the hypothesis that seeding increased the target area snow pack. The AgI plume was detected on the Main Ridge just upwind of the target on several occasions. Increased ice particle concentrations and snowfall rates were sometimes associated with the AgI plume at the Crest Observatory. Cross-wind sampling of the snow silver content revealed high levels downwind (ESE and SE) of the generator in the target area, decreasing to background levels on the north and south ends of the sampling line. Most important, target-control analysis of seasonal snow course measurements indicated approximately 40% more snow water equivalent in the target than predicted from nonseeded winters.

ACKNOWLEDGEMENTS

T. Abelin, the manager of Bridger Bowl ski resort, is gratefully acknowledged for his encouragement and facilitating many details. G. Langer, the inventor of the acoustical ice nucleus counter contributed his expertise and loaned some equipment. The Division of Atmospheric Resources Research, U.S. Bureau of Reclamation, loaned some key pieces of research equipment. Support for operations was from the Bridger Bowl Ski Resort and the Montana Science and Technology Alliance (contract no. 86-045). Research aspects were supported by National Science Foundation Grants ATM-8413143 and ATM-8613604.

REFERENCES

Garvey, D.M., 1975: Testing of cloud seeding materials at the Cloud Simulation and Aerosol Laboratory, 1971-1973. J. Appl. Meteor., **14**, 883-890.

Finnegan, W.G. and R.L. Pitter, 1987: Rapid ice nucleation by acetone-silver iodide generator aerosols and implications to winter orographic seeding strategies. Proceedings of 11th Conf. on Weather Modification, 6-9 October, Edmonton, Alberta, Canada, 9-10.

Holroyd, E.W., 1987: Some techniques and uses of 2D-C habit classification software for snow particles. Accepted for publication in J. Atmos. Ocean. Tech., **4**.

Langer, 1970: Counter for number of snowflakes falling per unit area. Proceedings of Conf. on Cloud Physics, Ft. Collins, CO, Aug. 24-27, 105-106.

_____, 1973: Evaluation of NCAR ice nucleus counter. Part I: Operation. J. Appl. Meteor., **12**, 1000-1011.

Magono, C. and C.W. Lee, 1966: Meteorological classification of natural snow crystals. J. Fac. Sci., Hokkaido Univ. 2:321-325.

Rauber, R.M. and L.O. Grant, 1981: Microphysical processes and weather modification potential of two stably stratified orographic storms. Extended abstracts, Eighth Conf. on Inad. and Plan. Wea. Mod., Oct. 5-7, Reno, NE, 58-59.

Rogers, D.C., D. Baumgardner and G. Vali, 1983: Determination of supercooled liquid water content by measuring rime rate, J. Clim. Appl. Meteor., **22**, 153-162.

Super, A.B., 1974: Silver iodide plume characteristics over the Bridger Mountain Range, Montana. J. Appl. Meteor., **13**, 62-70.

_____, 1986: Further exploratory analysis of the Bridger Range winter cloud seeding experiment. J. Clim. Appl. Meteor., **25**, 1926-1933.

_____, and J.A. Heimbach, Jr., 1983: Evaluation of the Bridger Range cloud seeding experiment using control gages. J. Clim. Appl. Meteor., **22**, 1989-2011.

_____, and _____, 1988: Microphysical effects of wintertime cloud seeding with silver iodide over the Rocky Mountains. Part II: Observations over the Bridger Range, Montana. J. Appl. Meteor., submitted.

_____, B.A. Boe, and J.A.Heimbach, Jr., 1988: Microphysical effects of winter cloud seeding with silver iodide over the Rocky Mountains. Part I: Experimental design and instrumentation. J. Appl. Meteor., submitted.

Takahashi, T., C. Inoue, Y. Furukawa, T. Endoh and R. Naruse, 1986: A vertical wind tunnel for snow process studies. J. Atmos. Ocean. Tech., **3**, 182-185.

SEEDING PATH AND THE SEEDING START TIME FOR THE HAIL SUPPRESSION ROCKETS

Nenad M. Aleksic
Institute of Meteorology
University of Belgrade
11001 Belgrade, Yugoslavia

and

Zlatko Vukovic
Hydrometeorological Institute of SR Serbia
Kneza Viseslava 66
11000 Belgrade, Yugoslavia

ABSTRACT: A study has been conducted to determine the operational suitability of certain cloud seeding rockets used in Yugoslavia. Examination of the properties of hail suppression rockets used in Serbia shows that all of them have seeding paths that should be extended for about 1 km.

INTRODUCTION

The essence of the Soviet hail suppression concept, operationally applied in Yugoslavia, is rapid and massive seeding of the assumed hail embryo formation region (EFR). With some variations, depending on the type of the cloud seeded, the general goal (Bibilishvili et al., 1981) is to directly inject reagent into the layer bounded by -5°C and -15°C isotherms, preferably into the (-8°C, -12°C) layer.

In Yugoslavia, the seeding is performed by the rockets. Characteristics of the rockets used in the Socialist Republic of Serbia are summarized in the Table 1. These values are somewhat arbitrary, chosen after the performances of the Soviet models.

The purpose of this study was to check them with regard to the operational suitability. Particularly, we were interested in the seeding paths and the timing of the seeding.

Both of these values are supposed to satisfy two constraints. First, the rocket should seed on the segment of the trajectory through the targeted layer. Second, during the time available for the reagent activation, concentration of the dispersed reagent should not fall below the prescribed value of 0.1 cm^{-3}. Otherwise, the seeding path should be shortened or the total number of active nuclei released from the rocket increased.

2. BALLISTIC CONSIDERATIONS

Segments of trajectory through the designated layer are determined by the position of the target layer and the ballistic properties of the delivery vehicle.

2.1 Position of the Target Layer

Heights of the isotherms of interest vary from month to month. Because of this, all the calculations were repeated for each month of the hail suppression season, using mean monthly values of isotherm heights in the free atmosphere.

In-cloud temperatures are higher than those in the surrounding atmosphere (at least in updrafts in the lower part of the cloud). To account for this factor, we have lowered all the isotherm heights for an arbitrary value of 200 m.

The values obtained in this way are assumed to give altitudes of the in-cloud target layer above the mean sea level. Additional factor to be considered is that effective layer heights may be considerably lower, since the altitudes of launchers range up to 1400 m above the sea level. Thus, for each month of the season we have worked with a range of effective layer heights, using 200 m intervals for launching pad altitudes.

2.2 Trajectory Calculations

For all calculations we have used interpolated values from the empirical rocket trajectories, given by Jeftic (1986).

For each type of the rocket and for each possible position of the target layer, we have calculated the length of the trajectory whose top is in the middle of the layer. There were other possible choices. However, according to the seeding concept, the seeding is performed in the updraft area, and reagent released near the upper boundary of the layer would be carried outside too fast to be effective.

Table 1. Rocket Characteristics

ROCKET TYPE	TG-10	TG-5	SAKO-6	PP-6
Caliber (mm)	72	72	80	72
Length (mm)	1050	1030	1096	950
Weight (kg)	4.35	6.2	5.7	5.75
Weight of the pyrotechnic mixture (g)	400	400	400	400
Percentage of AgJ	15	15	25	20
Activity at $-10^{o}C$ (g^{-1})	$1.2x10^{12}$	$1.2x10^{12}$	$1.7x10^{12}$	$3.0x10^{12}$
Vertical range (m)	8500	5000	5200	5200
Horizontal range (m)	10000	4000	4000	4000
Elevation range (deg)	45-85	45-85	45-85	55-85
Seeding start time (s)	5-25	9-18	8-22	6-16
Seeding duration (s)	27	20	14	20
Seeding path (km)	6-7	3-3.5	2-2.5	2.5-3

The starting time for the seeding was determined as the time when the rocket reaches lower base of the layer.

Calculations were done both for ($-8^{o}C$, $-12^{o}C$) and ($-5^{o}C$, $-15^{o}C$) layers. An example is shown in the Table 2, and the resume of all the calculations in the Table 3.

The Table 3 shows that for all the rockets seeding paths should be extended for about 1 km. As for the seeding start times, they may be considered to be adequate.

It should be mentioned that empirical rocket trajectories we used for calculations were determined from the measurements in the free atmosphere. In-cloud circulations may cause deviations we did not account for. In fact, deviations from these trajectories occur even in the free atmosphere. In our opinion, however, this is a problem to be handled by the increased number of rockets used for particular seeding and not by changing the seeding path or seeding start time of the individual rocket.

3. SUFFICIENCY OF THE REAGENT CONCENTRATION

Reagent released from the rocket has a limited time to induce formation of hail embryos. This time is mainly determined by the cloud dynamics. due to the reagent being carried outside EFR. Sljnn (1971) estimates this time as being around 10^{2}s. It is important that during this time concentrations of the dispersed reagent remain above or at least in the prescribed range of 0.1-1 cm^{-3}. Otherwise, the seeding path should be shortened.

Dispersion of the reagent is estimated after WMO (1980), by the formula

$$\sigma = \sigma_0 + C\epsilon^{1/2} t^{3/2}$$

σ is the spread parameter, σ_0 the initial spread, t time from the release and C constant (~ 0.25). ϵ is the turbulent dissipation. For organized convention it has representative values in the range of 100-500 $cm^{2}s^{-3}$. Neglecting σ_0, which has the order of a few meters, for this range of ϵ and t = 100 s, σ will range from 25 to 60 m. It appears that we may use 50 m as the representative value of the spread parameter.

If we adopt the Top Hat model of dispersion, the spread parameter may be interpreted (WMO, 1980) as the radius of the uniformly seeded cylinder. In the present context, length of this cylinder is approximately equal to the length of the seeding path.

From the Tables 1 and 3, the rocket TG-10 carries

Table 2. Seeding path and the seeding start time for the ($-8^{o}C$, $-12^{o}C$) target layer and the rocket TG-10 as a function of the launching pad altitude for the July.

Altitude (m)	Start time (s)	Seeding path (m)
0	17	3100
200	15	3300
400	13	4800
600	16	2850
800	14	3900
1000	12	4850

Table 3. Current and calculated values of seeding start time and seeding path

Rocket type		TG-10	TG-5	SAKO-6	PP-6
Current valve	Seeding start time (s)	5-25	9-18	8-22	6-16
	Seeding path (km)	6-7	3-3.5	2-2.5	2.5-3
For the (-8^{o},-12^{o}) layer	Seeding start time (s)	12-17	15-22	16-20	10-20
	Seeding path (km)	3-5	1-2	1-2	1.5-2.5
For the (-5^{o}.-15^{o}) layer	Seeding start time (s)	7-12	11-19	8-14	8-16
	Seeding path (km)	5-8	1-2.5	1.5-3.5	2-4

the smallest number of the active nuclei (4.8×10^{14} at $-10^{o}C$) and requires the longest seeding path (8 km). According to the considerations described above, at the end of the time available for the reagent activation, concentration of the reagent released from this rocket will be above 7 cm^{-3}, which is more than required. This being the case, the sufficiency condition is also satisfied for the other types of the rockets.

4. CONCLUSIONS

Our analysis has shown that hail suppression rockets in the use by Serbian hail suppression system are adequate for the seeding operations as far as the seeding start time and the amount of reagent carried are concerned. For all types of the rockets, the seeding paths should be extended for about 1 km.

During this study we also noted that long-range rocket TG-10 might be uneconomical for the use on the launchers with altitude above 800 m. In these situations, TG-10 is able to seed the target layer only on the rising or descending branch of its trajectory, thus wasting much of the reagent.

REFERENCES

Bibilishvili, N.Sh., Burtsev, I.I. and Seriogin, Yu.A., 1981: "Manual on the Organization and Execution of the Hail Suppression Activities" (in Russian). Gidrometeoizdat, Leningrad, 168 pp.

Jeftic, M., 1986: "An Overview of the Operational and Technical Characteristics of the Hail Suppression Rockets" (in Serbian). Hydrometeorologic Institute of S.R. Serbia, 14 pp. (available upon request from the authors).

Slinn, W.G.N., 1971: "Time Constants for Cloud Seeding and Tracer Experiments. J. Atmos. Sci., 28, 1509-1511.

WMO, 1980: "Dispersion of Cloud Seeding Reagents". Precipitation Enhancement Project, Rep. No. 14, Weather Modification Programme, WMO, Geneva, 28 pp.

SOME RESULTS RELATED TO THE SUPPRESSION HAIL PROJECT IN ALBACETE

J.L. Sanchez *; M.L. Sanchez **; A. Castro *; M.C. Ramos **

* Dpto Fisica. Lab. Fisica de la Atmosfera. Univ. de Leon. Spain
** Dpto Fisica Aplicada I. Fac. de Ciencias. Univ. de Valladolid. Spain

ABSTRACT

A characterization of unseeded hailstorms and a comparison between seeded and unseeded hailstorms observed in the protected area of the province of Albacete (Spain) have been carried out by the use of the t-statistic distribution. For this case study several direct parameters gathered by meteorological radar and the growth factor as an indirect parameter have been selected. The results indicate that the only parameter able to distinguish the behaviour of both types of hailstorms was the growth factor which was 25% less for seeded hailstorms which is significant at the 5% level. Based on these results, a linear correlation between the growth factor and remaining radar variables has performed. The final results suggest a better correlation between most variables for the unseeded than for seeded hailstorms.

1. INTRODUCTION

Direct and indirect losses by hail on crops are dramatic around the world (Dessens, 1986; Romero and Balasch, 1985; Humphries et al.,1987). This problem is particulary important in Spain since our country mainly depends on its agricultural production.

The devastating effects of hail have focused attention on the use of weather modificaction techniques to alleviate the problem. Therefore, different countries have initiated a wide range of projects in order to study hailstorms and to design adequate technological methods for suppressing hail (Colino, 1987; Dessens, 1987; Henderson, 1975).

There is a lot of controversy over the effectiveness of hail suppression projects developed in different countries. The main part of the projects described in the literature show positive benefits for the hail suppression programes (Dessens 1987; Santolaya and Santos, 1987). However, according to the WMO, there is no scientific experimental evidence supporting the effectiveness of hail suppression (WMO, 1983, 1985, 1986). Despite this, the WMO recognizes the need for an important advance in seeded technologies and it encourages the development of experimental projects conducted to analyse the results obtained.

For the years 1978 to 1983, and from the period June through September, a hail suppression program was operated in the province of Albacete (Spain). The protected area was about 600 km^2. This area was chosen by the Ministry of Agriculture on the basis of historical data concerning hail losses encurred by insurance companies. During these operations hailstorms were seeded by aircraft flying at the -10 °C altitudes. Ejectable AgI pyrotechnics were used as the seeding material. The aircrafts were flown directly into the cloud masses based on vectors from a meteorological radar located at the control site in the protected area. The cloud with reflectivity values near 45 dbz and with vertical development greater than 6,500 meters, were considered to contain a risk of hail. When the reflectivity was higher than 35 dBZ at 6,500 meters then the clouds were seeded, subsequently the spatial and temporal evolution of the radar echoes were followed and stored in the computer. Therefore, an extensive collection of information relative to the most common radar parameters was available to study the clouds. However,

neither microphysical observations of the clouds nor information on hail at the ground (i.e., size spectrum, kinetic energy...) were available.

The purpose of this paper is to present some of the results obtained concerning the main radar characteristics of the unseeded hailstorms occuring over the protected area (or in the nearby areas), to compare the characteristics and identify any statistical differences. To do this, we have used some of the most relevant radar parameters. Also, a comparison has been performed by using the "growth factor" of hailstorms proposed by Goyer (1975).

2. DATA

From all the data recorded by the radar/computer system, we have focused our attention on the clouds with hail risk. Therefore, we have selected only those clouds with reflectivities greater than 45 dBZ. In addition, we have only considered clouds with lifetimes greater than 10 minutes. The interval of time was chosen as a compromise between obtaining enough statistical data and having echo lifetime with sufficient duration in order to compare the results of seeded versus non seeded clouds. (Foote and Mhor, 1979)

For this case study, we have chosen the following direct parameters measured by the radar:

- HM maximum height of the hailstorms (Km)
- H10 height related to the 10 dBZ echo (Km)
- T lifetime of hailstorms (min)
- MR maximum reflectivity (dBZ)
- HMR height corresponding to the maximum reflectivity (Km)
- X total distance traveled by the hailstorms (Km)

As an additional part of this preliminary study, we have included an factor which takes into account the vertical growth rate of hailstorms. The factor chosen and which is referred to as GF, is defined as follow for seeded and unseeded hailstorms (see Goyer for details):

$$GF = T_1 / T_0$$

If 't_0' is the time of initiation of seeding for seeded storms, the time is perfectly known, but t_0 for unseeded storms is defined as the time when echo tops first reached 10 Km.

Then:

- 'T_0' (Km.min), the initial hailstorm magnitude, is defined by the echo top integrated from 20 min before, to the time of initiation of seeding (t_0).

- 'T_1' (Km.min) is the total storm magnitude, and it is defined by its echo top integrated from 20 min before 't_0' to the time the echo drops below 7.6 Km.

3.CHARACTERISTICS OF UNSEEDED HAILSTORMS

Table 1 shows the arithmetical mean, the arithmetical standard deviations, the maximum and minimum values of each radar variable and the geometrical average and the standard deviations. There were 43 hailstorm cases studied.

PARAMETERS	M_a	σ_a	MAX	MIN	M_g	σ_g
HM	11.60	1.30	15.0	9.4	11.62	1.13
H10	10.70	1.43	14.3	9.5	10.71	1.13
T	71.50	62.08	282.0	10.0	57.43	2.38
MR	56.55	7.51	68.0	45.0	56.21	2.38
HMR	3.41	1.90	7.0	0.6	2.80	1.94
X	46.14	31.25	148.0	7.0	39.40	1.95
GF	5.71	3.99	22.2	2.9	4.85	1.95

Table 1 : arithmetic average (M_a), arithmetic standard deviation (σ_a), maximum (MAX), minimum (MIN), geometric average (M_g), and geometric standard deviation (σ_g) for unseeded hailstorms.

The examination of the frequency histograms revealed the tendency of the values of most of the variables to be lognormally distributed. Using Probits analysis, (Murray, and Spiegel, 1961), the figure 1 shows the cumulative frequency distribution of each variable expressed in terms of the standardized "u" variable versus the logarithms of the values *. The linear plots obtained for each variable are indicative of the lognormality of the values. The correlation coefficient related to each linear fit was never below 0.99 as may be seen in Table 2.

* u is defined by $u = (L x - m)/\sigma$, where x is an individual storm value (either GF, MR, T, X, H10 or MR), m is the mean of that value over all storms, and σ is the standard deviation of that value over all storms.

PARAMETERS	r	p	V(50)	V(95)	V(5)
HM	0.990	0.1188	11.70	14.23	9.62
H10	0.998	0.1137	10.79	13.00	8.95
T	0.991	0.8077	52.65	198.80	13.94
MR	0.990	0.1105	55.50	65.56	46.30
HMR	0.998	0.4554	3.52	7.4	1.67
X	0.995	0.6451	37.23	107.6	12.89
GF	0.995	0.4861	4.61	10.25	2.07

Table 2 :correlation coefficient (r), slope (p) and values for different percentiles related to unseeded hailstorms.

In order to check the validity of the hypothesis of the lognormal frequency distribution, the Kolmogorov-Smirnov test was performed. The values obtained for the statistics confirmed the validity of this assumption at a significance level below 5%. Based on these results the geometric average and the geometric standard deviations have been determined to properly characterize the frequency distributions.

After looking at Figure 1 and the results related to different percentiles (see Table 2), the following general considerations can be drawn.

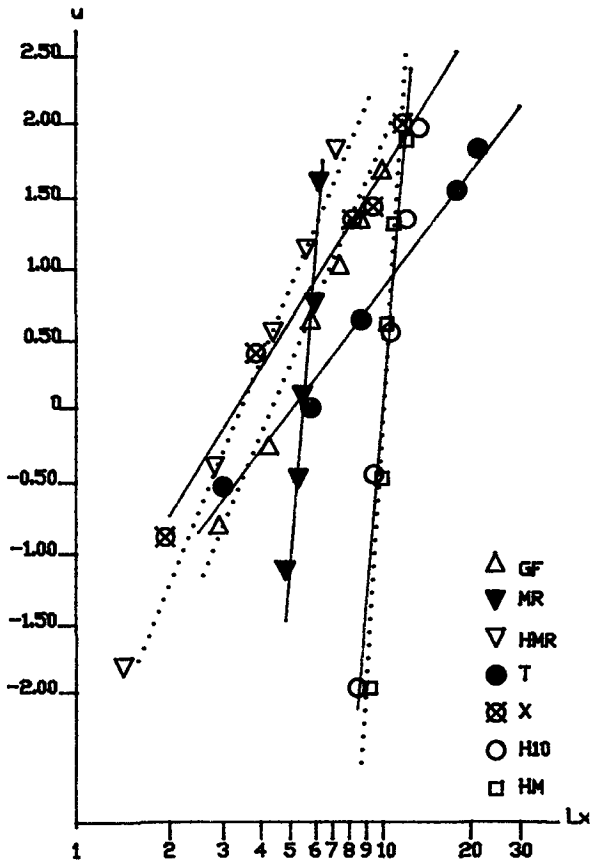

Figure 1 : cumulative frequency distribution versus logarithms of the values related to unseeded hailstorms

The lifetime of the hailstorms in the area of Albacete can be considered as moderately long because average geometric value is near 1 hour and the frequency of hailstorms whose lifetime was below 15 minutes is only 5%. This variable presents the highest geometric standard deviation, which reveals the heterogeneity of the lifetime of hailstorms. Similar results are obtained for the distance traveled.

The ratio between the average distance and lifetime is around 12 ms^{-1} , which may be considered as a realistic wind speed.

The parameters HM, H10 and MR have standard deviations quite small as can be seen in the similar slopes in the cumulative frequencies plots indicated in figures 1 and 2. The average value obtained in the reflectivity observed indicates that the hailstorms observed in the area of Albacete are not very severe compared to other continental areas (see Foote and Mhor; 1979).

It is also interesting to note that the height of the maximum reflectivity should also be considered as average, since only 5% of the hailstorms have the maximum reflectivity located at 1.7 Km above ground.

4. COMPARISON BETWEEN SEEDED & UNSEEDED HAILSTORMS

Table 3 shows the arithmetical mean, arithmetical standard deviation, maximum and minimum values, the geometric mean and geometric standard deviations of each radar parameter related to seeded hailstorms. The number of cases analyzed was 29.

PARAMETERS	M_a	σ_a	MAX	MIN	M_g	σ_g
HM	12.20	1.32	14.8	9.8	12.08	1.65
H10	11.32	1.58	14.8	9.0	11.27	1.06
T	83.50	56.40	255.0	16.0	67.50	2.25
MR	57.11	6.40	71.0	45.0	56.87	1.12
HMR	3.90	1.89	9.8	0.7	3.50	1.65
X	64.10	42.24	144.0	19.0	49.21	1.84
GF	3.99	1.72	7.6	1.5	3.65	1.50

Table 3 : arithmetic average (M_a), arithmetic standard deviation (σ_a), maximum (MAX), minimum (MIN), geometric average (M_g), and geometric standard deviation (σ_g) for seeded hailstorms.

Figure 2 shows the cumulative frequency distributions versus the logarithms of the values related to each parameter. The linear fits were again rather satisfactory as can be seen in Table 4. The Kolmogorov-Smirnov test was also performed in order to check types of storms. In fact, the examination of the geometric average values shown in Table 1 and 3 indicate a slight increase for the most of the variables. The growth factor was the only parameter which decreased for the seeded hailstorms. In order to analyze if the differences between the average values were significant from a statistical point of view, the Student t-test was applied to each variable. Table 5 shows the differences between the logarithms of each variable and the " t " statistical value. The symbol 'Y' written in the last column indicates that the differences were statistically significant at the 5% level and the symbol 'N' means that they were not.

PARAMETERS	r	p	V(50)	V(95)	V(5)
HM	0.998	0.1028	12.11	13.42	10.23
H10	0.992	0.1490	11.14	12.94	8.72
T	0.994	0.6481	67.11	194.91	23.11
MR	0.997	0.1107	56.71	68.04	47.27
HMR	0.998	0.5802	56.71	7.37	1.24
X	0.978	0.5997	45.98	17.14	123.29
GF	0.996	0.5087	3.62	8.38	1.57

Table 4 :correlation coeffient (r), slope (p) and values for different percentiles related to seeded hailstorms.

From the results shown in Table 5, we can conclude that there is not a significant difference between the radar parameters measured by the radar when unseeded and seeded storms are compared. However, for the growth factor used in this report, there is a 32.1% decrease for the seeded when compared to the unseeded hailstorms (results in table 6).

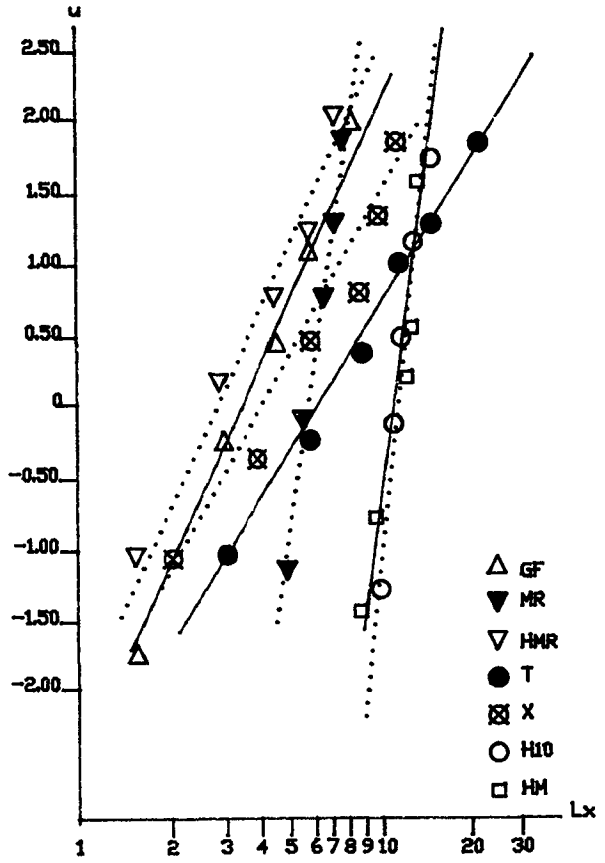

Figure 2 : cumulative frequency distribution versus logarithms of the values related to seeded hailstorms

PARAMETERS	DIF	t	S(5%)
HM	0.0388	1.59	N
H10	0.0509	1.71	N
T	0.1615	0.78	N
MR	0.0117	0.43	N
HMR	0.2231	0.18	N
X	0.2222	1.41	N
GF	-0.2842	2.02	Y

Table 5 : results of the t-statistic at the 5% significance level.

GF (SEEDED) N=29				GF (UNSEEDED) N=43			
5.6	3.6	3.7	2.9	3.2	5.2	6.0	2.6
1.6	5.4	3.0	2.9	8.5	3.5	5.0	2.9
2.7	2.7	3.6	4.7	2.6	6.5	1.7	5.8
3.9	3.5	3.3	2.7	3.7	4.7	2.4	6.0
2.7	1.5	3.5	2.6	3.3	3.4	5.0	1.7
2.7	4.7	3.5	6.4	4.8	4.9	4.4	8.5
4.7	7.6	1.7	8.3	6.5	3.8	4.5	5.4
7.5				7.5	17.2	22.3	6.5
				5.9	10.4	7.2	5.3
				2.1	2.4	9.1	4.6
				2.8	5.5	10.7	

Table 6 : Values of GF for seeded and unseeded hailstorms.

5. LINEAR CORRELATION AMONG THE GROWTH FACTOR AND THE DIRECT RADAR PARAMETERS

Since the only parameter which showed a difference between the two groups of hailstorms was the growth factor we tried to establish if there was any correlation between this factor and the other radar parameters. Tables 7 and 8 show the correlation coefficient, the slopes and the intercept for the unseeded and seeded hailstorms respectively. In the last column we have included the significance level of each linear fit. The symbol 'N' means that the fit was not significant at a level below 5%.

The unseeded hailstorms correlated better with most of the parameters than did the seeded ones. A similar correlation was found with the lifetime of the hailstorms. This difference in behaviour could be indicative of a modification to the seeded hailstorms.

PARAMETERS	r	b	a	sl
HM	0.661	0.14	11.66	0.002
H10	0.637	0.22	9.62	0.002
T	0.795	0.07	2.16	0.002
MR	0.441	1.08	46.00	0.005
HMR	0.563	0.28	1.95	0.002
X	0.733	4.73	15.34	0.002

Tabla 7 : linear fits between the growth factor and the direct parameters for unseeded hailstorms.

PARAMETERS	r	b	a	sl
HM	0.180	0.140	11.66	N
H10	0.006	0.006	11.31	N
T	0.590	0.018	2.48	0.002
MR	0.322	1.204	52.47	N
HMR	0.002	0.002	4.01	N
X	0.084	1.641	50.32	N

Table 8 : linear fits between the growth factor and the direct parameters for seeded hailstorms.

6. CONCLUSIONS

A characterization of hailstorms developed in the province of Albacete has been performed with the aid of the information recorded by a meteorological radar located in the protected area. In order to describe properly the main characteristics of each of the parameters studied, two lognormal frequency distribution tests were performed : the Kolmogorov - Smirnov test and a Probits analysis. The results obtained for unseeded and seeded hailstorms have revealed that the values of all parameters were well fitted to the lognormal frequency distribution.

The unseeded storms, whose reflectivities were greater than 45 dBZ when lifetimes were greater than 10 minutes, were analyzed for the protected area. They are characterized by moderate lifetime and with long travel distances, although they were not very severe according to the reflectivity values.

The comparison between the geometric average values of each studied parameter has indicated that there is no significant difference between seeded and unseeded hailstorms. The only parameter which was demonstrated to have a significant difference was the growth factor. There was a decrease for the seeded cases.

The correlations between the growth factor and the various parameters obtained for both seeded and unseeded hailstorms revealed that there was a different behaviour for seeded and unseeded storms. The unseeded storms correlated rather satisfactorily with most of the direct radar parameters, while the linear fits were very poor for the seeded cases. This result suggests that the influence of the seeding process may have changed the radar characteristics of the hailstorms.

It should be noted that these results are based on radar observations only. In order to obtain definitive results, and according to the suggestions of the WMO, it would be important not only to complete this study with cloud microphysical information and ground truth data concerning hail size characteristics, but also to conduct these studies on the basis of a randomized seeding experiment.

7. ACKNOWLEDGMENT

We want to express our most sincere thanks to the Servicio de Plagas of Ministry of Agriculture.

8. REFERENCES

Colino, J.A., 1987: Cloud Seeding: a technique in the service of the agriculture. Proc. First Int. Meet. on Agr. and Wea.Mod., 253-255. Leon, Spain

Dessens, J., 1986: Hail in southwestern France. Part II. Results of 30 years hail prevention project with silver iodide seeding from the ground. J. Climate Appl. Meteor., 25, 48-58.

------, 1987: Efficiency of hail prevention by ground seeding as a function of the number of generators. Proc. First Int. Meet. on Agric. and Wea. Mod. 177-181. Leon. Spain.

Foote G.B., C.G. and Mhor, 1979: Results of a randomized hail supression experiment in Northeast Colorado: Part IV. Post hoc stratification by storm intensity and type. J. Appl. Meteor. 18, 1589-1600.

Goyer G.G., 1975: Time integrated radar echo tops as a mesure of cloud seedings effects. J. Appl. Meteor. 14, 1362-1365.

Henderson T., 1975: The Kenya hail supression program. J. Wea. Mod. 7, 192-199.

Humphries R.G., M. English and J. Renick, 1987: Weather Modification in Alberta. Proc. First Int. Meet. on Agr. and Wea. Mod. 235-247. Leon. Spain.

Murray R. and R. Spiegel 1961: Estadistica. MacGraw Hill. 357 pp.

Romero R. and S. Balasch, 1985: Evaluacion de la efectividad de las actuaciones de defensa aerea antigranizo en la zona de Levante. Bol. Serv. Plagas

Santolaya A. and L. Santos, 1987: Hail prevention in Alava, La Rioja and Navarra regions: study of efficiency, effects upon precipitation. Proc. First Int. Meet. on Agr. and Wea. Mod. 225 - 234. Leon. Spain.

WMO, 1983; First WMO Long-term Plan Part I : Overall policy and strategy. WMO No. 616.

----, 1985: Review of the Present Status of Weather Modification. Annex of the abridged report with resolutions, thirty-seventh session of the executive council. WMO No. 648.

----, 1986: Report of the Meeting of experts on the evaluation of hail supression experiments. WMO/TD No. 97.

RADAR OBSERVATIONS OF WINTERTIME MOUNTAIN CLOUDS OVER COLORADO AND UTAH

Lewis O. Grant and Robert M. Rauber
Department of Atmospheric Science
Colorado State University
Fort Collins, Colorado 80523

Abstract. Ludlam (1955) postulated that seedable clouds for initiating snowfall are the extensive, shallow orographic clouds. He referred to these as "extensive low clouds". He specifically excluded clouds that contain persistent vertical motions not associated with localities where the airstream flows over mountains. The orographic, randomized Climax, Colorado cloud seeding experiment conducted during the 1960's followed the seeding hypothesis for orographic clouds as proposed by Ludlam (Grant, 1987). This paper presents the results of recent radar observations of the characteristics of differing types of clouds that form over the mountains of Colorado and Utah.

Cloud radar echo observations show that deep, stable and deep, convective cloud systems in the interior areas of the western United States during winter generally extend to elevations higher than the 50 Kpa pressure level where temperatures during winter are sufficiently cold to permit efficient ice nucleation processes to occur. Shallow, orographically forced clouds, on the other hand, almost always occur in their entirety at elevations below the 50 Kpa level where wintertime temperatures are variable with respect to temperatures at which natural ice nucleation can be either efficient or inefficient.

1. INTRODUCTION

The Ludlam (1955) concepts for seedable orographic clouds for initiating snowfall were postulated for extensive, shallow orographic clouds. He referred to these as "extensive low clouds...". He excluded "...clouds (that) contain persistent vertical motions of a magnitude sufficient to sustain any considerable precipitation, except in localities where the airstream containing the clouds flows over the mountains." The Climax randomized cloud seeding experiments were designed and conducted following considerations of orographic clouds as proposed by Ludlam (Grant, 1987). Climax experiments placed emphasis on the generally shallow orographic clouds that form as moisture is advected into the area in association with various weather systems. Large, organized cloud systems passing through the region and deep convective clouds forming over the mountains were considered to be already efficient precipitation producers that could not have their efficiency as precipitation producers greatly enhanced. Consequently, it was assumed for these experiments that the precipitation from these deep cloud systems would be "noise" in the randomized experiment, and that similar "noise" should occur on both seeded and "non-seeded" experimental days. Following Ludlam, the bias in the seeded sample, was postulated for the Climax experiment to occur from a difference in precipitation from the "extensive low clouds."

Detailed, descriptive, and continuous observations of the cloud systems were not feasible at the time of the Climax experiments which were carried out during the 1960's. Descriptive observations of cloud characteristics, estimated depths, and cloud top were limited to (1) visual observations under partly cloudy conditions and from the clear areas to the lee of the barrier, (2) a few direct observations with a modified Navy's SO-12 X-Band search radar, and (3) pilot reports of cloud tops. Other estimates of cloud characteristics were made from analyses of a limited number of upper air soundings made in the vicinity of the experimental area. Descriptive observations of the orographic clouds in the vicinity of Climax, as well as at other locations in Colorado and Utah, have been made during the past few years with the aid of a Ku-Band radar assembled at Colorado State University in the late 1970s. This paper presents the results of some of these recent observations. These results provide climatological descriptions of cloud tops (and consequently cloud depths), maximum and cloud top radar reflectivity, and the cloud elevation of the maximum reflectivity. Data are presented and compared for Tennessee Pass, Colorado (in the immediate vicinity of the Climax experiments), the Park Range of northwest Colorado, and from Beaver, Utah, upwind of the Tushar Mountains. These results are considered in the context of the seedability criteria hypotheses which were utilized for analyses of the Climax statistical experiments.

2. THE OBSERVING RADAR

All of the cloud descriptions presented in this paper are based on observations made with the Colorado State University Ku-Band (1.79 cm) radar. Received echoes are digitized by an eight-bit analog-to-digital converter and thereafter loaded into the memory of a minicomputer. Data are written onto 9-track magnetic tape once every 30 seconds or multiples thereof. Storage of data in an array of 46 pulses by 200 range bins affords access to individual pulse values for statistical

*Present affiliation: University of Illinois, Urbana, Illinois

calculations such as signal variance and bias. The computer also produces a real time display of reflected power, calculated in dBZ, based on averages of 46 consecutive pulses. The real-time display is formated as a horizontal intensity profile with 80 positions, each corresponding to 100 meters vertical distance. The overall effect is to establish a time-height history of the cloud vertical structure from 0.4 to 8.0 km height above ground level. Since water droplets are very small in Park Range clouds and concentrations seldom exceed 300 cm^{-3} (see Part II), the radar return is virtually always due to ice particles. Greeson et al. (1979) have shown that attenuation losses in the low liquid water content clouds and at distances observed with the vertical pointing radar are not serious. Greeson (1983) has confirmed this conclusion with comparisons of radar determined values of cloud top compared with aircraft observations.

3. OBSERVATIONAL DATA

The observations for Tennessee Pass included in this analysis, were made during the late winter and early spring months of the 1979-80 and 1980-81 winter seasons. The site for these observations was at the Ski Cooper Mountain ski area, approximately 9 km WSW of Climax, Colorado. This site is at an elevation of 3201 m msl. The various results presented in this paper are based, respectively, on all usable observations recorded at one minute intervals.

The observations for the Park Range included in this analysis, were made during the 1981-82 winter season. The site for these observations was at the outlying parking area of the ski area at the south end of Steamboat Springs, Colorado. This site is immediately upwind of the Park Range of NW Colorado at an elevation of 2050 m msl. The various results presented in this paper are based, respectively, on all or part of 24,755 observations made at one minute intervals.

The observations for the Beaver, Utah site were made during the 1982-83 winter season. The site for these observations was just east of Beaver, Utah, at the upwind base of the Tushar Mountains, near the mouth of Beaver Canyon. The site is at an elevation of 1890 m msl. The various results presented are based, respectively, on all or part of 11,381 observations made at one minute intervals.

4. RESULTS

Figure 1 shows the cumulative percent of observations of cloud tops that reach to different elevations for each of the three sites. It can be noted that the median value of cloud top is the lowest at Beaver, Utah: 4280 m msl and near 60 Kpa. The median value of all cloud tops at the Park Range site is higher at 5350 m msl and at a pressure slightly greater than 50 KpA. The highest median value of cloud top was observed at Tennessee Pass at 5850 m msl near 50 Kpa. It can be noted that both the median and mean value of the cloud top elevation at Tennessee Pass are at an elevation slightly above 50 Kpa. These mean values are similar to those observed by Furman (1967) for three storms during the Climax experiments using a SO-12 X-Band radar. He reported mean heights for the three storms to

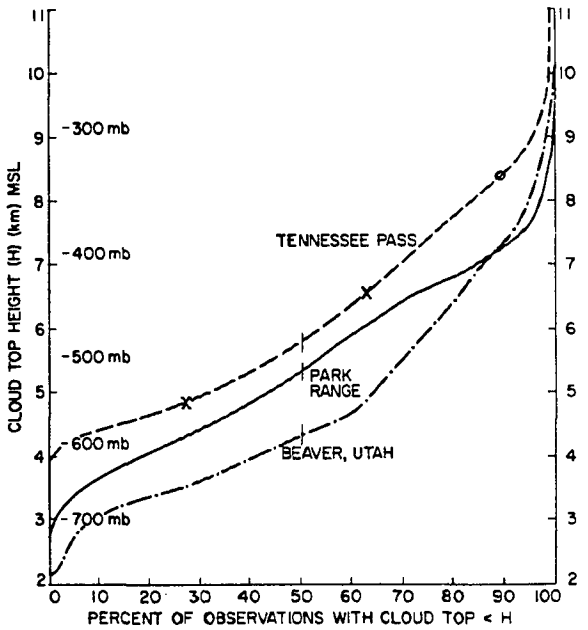

	Beaver, Utah	Park Range, Colo	Tennessee Pass, Colorado
Number of obs.	11,381	24,755	6824
Obs. frequency	1 min	1 min	1 min
Median	4280 m	5350 m	5850 m
Mean	4760 m	5468 m	6166 m
Standard deviation	1648 m	1393 m	1508 m
Radar elevation	1890 m	2050 m	3201 m

Figure 1. Cummulative frequency of cloud radar echo tops (msl) at three sites in the western United States

range from 4878 m to 6402 m msl with an extreme value of 8232 m msl. The range of the his mean values are shown on Figure 1 as X's and the extreme individual observation which he observed as a circle. The range of the mean values for his storm cloud tops bracket the mean and median values of the much larger Tennessee Pass observational sample. The cloud top climatologies in Figure 1, as in Furman's analysis, are for all cloud types not just for shallow, stable clouds which were the target of the experiment. In Figure 1, as in Furman's data for three storms, different types of cloud systems include shallow, stable clouds as well as convective cells and bands and deep synoptic scale cloud systems. The deeper convective and deep, stable cloud systems, as pointed out earlier, were considered to be naturally efficient and not the basic target clouds during the Climax experiments. The shallow orographic clouds targeted as having a potential for weather modification to augment precipitation during the Climax experiment were those that could be expected to be somewhat lower than the "mean" cloud top observed at the Tennessee Pass site. Grant et al., (1968) concluded that "the cloud system (with weather modification potential) is assumed to be embedded in the 700 mb to 500 mb layer...". The 50 Kpa level was used to index cloud tops for temperature partitioning as one of the criteria for the Climax statistical analyses.

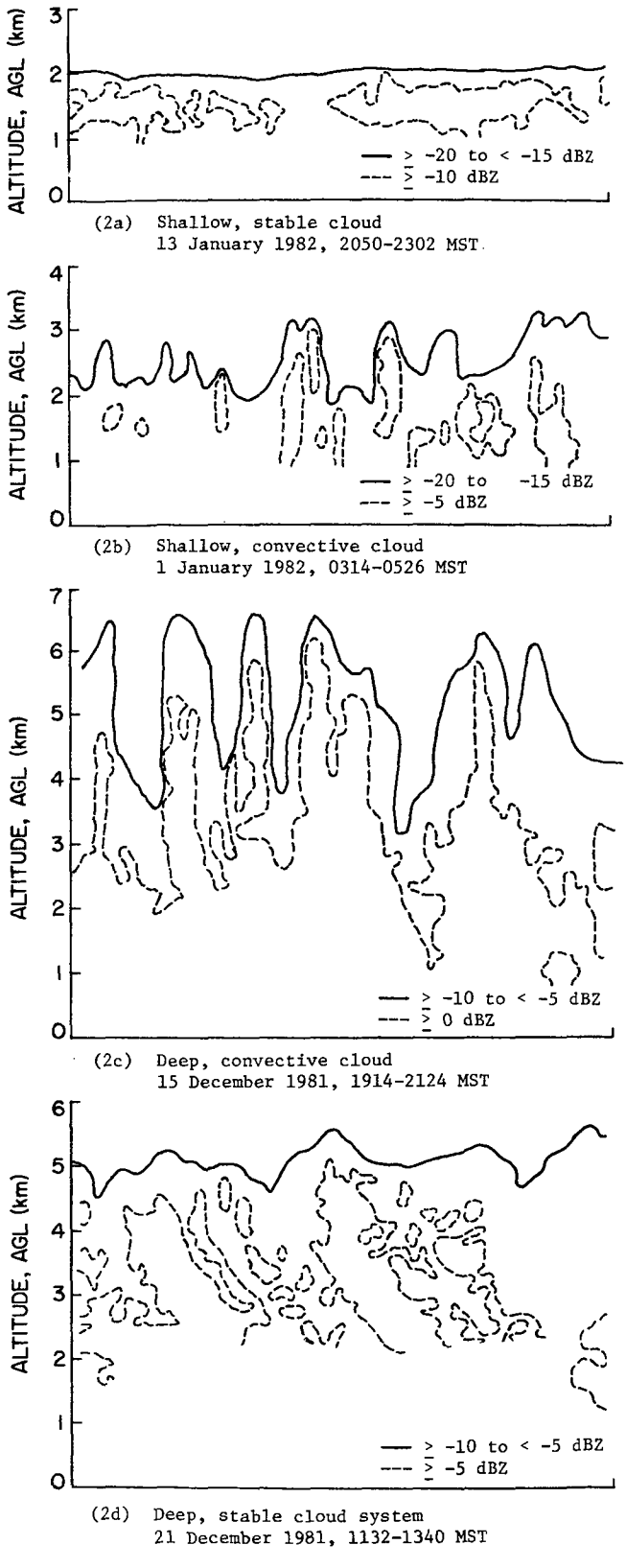

Figure 2. Radar reflectivity (dBZ) for four cloud types observed over western U.S. interior mountains.

The following sections explore the cloud characteristics for differing types of cloud systems for the present data set for the three western U.S. mountain sites.

4.1 Cloud Types

Cloud characteristics have been considered for four cloud types. These include shallow-stable; shallow-convective; deep-convective; and deep-stable cloud systems. The classifications are based on radar data but synoptic and precipitation data have also been utilized.

Figure 2a shows the radar display at two-minute intervals for a representative case of a shallow, orographic cloud over the Park Range. This shows the radar reflectivity values from 350 meters above ground level (AGL) to cloud radar top. The same type of display is used in Figures 2b, 2c, and 2d for the other types of cloud systems. All displays are from the Park Range site. The representative example of a shallow-stable cloud system in Figure 2a extends from 2014 to 2302 on 13 January 1982. This particular episode of a shallow cloud extended almost unchanged from 0745 MST on 12 January, through 13 January, to 0650 MST on 14 January. Precipitation for the 24 hour period on 13 January fell at an average rate of .125 mm/hr at the lower upwind elevations to an average rate of .425 mm/hr at the higher elevations.

Figure 2b shows a representative radar presentation for a shallow convective cloud system which occurred on 1 January 1982. The precipitation rate during the period for the display averaged approximately 0.2 mm/hr at the lower upwind elevations and up to an average of approximately 0.7 mm/hr at the higher elevations.

Figure 2c shows a representative radar presentation for a deep convective cloud system which occurred on 15 December 1981. The convective elements on 15 December 1981 went through several repetitions as was the case with the shallow convective cloud system on 1 January 1982. More isolated convective elements are also observed. The precipitation rate during the period of time shown in Figure 2c at the lower, upwind elevations was approximately 0.5 mm/hr and at the higher elevations was at an average rate of about 1.6 mm/hr.

Figure 2d shows a representative radar presentation for the deep, stable cloud system observed on 21 December 1981. The precipitation rate during the period used for this sample was at an average rate of 0.2 mm/hr at the lower upwind sites and up to an average rate of 1.9 mm/hr at the higher elevations. While this sample shows a little over two-hour interval, this particular episode extended for a period of about 6 1/2 hours on 21 December from 0744 to 1416 MST.

4.2 Frequency of Different Cloud Types at the Respective Sites

The frequencies of the different cloud types in this data set are shown in Table 1.

Table 1

Frequency of different cloud types

	Beaver	Park Range	Tennessee Pass
Shallow, stable	58%	53%	33%
Shallow, convective	9%	5%	9%
Deep, convection	15%	7%	21%
Deep, stable	11%	35%	37%

The percentages at Beaver total less than 100% since some of the Beaver, Utah data do not fit the classifications used in this paper. The frequency distributions of cloud types for the Park Range are for 4891 observations at two minute intervals during the periods 13-21 December 1981 and 11-16 January 1982. The frequency distributions for Tennessee Pass are based on 1760 observations at two- minute intervals during the periods 14 February-2 April 1980 and 16 February-27 March 1981 and 5 May 1981.

These frequency distributions show a predominant occurrence of shallow, stable clouds at all three sites. This limited sample suggests that shallow clouds constitute a higher percentage of the total cloud population in the Tushars of southwest Utah than at the Colorado sites. The Colorado sites, show a high frequency of deep, stable clouds as well as the high frequency of shallow, stable clouds. While it is believed that these data are generally representative, it must be remembered that at each site they are based on only a few storms in one or two particular seasons.

4.3 Cloud Top Climatology for Different Cloud Types

Median elevations of cloud echo tops for the respective cloud types are shown in Table 2.

Table 2

Median cloud top elevations in meters for elevation above ground (AGL) and above sea level (MSL).

	Beaver		Park Range		Tennessee Pass	
	AGL	MSL	AGL	MSL	AGL	MSL
Shallow, stable	2100	(3990)	2100	(4150)	2100	(5301)
Shallow, convective	2260	(4150)	3075	(5125)	2180	(5381)
Deep, convective	4320	(6210)	4940	(6990)	4340	(7541)
Deep, stable	4780	(6670)	4004	(6054)	4696	(7897)

The median cloud echo tops AGL are approximately the same at the various sites for the respective cloud systems. The elevation above sea level, consequently generally increases at the higher elevation sites. This would result in colder cloud top temperatures over the higher elevation mountain ranges.

4.4 Cloud Depth

Systematic observations of cloud bases are not available for these radar sites. For purposes of estimating cloud depth in this paper, it is assumed that cloud bases at the Park Range and Beaver radar sites are at around 400 m AGL and that they are 100 m AGL at Tennessee Pass. The primary estimates of cloud base are from estimates of the elevation at which cloud was observed to intersect the mountains. Balloon releases and rawinsonde observations have also been noted. Using these estimates for cloud base, estimates of cloud depths are presented in Table 3.

Table 3

Estimated median cloud thickness in meters.

	Beaver	Park Range	Tennessee Pass
Shallow, stable	1700	1700	2000
Shallow, convective	1860	2675	2080
Deep, convective	3920	4540	4240
Deep, stable	4380	3604	4596

The depths of the shallow, stable clouds at these sites, all located along continuous mountain ranges, are deeper than found for the cap clouds over the more isolated peak at Elk Mountain, Wyoming. Rogers and Politovich (1981) reported that typical Elk Mountain cap clouds have bases at 3000 m msl and tops at 4000 m msl and typically depths, consequently, of about 1000 m.

4.5 Cloud Top Radar Reflectivity

Cloud echo top reflectivity value for the Park Range and Tennessee Pass sites are shown in Table 4.

Table 4

Mean cloud top radar reflectivity values in DBZ.

	Park Range	Tennessee Pass
Shallow, stable	-15.0	-9.1
Shallow, convective	-12.7	-13.7
Deep, convective	-9.5	-9.6
Deep, stable	-10.9	-12.3

The median value of cloud top echo reflectivity values with all cloud types fall in the range of -9.0 to -15.0 dBZ at the Park Range and Tennessee sites. The differences between the

dBZ values for deep, convective echo systems from other cloud types, is probably significant. Particularly with this radar echo type, and on occasion with other types, the boundary reflectivity value at cloud radar top and "no signal" zone above is much stronger than typical values.

4.6 Cloud Maximum Radar Reflectivities

Median values of cloud maximum reflectivity are shown in Table 5.

Table 5

Median values of maximum radar reflectivity in DBZ.

	Beaver	Park Range	Tennessee Pass
Shallow, stable	9.8	-8.24	-9.8
Shallow, convective	10.8	-5.8	+0.2
Deep, convective	10.8	+4.7	+5.2
Deep, stable	19.7	-2.9	-4.1

It can be noted that there is little difference between the Park Range and Tennessee Pass values but that there is a large difference between the value at these two sites and the one at the Beaver site. At the Colorado sites, essentially all precipitation occurs in the form of snow with a large portion falling as single crystal snowfall. It is believed that the reflectivity values at these sites reflect this form of precipitation. The higher median values at Beaver result from cases with higher reflectivity associated with the occurrence of rain, as distinct from snow, from accreted and aggregated snow crystals that are larger than the single crystals generally observed at the other sites; and from the sometimes presence of a bright band.

Considering the Colorado sites, the reflectivity values for shallow, stable clouds are the lowest and similar. Higher, but still negative values, are observed with deep, stable cloud systems. Still higher median reflectivity values are observed with convective systems and particularly with deep convection.

4.7 Height of Cloud Maximum Radar Reflectivities

The elevations above ground of the maximum radar reflectivities are shown in Table 6.

The median value of the height of the maximum reflectivity is in the lower portions of the shallow cloud systems. The height of the maximum reflectivity in Colorado clouds is, however, considerably more complex. The maximum reflectivity with deep convective clouds frequently occurs both in the lower and upper portion of the clouds. In some cases, highest reflectivity values are observed very near cloud top. It can also be noted with the deep, stable cloud systems that the most common elevation of maximum reflectivity is near mid-cloud level.

Table 6

Median height AGL of maximum radar reflectivities in meters.

	Beaver	Park Range	Tennessee Pass
Shallow, stable	1180	1480	1430
Shallow, convective	1620	1800	1360
Deep, convective	1620	2020 3870*	1690 3000*
Area-wide synoptic scale	1380	1860	2580

*Second zone of maximum reflectivity present in many of the observations.

In many cases with deep, stable cloud systems, and on occasions with shallow, stable clouds, maximum reflectivity values develop at mid-cloud levels and remain essentially at the same elevation for an extended period of time.

5. DISCUSSION AND CONCLUSIONS

Mountain clouds over the interior mountains of the western U.S. are sometimes deep, extensive, area-wide cloud systems. At other times they are shallow, orographically forced clouds that blanket the mountains. At still other times, they can be convective in nature. This discussion follows from the differing characteristics of these respective cloud systems.

5.1 Deep, Stable Cloud Systems

The median depth of these cloud systems is typically 4000-4700 meters and they typically extend to 6000 m to 8000 m msl, and occasionally to above 10,000 m msl. They frequently last for a few hours and occasionally for 5-10 hours as a large synoptic scale weather system passes through the region. These deep cloud systems are generally preceded and/or followed by shallow, stable blanket clouds or orograhically forced convective clouds as low-level moisture and/or instability is advected into the mountain regions in association with the synoptic scale disturbance. Deep, stable clouds extend to elevations that nearly always have cold temperatures which favor ice nucleation during winter(Rauber and Grant, 1986; Rauber et al, 1986; Rauber, 1987; Uttal, 1988). Maximum radar reflectivity values in these clouds are consistently greater than in the shallow, stable blanket clouds but still low. These clouds constitute some 30-40% of the orographic cloud cover over the Colorado mountains but apparently, based on the limited sample, a much smaller portion (11%) of the cloud cover in southwest Utah.

5.2 Shallow, Stable, Orographic Clouds

Shallow, stable, blanket clouds are typically the most frequent cloud type over the mountains of Colorado and Utah. The limited data sets suggest

that they constitute over 50% of the cloud cover over the ranges directly exposed to approaching airflow and perhaps as little as 30-40% of the cloud cover over complex mountain areas such as Tennessee Pass that are protected from direct low-level lifting from some directions.

The median depth of these orographic blanket clouds is about 1700 m and their cloud radar echo tops extend to elevations from about 4000 to around 5000 m msl. While these clouds are relatively thin, condensate supply rates can be large as horizontal wind flow is rapidly lifted in passing over a mountain barrier. While the median maximum reflectivity is -8.24 DBZ in the Park Range, shallow, stable clouds, for example, values for individual cases range from less than -15 DBZ to greater than +10 DBZ. The median elevation of radar cloud tops in shallow clouds varies from about 2690 m to 4890 m msl at Beaver, 2650 m to 4250 m msl at the Park Range, and 4101 m to 5501 m msl at Tennessee Pass. These cloud radar echo tops for this cloud type were almost always at an elevation below the 50 Kpa level, which was used to index cloud top temperature for this cloud type which was hypothesized for the Climax experiments to have the main weather modification potential (Rauber and Grant, 1986; Rauber and Grant, 1987). The temperature at the 50 Kpa level, consequently, would almost always be equal to or colder than the actual cloud top temperatures. If the statistical partition of -20°C or warmer at 50 Kpa used in the Climax statistical analyses is considered (Mielke et. al, 1981), one can be confident that the actual cloud top temperature for these shallow clouds was at that 500 mb temperature or warmer. These shallow clouds are also the ones generally observed to have significant amounts of sub-cooled water for extended time periods (Rauber and Grant, 1983; Rauber et. al, 1986; Rauber and Grant, 1986).

5.3 Shallow, Convective Clouds

Shallow clouds were much less frequent in all study areas than the shallow, stable, orographic clouds. They were, however, typically only slightly deeper than the shallow, stable clouds. The general conclusions reached with respect to the weather modification potential for the more stable, shallow clouds may also apply to these clouds.

5.4 Deep Convective Clouds

The median depth of the deep, convective clouds in this study were from 3900 m to 4500 m with median cloud tops extending to elevations of 6200 m to 7500 m at the various sites. This cloud type constituted from 7% to 21% of the samples at the respective sites. The greater reflectivity values show the presence of larger hydrometers. Since over 95% of the deep convective clouds observed at the Park Range and Tennessee Pass sites had reflectivity values greater than -5 dBZ (75% > 0 DBZ), it must be concluded that even during their relatively short life span, a significant population of large ice particles form in these clouds either from accretion and/or aggregation.

6. SUMMARY

In summary, the cloud radar echo observations show that deep, stable and deep, convective cloud systems in the interior areas of the western United States during winter generally extend to elevations above the 50 Kpa pressure level where temperatures during winter are sufficiently cold to permit efficient ice nucleation processes to occur. Some liquid water can still occur in the lower portions of these clouds. Other studies, however, using parallel radiometric sensing and aircraft probes have shown, for the cases studied, that the amounts of liquid water present in these deep clouds is not large or present for very long periods of time (Rauber et al., 1986; Rauber and Grant, 1986). Shallow, orographically forced clouds, on the other hand, almost always occur in their entirety at elevations below the 50 Kpa level where wintertime temperatures are variable with respect to temperatures at which natural ice nucleation can be either efficient or inefficient.

7. ACKNOWLEDGEMENTS

Support for this research by National Science Foundation grants ATM-8109590 and ATM-8407543 is gratefully acknowledged. Other support from the Utah Department of Natural Resources is also gratefully acknowledged.

8. REFERENCES

Furman, R.W., 1967: Radar characteristics of wintertime storms in the Colorado Rockies. Atmos. Sci. Paper No. 112, Dept. of Atmospheric Science, Colorado State University, Fort Collins, Colorado, 53 pp.

Grant, L.O., 1987: Hypotheses for the Climax wintertime orographic cloud seeding experiments. Precipitation enhancement - A Scientific Challenge. AMS Meteor. Monograph, 21, 105-108.

Grant, L.O., C.F. Chappell, and P.W. Mielke, Jr., 1968: The recognition of cloud seeding opportunity. Proc. 1st National Conference on Weather Modification, Albany, New York, 372-385.

Greeson, J.S., 1983: The vertical and temporal characteristics of winter orographic clouds as assessed by vertical pointing radar. Atmos. Sci. Paper 368, Dept. of Atmospheric Science, Colorado State University, Fort Collins, Colorado, 147 pp.

Greeson, J.S., D.R. Cobb, L.O. Grant and L. Lillie, 1979: The use of the Ku Band radar for weather modification research. Proc. 7th Conf. on Inadvertent and Planned Weather Modification, Banff, Alberta, Canada, 108-109.

Ludlam, F.H., 1955: Artificial snowfall from mountain clouds. Tellus, 7, 277-290.

Mielke, P.W., G.W. Brier, L.O. Grant, G.J. Mulvey and P.N. Rosenzweig, 1981: A statistical reanalysis of the replicated Climax I and II wintertime orographic cloud seeding experiments. J. Appl. Meteor., 20, 643-659.

Rauber, R.M., 1987: Characteristics of cloud ice and precipitation during wintertime storms over the mountains of northern Colorado. J. Clim. Appl. Meteor., 26, 488-524.

Rauber, R.M. and L.O. Grant, 1983: Preliminary analysis of the hypothesis used in the Utah operational weather modification program. *Final Report to Utah Dept. of Natural Resources*, Dept. of Atmospheric Science, Colorado State University, Fort Collins, Colorado, 9-16,23-82.

Rauber, R.M. and L.O. Grant, 1986: The characteristics and distribution of cloud water over the mountains of northern Colorado during wintertime storms. Part II: Spatial distribution and microphysical characteristics. J. Clim. Appl. Meteor., 25, 489-504.

Rauber, R.M., L.O. Grant, D. Feng, and J.B. Snider, 1986: The characteristics and distribution of cloud water over the mountains of northern Colorado during wintertime storms. Part I: Temporal variations. J. Clim. Appl. Meteor., 25, 468-488.

Rauber, R. M. and L. O. Grant, 1987: Supercooled liquid water structure of a shallow orographic system in southern Utah. J. Clim. Appl. Meteor., 26, 208-215.

Rogers, D.C., and M.K. Politovich, 1981: Meteorology of the wintertime Elk Mountain cap clouds. Second Conference on Mountain Meteorology, AMS, Steamboat Springs, Colo., 371-374.

Uttal, T., R.M. Rauber and L.O. Grant, 1988: Distributions of liquid vapor and ice in an orographic cloud from field observations. J. Atmos. Sci., accepted for April publication.

COMPARISONS OF THE BEHAVIOR OF AgI-TYPE ICE NUCLEATING AEROSOLS IN LABORATORY-SIMULATED CLOUDS

Paul J. DeMott
Department of Atmospheric Science
Colorado State University, Fort Collins, CO 80523

Abstract. A variety of commonly used ice nucleants have been tested for comparable simulated adiabatic parcel ascents in the Colorado State University dynamic cloud chamber. Atmospheric adiabatic expansion and cooling of a parcel of air is simulated by evacuation and wall temperature control within the working volume. Ice nucleation characteristics have been studied for the injection of nuclei preceding the formation of clouds at a temperature near 0°C and following nuclei injection directly into cooling cloud parcels.

A summary and comparison of the nucleation rates and mechanisms observed for four different ice nucleating aerosols is presented. In some cases, the results observed in the simulations of real cloud processes were quite different than found previously in the static conditions of the CSU isothermal cloud chamber containing an artificially generated cloud. In particular, complexed hygroscopic nucleating aerosols (2AgI·NaI and 2AgI·KI) display much higher nucleation rates during expansional cooling than for injection into supercooled isothermal cloud. Some implications of the experimental results to the expected results of seeding atmospheric clouds are discussed.

1. INTRODUCTION

New and significant informaton on the ice nucleating behavior of various nucleating aerosols used now and in past weather modification programs has been gained during concentrated testing at the Colorado State University Cloud Simulation Laboratory in the last several years. The isothermal supercooled cloud chamber (ICC) and the continuous slow expansion (dynamic) cloud chamber (DCC) have proved useful for the identification of the activities, rates and mechanisms (modes of nucleation) of various AgI-type aerosols for equivalent cloud conditions. Some of the findings have been discussed separately in recent weather modification conference proceedings. In this paper, the results for four common ice nucleating aerosols produced by solution combustion are summarized. These are silver iodide-silver chloride (AgI-AgCl), silver iodide-silver chloride-sodium chloride (AgI-AgCl-4NaCl), silver iodide-sodium iodide (2AgI·NaI) and silver iodide-potassium iodide (2AgI·KI) nucleating aerosols. The new insights into the complex and varied response of different ice nuclei to the cloud type and seeding method suggest careful evaluation of which nucleating aerosols are "best" for use in a particular field application.

2. FACILITIES

2.1 Isothermal Cloud Chamber

The CSU isothermal cloud chamber has been described in numerous publications (e.g., Garvey, 1975; DeMott et al., 1983). The chamber characteristics are described only briefly here. A cloud of known droplet concentration and liquid water content is physically continuously supplied to the 1000 L cloud chamber and a water saturated environment results at a constant cloud temperature for nucleation tests. The chamber has proved useful for the definition of the relative total yield (effectivity) of ice crystals per gram of nucleant dispersed (from actual field-type generators) as a function of cloud temperature for the conditions present. The constant conditions in the cloud chamber can be altered to the extent that cloud droplet concentrations can be varied at any one temperature or saturation ratio can be raised above water saturation by the purposeful introduction of humid air with aerosols. These features have proved useful for the delineation of the dominant nucleation mechanisms using observations of changes in ice crystal formation rates (kinetics) with changes in cloud conditions (DeMott et al., 1983; Blumenstein et al., 1987).

2.2 Dynamic Cloud Chamber

The CSU dynamic cloud chamber has been described in its current configuration, only in conference proceedings. Its primary characteristics relevant to the data presented here will now be discussed. A more technically detailed description is being prepared for separate publication.

The DCC and its support systems are shown schematically in Fig. 1. Adiabatic expansion is simulated in the DCC by the evacuation of a 2 m^3 volume surrounded by stainless steel. A 1.2 m^3 volume of air within the chamber is further isolated by a force-cooled copper liner that is only open to the outer 0.8 m^3 volume by small holes. The temperature of the inner liner is controlled empirically (by providing coolant

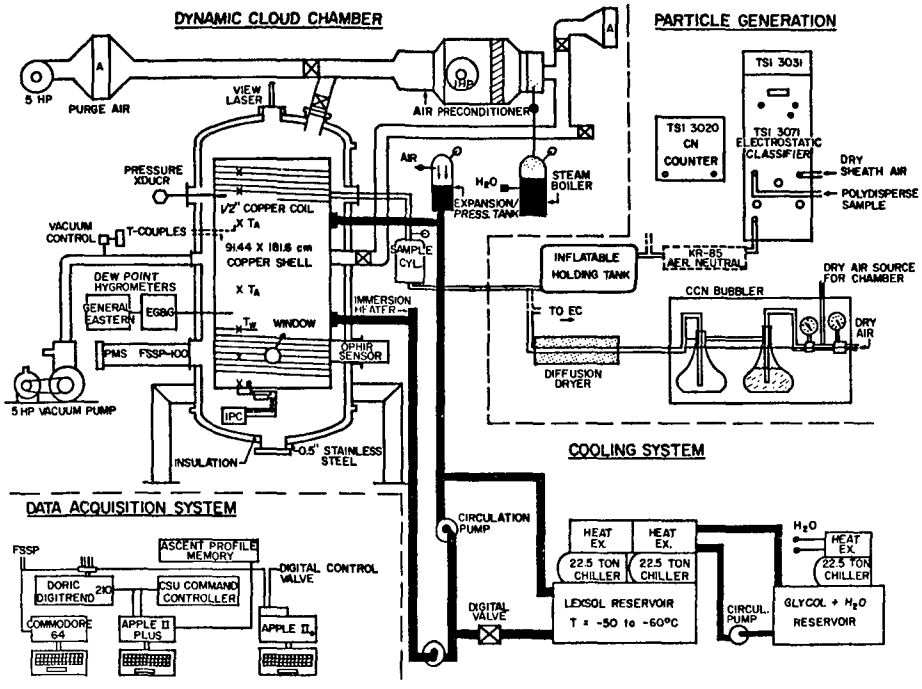

Fig. 1. Schematic diagram of the CSU dynamic cloud chamber facility, including particle generation, cooling and data acquisition systems. Additional descriptions and discussion of capabilities utilized are in the text.

through a digital flow valve) to follow as closely as possible the simulated adiabatic cooling from evacuation. Thus, the cloud that forms is contained within the inner liner. Temperature, pressure, humidity, cloud droplet sizes and concentrations, and the number of ice crystals settling from the volume are measured in time, within the inner volume.

Temperature is measured continuously using an array of ten Cu-Constantin thermocouples located on the inner liner and two faster response thermocouples located ten inches into the air volume from the inner wall. Pressure is measured using a transducer. Humidity is measured using a optical condensation-type dewpoint hygrometer. A differential-absorption infrared hygrometer (OPHIR Corporation) has recently been installed, but was not employed in these studies. Cloud droplet spectra are measured with a Particle Measuring Systems FSSP-100. A specially designed sampling inlet protrudes into the chamber to draw cloud in, accelerate it to 25 m s^{-1}, and focus it in the laser beam. Ice crystals are detected by a laser-based extinction device (~ 20 μm size threshold) similar to that of Lawson and Stewart (1983) that has been calibrated versus ground truth measurements on microscope slides. This is denoted as the ice particle counter (IPC) in Fig. 1. The device depends on the settling of ice crystals from the cloud for measurement. This causes a slight measurement lag because crystals must both grow and settle. Pulse nucleation tests using CO_2 have shown this time to be between 30 and 60 s. Since a transfer function has not been determined yet, ice counts were adjusted 30 s back in time to determine their nucleation temperature. A PMS 2D-C ice crystal sensor has also been used in the DCC (see, for example, DeMott et al., 1984), but all results reported here are from the IPC.

Concentrations of CCN (ammonium sulfate aerosols) and initial temperature and dewpoint temperature can be specified to form a cloud of known characterisitics at a desired temperature and pressure. Evacuation control, cooling control, and data acquisition are currently done by three microcomputers. One (Commodore 64) is devoted to cloud droplet measurements, one to cooling control (Apple IIe), and the other (Apple II+) handles data acquisition, display and control. Data are recorded at 15 s intervals. Simulated ascents are programmed based on equations for dry adiabatic expansion to cloud point and moist adiabatic expansion in cloud. Ice nucleus aerosols can be vented into the DCC and mixed briefly at any point during expansion. The DCC thus permits a large variety of comparative studies of nucleation by different aerosols for cloud conditions that are more like atmospheric cloud conditions than the conditions in the isothermal cloud chamber. Ice nucleus aerosol generation was done within a vertical dilution wind tunnel (Garvey, 1975) and samples were transported by syringe to the DCC. The mass of nucleating material in each sample was determined by standard procedures.

3. YIELDS, MECHANISMS AND RATES OF NUCLEATION

Ice nucleation yield, mechanism and rate are intimately related for a given set of cloud conditions, as shown in the referenced isothermal cloud chamber studies. A population of ice

nucleating aerosols has an inherent yield by a given nucleation mode, that can only be measured experimentally. However, this yield can be a function of time due to the kinetic details of the mechanism (e.g., how nucleation rate depends on temperature, cloud droplet distribution and saturation ratio). These interactions vary for different ice nucleants and together define the utility of an ice nucleus for weather modification by cloud seeding. Four examples of nucleating aerosol systems are discussed in this paper. All were generated using the CSU standard generator, which functions by aerosolizing acetone-based solutions into a propane flame.

3.1 AgI-AgCl Aerosols

AgI-AgCl (silver iodide-silver chloride) aerosols are produced by the combustion of solutions of AgI, acetone, ammonium iodide, ammonium perchlorate and water. These have been found to act predominantly as contact-freezing ice nuclei at temperatures warmer than -15°C in the isothermal cloud chamber (DeMott et al., 1983). This was noted by the fact that the kinetic rate of ice crystal production in the chamber was linearly related to the cloud droplet concentration at any temperature. Thus, although they are highly efficient ice nucleating aerosols (see Fig. 2), the potential efficiency of the AgI-AgCl aerosols in the atmosphere may be controlled by the existing droplet concentrations and sizes, and the time available to scavenge the aerosols. An exception to this behavior may occur when solutions are burned in propane flame within cloudy air (see, for example, Finnegan and Pitter, 1987). In this case, high transient supersaturations may force a rapid nucleation mechanism, despite the hydrophobic nature of these aerosols. In any case, it is clearly difficult to attempt to generalize or predict nucleation effects a priori in particular atmospheric conditions. Pure AgI aerosols have these same characteristics.

Comparative simulations of in-cloud and below-cloud (before cloud formation at warm temperatures) seeding using AgI-AgCl nucleating aerosols were performed in the DCC by DeMott et al. (1984). Similar clouds were formed close to 0°C during simulated 2.5 m s^{-1} parcel ascent and nuclei were introduced before or after cloud formed, as appropriate. In-cloud seeding was done at -7°C, the temperature at which ice was first detected in the pre-cloud seeded tests. The essential results of this research are displayed in Fig. 3 and Fig. 4. Fig. 3 shows the cumulative yield of ice crystals at various temperatures during adiabatic cooling at near 1°C min^{-1} (in-cloud). The AgI-AgCl nuclei, are strongly sensitive to the seeding method. When introduced before cloud formation, much time is available for collision with cloud droplets and the immersion-freezing nucleation mechanism must be considered in addition to contact-freezing nucleation. The immersion-freezing mode is apparently much less efficient for these aerosols than for a direct contact-freezing mode at supercooled cloud temperatures. It is also shown (Fig. 4) that the rate of ice crystal generation by AgI-AgCl aerosols is dependent on the cloud droplet concentrations present in the cloud. Lower droplet concentrations result in fewer ice crystals in the same time period. Finally, it is notable that the

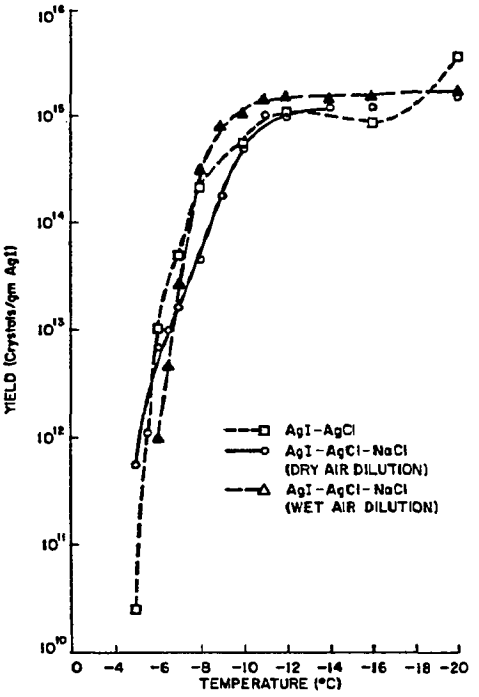

Fig. 2. Comparison of total yield as a function of isothermal cloud chamber temperature for AgI-AgCl versus AgI-AgCl-4NaCl ice nucleating aerosols. Data for injections with humid air are denoted as "wet air dilutions".

cumulative yield during cooling approaches the yield in the ICC only at the coldest temperatures. This is consistent with the nucleation mechanisms hypothesized.

3.2 AgI-AgCl-4NaCl Aerosols

The AgI-AgCl-4NaCl ice nucleating aerosols were synthesized (Finnegan et al., 1984; Feng and Finnegan, 1985) as a way of producing an uncomplexed and hygroscopic nucleant that forms ice rapidly by condensation-freezing nucleation at water saturation and also retains nearly the effectivity of the AgI-AgCl system in the isothermal cloud (see Fig. 2). Comparative simulations of in-cloud versus below-cloud seeding with the AgI-AgCl-4NaCl aerosols in the dynamic cloud chamber were also performed by DeMott et al. (1984) and the primary results appear in Figures 3 and 4. In-cloud injection was made at -9°C, the temperature at which ice was first detected in the pre-cloud seeded tests. These condensation-freezing nuclei appear to function in the same way whether introduced before or after cloud formation. This implies that the freezing step is rate determining for nucleation and also that the occurence of the condensation step at warmer temperatures during cooling does not decrease yield due to potential dissolution effects. No dependence of nucleation rate or yield on droplet concentrations present was found in the simulated adiabatic parcel ascents (see, for example, Fig. 4). This is consistent with the nucleation mechanism envisioned and the ICC results of Feng and Finnegan (1985). In general, the AgI-AgCl-4NaCl aerosols would be expected to act in a more consistent manner in a wide variety of atmospheric cloud conditions than AgI-AgCl aerosols based on this information.

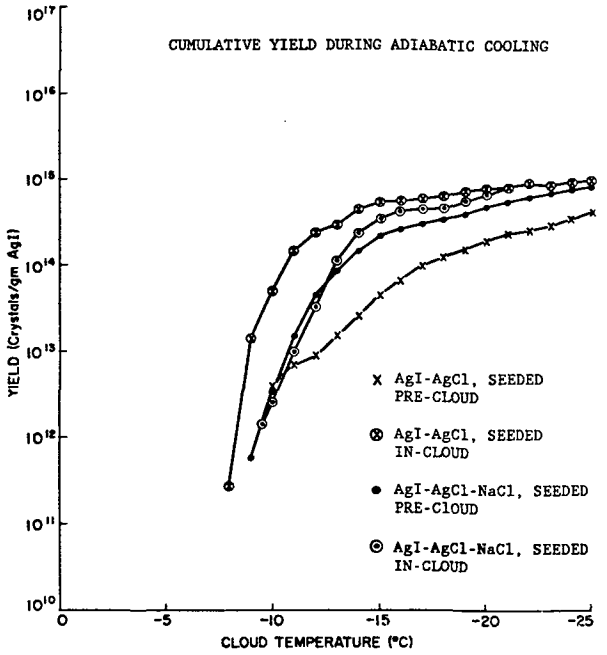

Fig. 3. Cumulative yields of ice crystals formed as a function of cloud temperature during simulated adiabatic cooling in four equivalent dynamic cloud chamber tests for AgI-AgCl and AgI-AgCl-4NaCl aerosols. Cooling rate in-cloud was approximately 1°C min in these tests. Cloud was formed at 0°C in each case (except -x- formed at +5°C). The AgI-AgCl aerosols were introduced at -7°C in the in-cloud seeding test, while the AgI-AgCl-4NaCl aerosols were introduced at -9°C.

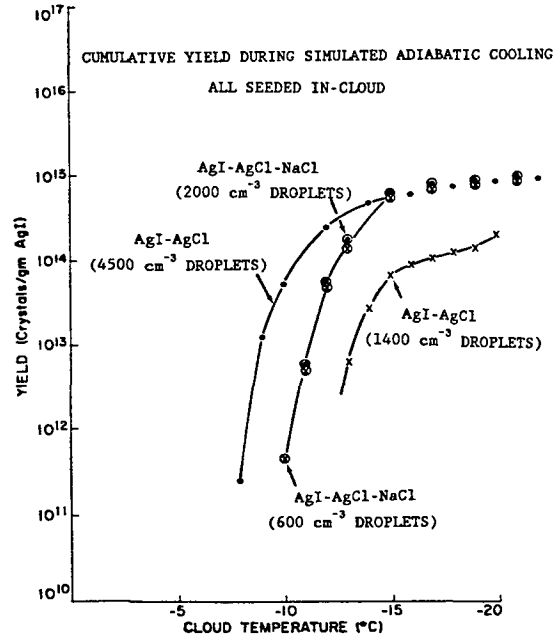

Fig. 4. Results from experiments in the DCC as shown in Fig. 3, but for different droplet concentrations at the point of ice nuclei injection. Droplet concentrations are indicated in parenthesis. All injections shown were directly into cloud. AgI-AgCl aerosols were injected at -7°C, while AgI-AgCl-4NaCl aerosols were injected at -9°C.

3.3 2AgI·NaI and 2AgI·KI Aerosols

The 2AgI·NaI and 2AgI·KI ice nucleating aerosols are grouped together here due to their similar chemistry and ice nucleation behavior. 2AgI·KI aerosols are fully complexed upon generation and the 2AgI·NaI aerosols are fully complexed upon the formation of a tri-hydrate. The 2AgI·NaI aerosols have been used in the Climax and Israeli weather modification programs among others and the 2AgI·KI aerosols are most familiarly associated with Project Whitetop. The yield curves for 2AgI·NaI in the isothermal cloud chamber are shown in Blumenstein et al. (1987). The ICC results for 2AgI·KI aerosols are shown in Fig. 5 (unpublished, from a study by Rilling et al., 1984). Nucleation rate constants for standard water saturated conditions are typically as low as 0.05 min^{-1} (47 minutes for 90% of the the total ice crystals formed to nucleate at one temperature) for both aerosols. The slow rates are apparently the result of the multiple stage process leading to ice formation (Blumenstein et al., 1987). The complexes must first be broken within a solution droplet, freeing the AgI, before nucleation can occur. Recognizing that the isothermal cloud does not truly simulate atmospheric clouds where water saturation is probably a more transient state and water supersaturations can occur, and realizing that the effect of intermediate stages to nucleation might be eliminated when supersaturations exist, Blumenstein et al. induced transient supersaturations in the isothermal cloud chamber by injecting the 2AgI·NaI aerosols with varying amounts of moisture. Nucleation yield was markedly increased and nucleation rate was faster than the fallout rate of ice crystals, so it could not be measured. The implications of this potentially fast and efficient mechanism to the quantity and location of ice formed in 2AgI·NaI seeded clouds

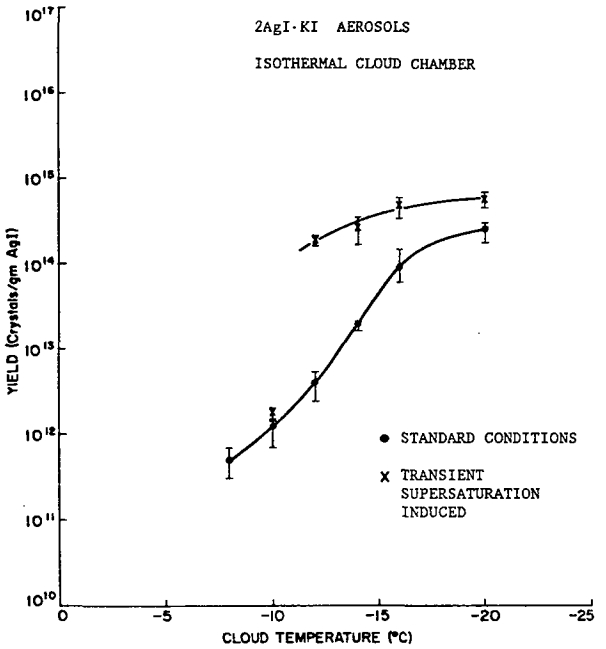

Fig. 5. Average total yields of ice crystals for 2AgI·KI aerosols in the CSU isothermal cloud chamber (data courtesy of Mr. Robert Rilling). Error bars display one standard deviation from mean values (6-10 tests for each set of conditions). These errors are typical for most ICC data.

was demonstrated, using a simple 2-D orographic cloud model, by Blumenstein et al. The 2AgI·KI aerosols displayed similar results to the 2AgI·NaI aerosols when transient supersaturations were induced in the isothermal cloud chamber tests (Fig. 5). The only questions that have remained concern the magnitude of the induced supersaturations and their validity to atmospheric conditions.

The nucleating behavior of 2AgI·NaI and 2AgI·KI aerosols in the presence of realistic atmospheric supersaturations has now been examined using the dynamic cloud chamber. The aerosols were introduced to the cloud chamber either at temperatures of +2°C or -7°C during simulated adiabatic ascents at 2.5 m s^{-1}. Cloud was set to form at 0°C in concentrations comparable to the tests discussed in sections 3.1 and 3.2. The results of the cumulative yield of ice crystals formed as a function of cloud temperature for characteristic tests of the two nucleating aerosols are shown in Fig. 6. Comparing to Figure 2 in Blumenstein et al. and Fig. 5 here, these results can certainly not be explained by the inefficient nucleation mechanism noted for standard ICC conditions. This is particularly true since the nucleation rates were very slow in the standard (no supersaturation induced) ICC tests. With slow nucleation at any given temperature and given the approximately 1°C min^{-1} cooling rates in the DCC tests, the standard ICC yields would never be achieved. Clearly the nucleation mode is different in the DCC. The results agree more with the higher yields and fast rates noted when transient supersaturations were induced in the isothermal tests. These results agree with findings in warm cloud base seeding tests of 2AgI·NaI aerosols, produced by burning solution-impregnated coke samples, reported by DeMott et al. (1985). Those tests also demonstrated the potential of long survival times through warm cloud for these aerosols. In-cloud seeding tests of the 2AgI·NaI and 2AgI·KI nucleating aerosols in the DCC show a slightly higher activity compared to the pre-cloud seeding results. The significance of this is not known at this time.

The 2AgI·NaI and 2AgI·KI complex nuclei are far more efficient than previously thought for the clouds and seeding method simulated, particularly in comparison to the two uncomplexed aerosols. Figures 7 and 8 show the cloud characteristics and ice crystal flux (from the chamber volume) in the below-cloud seeding simulations with similar concentrations of 2AgI·KI and AgI-AgCl aerosols respectively. Ice flux is determined from the number of ice crystals settling from the chamber in each 15 s interval divided by the time and the mass of aerosol injected (based on generator burn rate and sample dilution factors). The scale factors for the ice flux differ due to different generator burn rates (different solution densities). Normalization was not done because the differences were small. The comparison of results in Figures 7 and 8 clearly shows the higher efficiency of the complexed 2AgI·KI aerosols for equivalent seeding simulations. The ultimate activity of the 2AgI·KI aerosols is probably underestimated at temperatures below -14°C, as cloud was completely consumed. This also occurred for 2AgI·NaI aerosols.

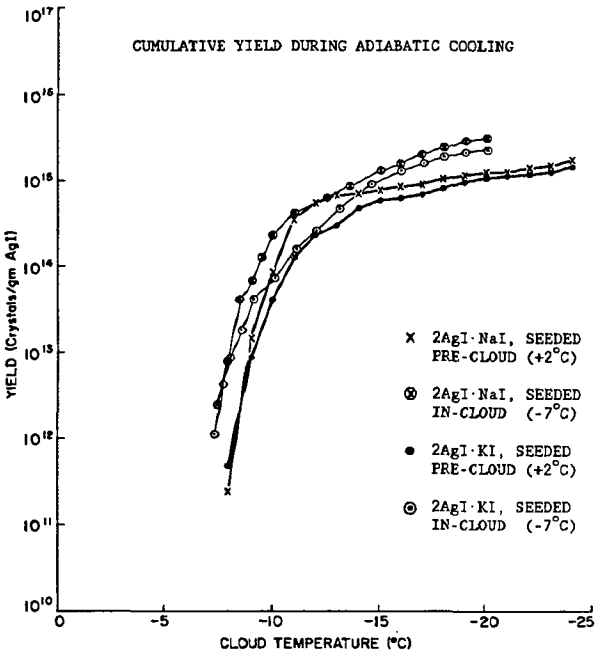

Fig. 6. Cumulative yields of ice crystals formed as a function of cloud temperature for equivalent adiabatic ascent simulations in the DCC using 2AgI·NaI and 2AgI·KI aerosols. The nucleating aerosols were injected at +2°C or -7°C as indicated. Cloud formed at 0°C in all cases, and the cooling rate was ~ 1°C/min (2.5 m s ascent) in cloud.

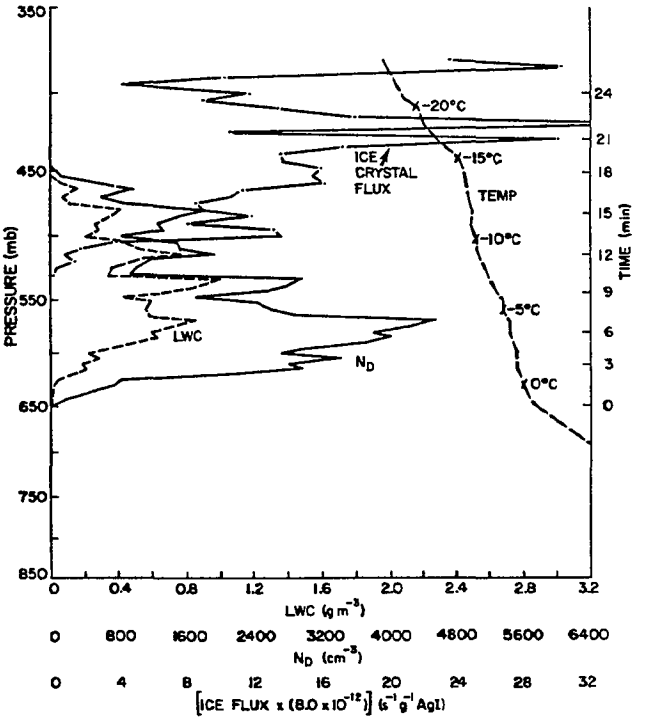

Fig. 7. Temperature, pressure, cloud droplet concentration (N_D), liquid water content (LWC) and ice crystal flux as a function of time after cloud forms in a simulated adiabatic ascent in the DCC seeded with 2AgI·KI aerosols at +2°C.

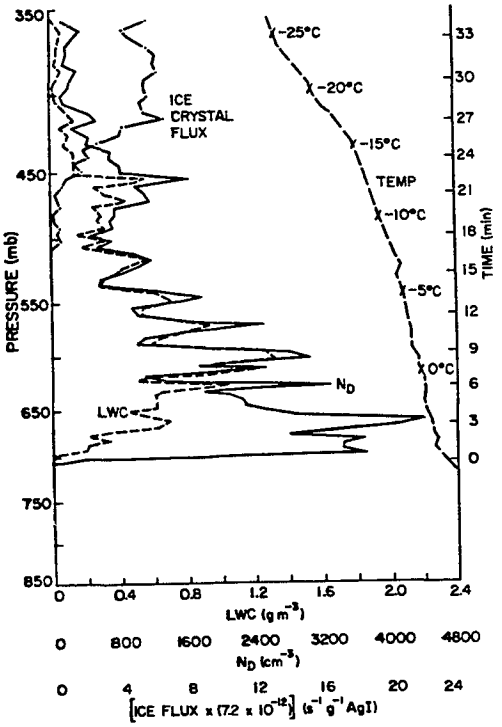

Fig. 8. As in Fig. 7, but for seeding with AgI-AgCl nucleating aerosols prior to cloud formation. The scale factor on ice crystal flux differs slightly due differing mass generation rate.

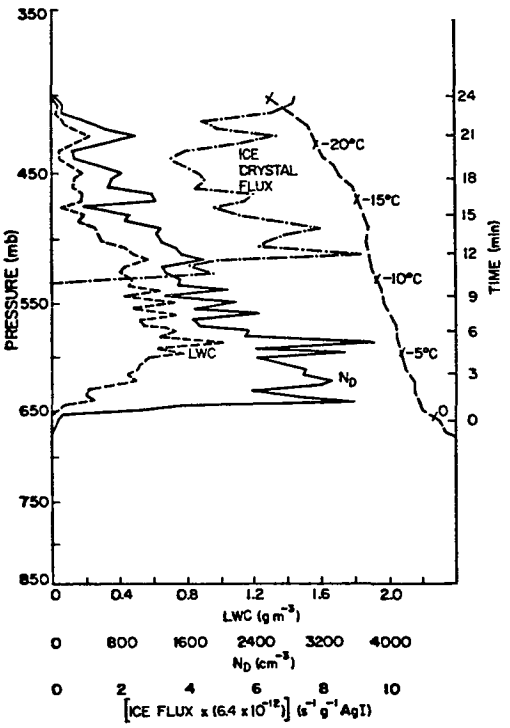

Fig. 9. Same type of data as shown in Fig. 7, but in this case AgI-AgCl-4NaCl nucleating aerosols were injected into cloud in the DCC at -9°C.

In-cloud seeding with AgI-AgCl-4NaCl mixed particle aerosols and the 2AgI·KI aerosols are compared in Figures 9 and 10. The only differences between the two experiments shown were the somewhat lower drop concentrations present with 2AgI·KI (should not matter for condensation-freezing) and the difference in seeding temperatures (-7°C for 2AgI·KI and -9°C for AgI-AgCl-4NaCl). The 2AgI·KI aerosols outperform even the rapid nucleating AgI-AgCl-4NaCl aerosols for this seeding situation. All results were repeatable.

4. CONCLUSIONS

A review of studies of the ice nucleating behavior of various artificial ice nucleating aerosols made during the past several years at the CSU Cloud Simulation and Aerosol Laboratory indicates that the judgement of the potential utility of the aerosols cannot be based on one set of test conditions. The potential mechanisms and rates of nucleation and how these change with cloud conditions must be known in order to quantify or even assess the behavior and ultimate utility of a given ice nucleant in weather modification.

Four nucleating aerosol systems have been discussed to demonstrate the specious nature of a one-dimensional characterization of artificial ice nuclei. AgI-AgCl aerosols show high effectivities as contact-freezing ice nuclei, but long nucleation time constants (due to details of the "contact" step) can prevent this yield from being achieved in real clouds. Also, an immersion-freezing nucleation process which appears to be much less efficient than contact-freezing on these

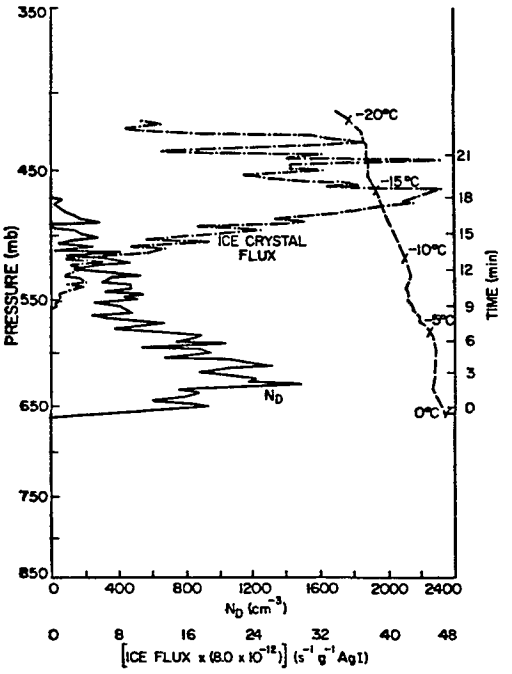

Fig. 10. Same as in Fig. 9, but for 2AgI·KI aerosols injected into cloud in the DCC at -7°C.

aerosols, is active during parcel ascent and cooling in cloud. There was no evidence of rapid nucleation on these hydrophobic aerosols, induced by the naturally occurring supersaturations generated in the DCC. AgI-AgCl-4NaCl aerosols appear to always function by a rapid freezing mechanism at water saturation and above. Although the rate of ice crystal formation is somewhat temperature dependent, yield in atmospheric clouds during parcel ascent (and at least water saturated conditions) might justifiably be approximated as a simple function of temperature. 2AgI·NaI and 2AgI·KI aerosols, once considered inferior ice nucleants based on their low effectivities and slow nucleation rates in standard ICC tests, appear to be ideal for seeding in dynamic cloud conditions. Specific experiments have now been defined to quantitatively characterize the function of all these common ice nucleating aerosols over a broad range of simulated atmospheric conditions. This will allow the most accurate evaluation of seeding effects using numerical cloud models and should help to guide field studies to detect seeding effects.

5. ACKNOWLEDGEMENTS

This research was performed partially under contracts ATM-8407543 and ATM-8519370 with the National Science Foundation. Developments of the dynamic cloud chamber since 1980 have been funded with the support of the Alberta Research Council and the U.S. Air Force. The research reported here was not possible without the efforts and support of Dr. William Finnegan, Ms. Rochelle Blumenstein, Mr. Robert Rilling, Mr. Randy Horn, Mr. Cleon Swain, Mrs. Marion Haurwitz, Mr. Mark Branson and Mrs.Lucy McCall.

6. REFERENCES

Blumenstein, R.R., R. M. Rauber, L.O. Grant and W.G. Finnegan, 1987: Application of ice nucleation kinetics in orographic clouds. J. Clim. Appl. Meteor., 26, 1363-1376.

DeMott, P.J., W.G. Finnegan and L.O. Grant, 1983: An application of chemical kinetic theory and methodology to characterize the ice nucleating properties of aerosols used in weather modification. J. Clim. Appl. Meteor, 22, 1190-1203.

DeMott, P.J., R.D. Horn, W.G. Finnegan, R.R. Blumenstein and L.O. Grant, 1984: Comparison of pre-cloud versus in-cloud seeding using mechanistically different ice nuclei in a "Dynamic" cloud chamber. Extended Abs. 9th Conf. on Wea. Mod., AMS, 4-5.

DeMott, P.J.,W.G. Finnegan and L.O. Grant, 1985: On the effectiveness of artificial seeding from below cumulus cloud base. Proc. 4th WMO Scientific Conference on Weather Modification, 12-14 Aug., 1985, Honolulu, Hawaii, 225-228.

Feng, D. and W.G. Finnegan, 1985: An efficient, fast functioning nucleating agent - Composite AgI-AgCl-NaCl ice nuclei. In, Collected Papers on Met. Sci. and Tech., Selection of cooperative papers by Chinese and American authors, Chang Shu Ping, ed., Meteorological Press, 37-42.

Finnegan, W.G. and R.L. Pitter, 1987: Rapid ice nucleation by acetone-silver iodide generator aerosols and implications to winter orographic storm seeding strategies. Preprints, 11th Conference on Weather Modification, Oct. 6-8, Edmonton, Alta., Canada, 9-10.

Finnegan, W.G., D. Feng and L.O. Grant, 1984: Composite AgI-AgCl-NaCl ice nuclei: Efficient, fast functioning aerosols for weather modification experimentation. Ext. Abs. 9th Conf. on Wea. Mod., 21-23 May, Park City, Utah, 3.

Garvey, D.M., 1975: Testing of cloud seeding materials at the cloud simulation and aerosol laboratory, 1971-1973. J. Appl. Meteor., 14, 883-890.

Lawson, R.P. and R.A. Stewart, 1983: An improved optical ice particle counter. 5th Symp. Meteor. Obs. and Instr., 11-15 April, Toronto, Canada, 46-53.

Rilling, R.R., R.R. Blumenstein, W.G. Finnegan and L.O. Grant, 1984: Characterization of silver iodide-potassium iodide ice nuclei: Rates and mechanisms and comparison to the silver iodide-sodium iodide system. Ext. Abs. of 9th Conf. on Wea. Mod., 21-23 May, Park City, Utah, 16-17.

RAPID ICE NUCLEATION BY ACETONE-SILVER IODIDE GENERATOR AEROSOLS

William G. Finnegan and Richard L. Pitter
Atmospheric Sciences Center
Desert Research Institute
Reno, Nevada 89506, U.S.A.

ABSTRACT. A field test conducted on 10 January 1987 confirmed a postulate that rapid ice nucleation occurs on wet silver iodide aerosols at temperatures below -6 C. The postulate was developed from laboratory tests and is consistent with results from winter orographic cloud seeding programs which have used ground generators sited at mountain tops and along ridges, where they are located within supercooled water clouds during their operation.

1. INTRODUCTION

Winter orographic storm seeding strategies, involving release of hydrophobic silver iodide (AgI) aerosols from ground-based acetone combustion generators, generally assume that the nucleant aerosol is dispersed and that ice nucleation occurs by contact of aerosol particles with supercooled cloud droplets (contact nucleation mechanism) at temperatures of -6 C and lower.

Therefore, ground generators in winter orographic cloud seeding programs are frequently sited at some distance from the target area to allow for transport and dispersion of the AgI aerosol particles. If the generators are located at lower elevations and warmer temperatures, contact nucleation is probably the dominant nucleation mechanism of the AgI aerosols reaching the cloud.

Ground generators are occasionally located at higher elevations and lower temperatures in winter orographic cloud seeding programs. In the Lake Almanor, CA program of the Pacific Gas and Electric Company, the generators are located on ridges immediately upwind of the target area (Stone and Warburton, 1985). Analytical studies of silver (Ag) and indium (In) tracer content in snow from the target area have found that the majority of snow samples from the target area contained Ag and In, despite their proximity to the generators (Stone and Warburton, 1985). If contact nucleation were operating, one would expect the sampling sites in close proximity to the generator either to have no silver or to have silver in a 1:1 ratio with indium, indicating scavenging, because of the slow rate at which contact nucleation proceeds. Thus, modeling studies (Chai, 1987) are unable to account for the 15:1 ratio of Ag to In in the snow close to the generators if it is assumed that AgI functions by contact nucleation. These studies have conclusively demonstrated that there was a much more efficient incorporation of silver into snowfall than possible by contact nucleation. Thus, in the cloud seeding program, the mode of function of AgI aerosol was not by contact nucleation, but rather by some other, more efficient mechanism.

Similarly, in the Bridger Range, Montana, program (Super and Heimbach, 1983), the ground generators were located along a mountain ridge where the ambient temperatures during storms were generally below -6 C. The generators were often in cloud. Aggregated ice crystals in high concentrations were observed at the first ridge top, approximately 2 km from the generators (A. Super, personal communication). The aggregation may have been promoted by high ice crystal concentrations close to the generators. The results from this program also indicate that a fast ice nucleation mechanism, other than contact nucleation, was occurring.

Laboratory studies using the isothermal cloud chamber at Colorado State University have demonstrated that AgI aerosols from field scale generators function exclusively by the contact nucleation mechanism when they are diluted with dry air and injected into the cloud chamber operating at water saturation, and with a liquid water cloud, down to and including -16 C (DeMott et al., 1983).

Laboratory studies (Rilling et al., 1984; Finnegan et al., 1984; Blumenstein et al., 1987) have also demonstrated that the injection of wet AgI-containing aerosols (after dilution with saturated room-temperature air) into the Colorado State University isothermal cloud chamber resulted in very rapid formation of ice crystals at temperatures between -6 and -20 C. Unlike chamber runs when contact nucleation acted, which typically took

30 - 40 minutes to generate the ice, the "wet" aerosols functioned within the first two minutes (including time to fall to the microscope slides). In addition to the rapid rate, the yields of "wet" aerosols at -10 C are a factor of 5 higher than in dry aerosol injection experiments.

It is not generally appreciated that an acetone solution burning AgI generator using an auxiliary propane flame cogenerates copious quantities of water vapor. On complete combustion, acetone and propane yield 0.93 and 1.64 grams of water, respectively, per gram of material burned. Thus, AgI aerosols produced in the field may function by mechanisms other than contact nucleation, due to the presence of the accompanying water vapor when the aerosols are generated into the atmosphere at temperatures below -6 C, the nominal activity threshold temperature for AgI aerosols.

Considering the preceding laboratory and field evidence, it was postulated that acetone burning AgI aerosol generators that use auxiliary propane flames produce ice nucleus aerosols that exhibit rapid and highly efficient nucleating characteristics in cloud or near water saturation conditions and at temperatures of -6 C or lower. This paper describes the field experiment conducted to test the postulate.

2. EXPERIMENTAL

An experiment was conducted between 0500 and 0615 local time on 10 January 1987 at Stead, a rural suburb north of Reno, Nevada. The objective was to determine whether ice crystals would form close to two acetone solution combustion ground generators of AgI aerosols operating below -6 C in a supercooled fog.

The Desert Research Institute (DRI) and the Bureau of Reclamation each operated ground generators during the experiment. The former burned an AgI - NH_4I - acetone - water solution (2% AgI and 0.26% H_2O by weight) in a propane flame (708 liters of propane per hour) to produce 7.3 g AgI per hour. By calculation, it produced 0.63 g H_2O and 0.002 g AgI per second. The latter generator burned an AgI - NH_4I - NH_4CLO_4 - acetone - water solution (3% AgI and 2% water by weight) in a propane flame (approximately 1127 liters propane per hour) to produce 30 g AgI per hour. By calculation, this generator produced a total of 1.25 g H_2O and 0.0083 g AgI per second. A cloud physics van was provided by the Bureau of Reclamation for measurement of wind, temperature, and humidity. It also contained a Particle Measuring System 2D-C ice crystal probe.

During the experiment, a supercooled fog deck covered the area, but did not extend down to ground level. The base was visually estimated to be 50 to 100 feet (15 to 30 m) aloft. The depth of the supercooled fog was unknown. The experiment was conducted in clear air. Initially, the temperature was -8 C, but it fell to -9 C by 0525. Data acquisition was terminated at that point due to mechanical problems. The relative humidity was initially 50%, rising to 60% by 0525. The air was thus about 60% saturated with respect to ice, initially. During the experiment, the winds were light, about 3 m/s, initially from the southwest and changing to easterly by 0530.

Observations of both generators disclosed that visible water vapor (steam) plumes could be seen at the exits, extending a few meters upward. Very small ice crystals in high concentrations were visible in flashlight beams within 30 m downwind of the generators (about 10 s transport time). The ice plumes were tracked, with sporadic success, to 50 - 100 m during the first half hour. Frequent minor wind shifts and the low relative humidity with respect to ice may have impaired efforts to track the plumes. At 0530, the wind shifted and steadied. The temperature continued to decrease, and probably yielded higher relative humidity. The fog never did descend to ground level, however, and generator emissions continued into subsaturated air. After 0530, the plume could be traced 350 m downwind. The plume tracking was limited by a traversing creek. Even at the most distant observation, the ice crystal concentration remained high. Lacking ice replication techniques, we were unable to determine whether ice crystal growth or aggregation had occurred within that distance. The plume widths were estimated to be about 40 m at the most distant observation. The observers concurred that ice crystal concentrations in the Bureau of Reclamation generator plume were higher than those in the DRI generator plume. This may have resulted from the greater emission rates of AgI and H_2O of the Bureau of Reclamation generator.

On conclusion of the experiment, snow powder was observed on the roads approximately 2 km from the generator site in the two major directions downwind of the generators, but in no other directions. An independent observation by another DRI employee indicated that the snowfall signatures extended for several kilometers in the directions of the prevailing winds (Figure 1). The snow may have been produced by the top of the plume lofting into the supercooled fog. The dimensions of the snow swaths, and the extension for several kilometers in the direction of the prevailing winds, all point to the ground based generators as the sources of aerosol particles serving as ice nuclei responsible for the snow.

FIGURE 1

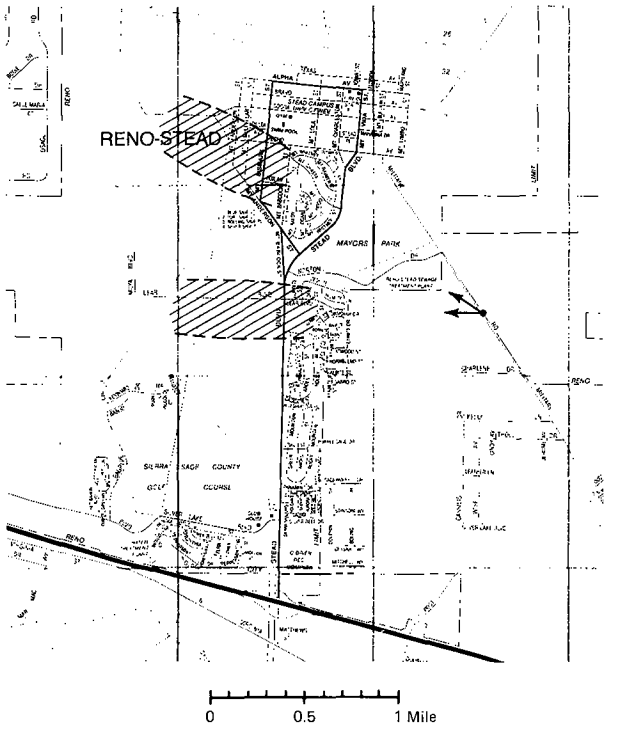

Map of Reno-Stead area of Nevada, showing ground-based generator site (location with two arrows denoting directions of prevailing wind) and areas where snow was observed on the ground after the experiment.

3. DISCUSSION AND CONCLUSIONS

Considering the atmospheric conditions prevailing during these experiments, we conclude that the ice crystals observed resulted from extremely rapid nucleation of aerosols from the generators. We believe the rapid nucleation rate was the result of generator-produced water vapor, and that the mechanism of nucleation was forced condensation-freezing.

There are several important implications of these results. Acetone solution combustion generators operating at temperatures below -6 C under ambient conditions of ice saturation or higher are now believed to rapidly produce high concentrations of small ice crystals, rather than produce AgI aerosols which slowly function by contact nucleation as they diffuse. The results obtained in the Lake Almanor, CA and Bridger Range, MT programs suggest that the fast nucleation process was operative in each program. Thus, seeding strategies in winter orographic cloud programs may be able to take the present observations into consideration to help explain previous results and to plan for future programs.

4. ACKNOWLEDGEMENTS

The authors gratefully acknowledge the participation of Drs. Dave Reynolds, Terry Deshler, and Jim Humpheries of the Bureau of Reclamation, and their enthusiastic operation of their generator and cloud physics van during the experiment. The authors also appreciate the efforts of Riza Oraltay and Renyi Zhang of the Desert Research Institute, who tracked ice plumes through the sagebrush in the dark. Funding was shared by the Desert Research Institute and the National Oceanic and Atmospheric Administration (NOAA) as part of the Federal-State cooperative program (Roger Reinking, Program Manager).

5. REFERENCES

Blumenstein, R.R., R.M. Rauber, L.O. Grant, and W.G. Finnegan, (1987). Application of ice nucleation kinetics in orographic clouds. **J. Climate and Appl. Meteorol., 26,** 1363-1376.

Chai, S., (1987). The theory of ice-nucleating aerosol capture. Report to National Oceanic and Atmospheric Administration.

DeMott, P.J., W.G. Finnegan, and L.O. Grant, (1983). An application of chemical kinetic theory and methodology to characterize the ice nucleating properties of aerosols used for weather modification. **J. Climate and Appl. Meteorol., 22,** 1190-1203.

Finnegan, W.G., Feng DaXiong, and L.O. Grant, (1984). Composite AgI·AgCl·NaCl nuclei: Efficient fast-functioning aerosols for weather modification experimentation. **Preprints,** 9th Conf. on Weather Mod., A.M.S., 3.

Rilling, R.R., R.R. Blumenstein, W.G. Finnegan, and L.O. Grant, (1984). Characteristics of silver iodide-potassium iodide ice nuclei: Rates and mechanisms and comparison to the silver iodide-sodium iodide system. **Preprints,** 9th Conf. on Weather Mod., A.M.S., 16-17.

Stone, R., and J. Warburton, (1985). Phase II - The use of trace chemistry for assessing the seeding effects in the Lake Almanor Watershed. Final Report to Pacific Gas and Electric Company.

Super, A.B., and J.A. Heimbach Jr., (1983). Evaluation of the Bridger Range winter cloud seeding experiment using control gages. **J. Climate and Appl. Meteorol.,** 22, 1989-2011.

FIELD OBSERVATIONS OF ICE CRYSTAL FORMATION IN CLOUDS AT WARM TEMPERATURES

Richard L. Pitter and William G. Finnegan
Desert Research Institute
Atmospheric Sciences Center
Reno, Nevada 89506

ABSTRACT. A field study of the effect of treating a shear line convective cloud with a 20% aqueous solution of ammonium carbonate is described. The results indicate that the presence of certain soluble salts in growing ice crystals may be sufficient to initiate ice crystal multiplication in clouds at temperatures of -4 to -5 C, as measured by a Rosemount instrument, or -3 C, as measured by a reverse flow thermometer. The field results are consistent with laboratory experiments conducted in the Desert Research Institute's cloud chamber, where ice multiplication was observed at temperatures as warm as -4 C. In the cloud chamber experiments, ice multiplication only occurred when crystals were growing rapidly and aggregating. Aggregation was more readily observed when certain soluble salts were added to the water which formed the supercooled cloud. A postulate is advanced as an explanation of the ice multiplication observed in the laboratory and field studies.

1. INTRODUCTION

Weather modification is typically conducted by inducing ice formation in supercooled clouds, either by introducing ice nucleating aerosol particles or by causing homogeneous nucleation with dry ice or liquid propane. A novel departure from this concept, treating clouds with sodium chloride to enhance the formation of large drops, was attempted in the Salt Shaker tests during 1967 (Schock, 1968) and the Cloud Catcher tests from 1969-1972 (Dennis et al., 1974).

Our recent laboratory results revealed an interesting phenomenon occurring in supercooled clouds. Ice multiplication occurred at temperatures from -4 to -30 C, without the presence of graupel particles. The study also found a strong correlation between the soluble salts contained in the water and whether a particular experimental run developed ice multiplication. When multiplication occurred, there was a strong correlation between the salt used and the rate with which ice multiplication occurred. Since the soluble salts were added to distilled, deionized water at 10^{-4} normal concentration, consistent with those found in cloud and precipitation water, we attempted a field experiment to see whether ice multiplication could be initiated in a cloud with a sufficient quantity of an appropriate soluble salt. The field experiment, described in the following section, dispensed a 20% solution by weight of ammonium carbonate [$(NH_4)_2CO_3$] in water into a shear line convective cloud at -4 C. The results, described in Section 3, reveal a high correlation between the detection of the treated volume, using sulfur hexafluoride as a tracer, and the presence of both some large, aggregated ice crystals and many small (less than 100 micrometers long) ice crystals. Section 4 describes the laboratory experiments which led to the field study, and Section 5 presents our postulate of how ice multiplication might have occurred. Section 6 presents a conclusion of the study and its impact.

2. PROCEDURE

During the NOAA-North Dakota field program at Dickinson, ND in June, 1987, arrangements were made for a seeding aircraft to dispense a concentrated solution of ammonium carbonate (20 percent by weight in water) from one wing, using a Lohse acetone-silver iodide generator with the flow restrictor removed. In this manner, the aircraft dispensed a few kilograms of solution on 1 July, 1987 between 11:34:41 and 11:40:24 while flying at -4 C in a cloud formed by shear line convergence. The drop size distribution produced by the pressurized spraying was not measured.

Simultaneously, 22.9 kg of sulfur hexafluoride gas were released from the aircraft to serve as a tracer for the treated volume of air. After dispensing the two agents, the seeder aircraft left the scene and the North Dakota Citation aircraft equipped with cloud physics instrumentation and a Scientech LDS-3 sulfur hexafluoride monitor repeatedly penetrated the cloud in search of the seeding signature.

The cloud selected for the experiment was a weak shear line cloud, selected primarily because of the unavailability of any isolated cumuli clouds during the short field season. Although the selected cloud was not considered ideal from a treatment/effect viewpoint, it allowed excellent repeated examination of the treated cloud volume.

The North Dakota Citation aircraft contained the usual cloud physics instrumentation: temperature, pressure, etc., and a 2D-C probe which was used in the identification of small ice particles.

The Citation investigated the cloud from 11:40 to 12:07. In that period, it detected strong pulses of the SF_6 tracer seven times. Although there is an unavoidable separation with time between a gas plume and a plume of water droplets released simultaneously, due to the terminal velocity of the drops, the SF_6 plume served as a tracer for the treated volume of the cloud. Thus, we sought differences in the nature of the ice particles between portions of the cloud tagged with SF_6 and otherwise.

3. FIELD STUDY RESULTS

The flight track (Figure 1) indicates that the seven intersections with the SF_6 plume were detected. The SF_6 monitor is sensitive to parts per trillion concentrations and has a response time of three seconds. Extrapolation of the air parcels where SF_6 peaks were detected backward in time, using the aircraft-computed winds, resulted in placement of the sampled parcels in close proximity to the treated parcel in space and time (shaded oval to west of flight path). In this sense, the selection of a weak shear line was probably optimal for allowing multiple plume intersections.

Table 1 summarizes ice particle sizes and concentrations detected during the experiment. During each of the seven plume intersections, the 2D-C probe detected ice crystals present in concentrations exceeding 1 per liter (as high as 70 per liter). In six of the seven intersections, the average ice particle size was 500 +/- 50 micrometers diameter, while the seventh event exhibited a mean ice particle size of about 1160 micrometers. By comparison, three occurrences of ice particles in excess of 1 per liter were found unassociated with SF_6 peaks. The ice concentrations varied from 1 to 6 per liter in these events, and the mean ice particle diameters varied from 840 to 1730 micrometers, with an average value of 1220 micrometers.

FIGURE 1

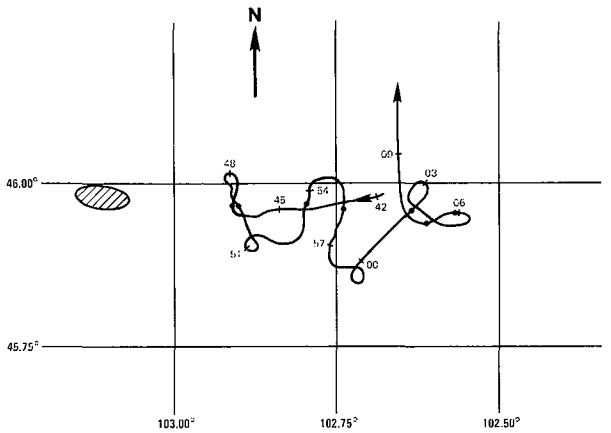

Flight track of cloud physics aircraft, with time pips (beginning at 1142 local time and ending at 1209) and circles to indicate where the sulfur hexafluoride plume was detected. The shaded oval to the west indicates where air parcels in which sulfur hexafluoride was detected would be extrapolated to, based on aircraft-detected winds, at the time of the tracer release. This region corresponds with the position of the seeder plane at the time of release.

TABLE 1

COMPARISON OF ICE CRYSTAL CONCENTRATIONS IN AND OUT OF SF_6 PLUMES

IN PLUME

TIME	TEMP. C	L.W.C. g/m^3	ICE CONC. $liter^{-1}$	MEAN ICE PARTICLE DIAM., um
11:46:48	-4.8	0.05	1 - 5	500
11:49:10	-5.0	0.05	35 - 40	500
11:53:26	-4.7	0.06	1 - 5	480
11:55:58	-4.6	0.10	5 - 10	450
12:01:47	-4.6	0.07	15 - 20	450
12:06:02	-4.6	0.12	65 - 70	1160
12:07:01	-5.2	0.00	20 - 25	550

OUTSIDE PLUME

TIME	TEMP. C	L.W.C. g/m^3	ICE CONC. $liter^{-1}$	MEAN ICE PARTICLE DIAM., um
11:51:20	-4.4	0.09	1 - 5	1730
11:56:50	-5.0	0.04	1 - 5	1110
12:04:30	-5.0	0.21	5 - 10	840

The Citation data was first analyzed by Dr. T. Grainger of the University of North Dakota, who brought attention to the strong coincidence of both high ice particle concentrations at -4 to -5 C and smaller particle sizes with the detection of SF_6.

The plume intersections occurred between six and 33 minutes after treatment, yet the ice particles in the treated parts of the cloud averaged about 500 micrometers diameter, independent of elapsed time from treatment. If the ice crystals were nucleated at the time of treatment, then we would expect an increase in size of the ice particles with time. Rather, the 2D images reveal that both larger, aggregated ice crystals and smaller (less than 200 micrometer) ice crystals present.

There is some similarity in the 1987 field experiments and one conducted in 1970, in which one end of a convergence line stratocumulus cloud was seeded with sodium chloride (Biswas and Dennis, 1971). The 1970 experiment released 150 kg of powdered salt just beneath cloud base in the southern part of the cloud. Although some communications (Havens, 1972; Blanchard, 1972) pointed to the complicating facets of prior silver iodide seeding and a cloud top temperature of -10 C, Biswas and Dennis (1972) indicated that the initial silver iodide treatment was ineffective.

The principal difference between the 1970 experiment and the present results lies in interpretation of the cloud physics mechanisms which were operating. Biswas and Dennis (1972) estimated that the salt seeding involved considerably fewer than 7×10^{14} condensation nuclei, while the induced shower consisted of roughly 2×10^{15} raindrops, and thus concluded that some chain reaction (drop breakup) operated in the cloud. They did not penetrate the cloud with aircraft, so they were unable to ascertain that ice was not present. We attribute the present results to ice multiplication, on the basis of the high concentrations of small ice particles at warm temperatures. We suggest that ice multiplication also may have occurred in the 1970 experiments.

The initiation of ice at temperatures warmer than -8 C by heterogeneous nucleation is rare, meteorologically, due to the scarcity of suitable ice nuclei. Silver iodide works poorly at -6 C, and more readily at temperatures of -8 C and below. Treatment with ammonium carbonate was not expected to yield ice forming nuclei. Additionally, studies with gaseous SF_6 dispensing during these NOAA-North Dakota experiments revealed no tendency for the SF_6 to nucleate ice crystals in clouds (personal communication, Don Griffith, North American Weather Consultants). Although the possibility of aircraft-produced ice particles (APIPs) (Rangno and Hobbs, 1983) exists, Rangno and Hobbs found APIPs only at much colder temperatures than were involved in the present study. They noted APIPs at between -12 and -20 C, with one exception at -7 C in descending virga. Their results don't indicate whether or not APIPs might be generated above -5 C.

The field study did not collect enough data to test a hypothesis with statistical rigor. Rather, it attempted to determine whether or not a signal could be sensed. It was designed after laboratory experiments indicated that ice multiplication occurs under conditions of rapid ice crystal growth and aggregation, and is enhanced by the presence of certain soluble salts initially dispensed within the cloud water. The field test demonstrated that higher concentrations of smaller crystals were found associated with the trace gas peaks, although the treatment was conducted with a 20 per cent solution of ammonium carbonate in water, which is not an ice nucleating agent. The following section details the laboratory experiments which led to the field study.

4. LABORATORY EXPERIMENTS

Laboratory experiments were conducted in the Desert Research Institute's 6.7 m^3 cloud chamber, which is described by Steele et al. (1981). The chamber was operated at ambient pressure (about 850 mb) and constant temperature during each experimental run. Temperatures investigated ranged from -2 to -30 C. The chamber contained a supercooled liquid water cloud of 1.5 to 3.0 g m^{-3}, generated by ultrasonic nebulizers, and was then nucleated by adiabatic expansion of moist air, similar to the technique described by Vonnegut (1948).

The water used to form the supercooled cloud was distilled, deionized water or water containing 10^{-4} normal solutions of dissolved salts. The concentrations of sodium nitrate ($NaNO_3$), sodium chloride (NaCl), ammonium sulfate [$(NH_4)_2SO_4$], or ammonium carbonate [$(NH_4)_2CO_3$] used are typical of the ionic concentrations found in clouds and precipitation.

The experimental results indicate that, under appropriate conditions, ice multiplication occurs between -4 and -30 C. The conclusions were based on several independent observations. The observations are as follows:

1. Time of ice presence -- the ice particles grow rapidly and settle out of the limited volume. Depending on the temperature (which controls the habit and drag characteristics), the ice particles fall out of the chamber within 3 to 8 minutes. However, experiments often lasted more than 10 minutes, occasionally more than an hour. One explanation for longer experiments is the action of ice multiplication generating new ice crystals.

2. Laser transmissivity characteristics. Petrushin (1983) noted that non-spherical ice particles scatter electromagnetic radiation of wavelength approximately their diameter much more strongly than other wavelengths. The laser transmissometer used in the experiments for measuring liquid water content (Gertler and Steele, 1980) always responded with increased attenuation just after the initial ice nucleation, as the crystals grew through 10.2 micrometers diameter (the CO_2 laser wavelength). Transmissivity then would normally increase as the liquid water cloud was consumed by the growing ice crystals. However, the longer-lasting experiments exhibited sporadic attenuation pulses in the laser, which were interpreted as effects of populations of newly-formed small ice crystals growing through the 10 micrometer size.

3. Dual-wavelength laser attenuation -- in addition to the CO_2 laser, a 0.55 micrometer wavelength HeNe laser, usually used to aim the CO_2 laser, was employed. During the longer experimental runs, the attenuation pulses of the CO_2 laser were preceded several seconds by similar attenuation pulses in the HeNe laser, indicating that crystals were first growing through the 0.55 micrometer size, and subsequently growing through the 10 micrometer size.

4. Microscopic observation -- crystals which fell onto glass microscope slides typically revealed ice crystals of similar size and shape during short experimental runs, indicating that they were nucleated together and grew at the same rate. During the longer runs, the ice crystal populations were polydisperse, with small crystals always present. This presence of smaller crystals is interpreted as evidence of new nucleation, at a later time, and hence to ice multiplication in the course of the run.

5. Microscopic observation -- signs of ice multiplication were only noted when aggregation of ice crystals also occurred.

6. Temperature and the solute present in the cloud water affected the probability of ice multiplication occurring during any particular experimental run.

Of significant importance, ice multiplication was only noted when existing ice crystals were rapidly growing and aggregating. The soluble salts contained in the supercooled cloud water exerted strong influence on whether or not ice multiplication occurred during any particular experimental run. Ice multiplication was also noted more readily at temperatures close to -6 and -16 C, where thin needles and dendrites are produced. The results were consistent with our previous studies of the factors which give rise to the greatest electric potentials across growing ice crystal interfaces, and led us to postulate that the intense electric fields which could result during the aggregation of such ice crystals might be capable of nucleating new ice crystals. The theory is expanded in the following section.

5. THEORETICAL BASIS

The North Dakota field studies indicate that small ice crystals may be continually generated by some process at warm temperatures due to the presence of the 20% ammonium carbonate solution liquid water plume, as traced by gaseous SF_6. The laboratory studies presented above substantiate the field experiments and further emphasize the effects of certain soluble salts on ice multiplication. The authors know of no existing theory that explains nucleation or ice multiplication under the observed conditions. Therefore, we take the liberty to postulate how ice multiplication may have occurred.

Finnegan and Pitter (1986) postulated the existence of electric multipoles in growing ice crystals due to the differential incorporation rate of anions or cations in the ice crystal matrix, an extension to three dimensions of the commonly-observed freezing potential called the Workman-Reynolds effect (Workman and Reynolds, 1950; Gross, 1968). This effect results in a potential difference of several to several hundred volts across a growing interface of ice and water. The potential difference is dependent on the rate of interface advance and the soluble ions present.

The electric multipole postulate states that the ice phase acquires an electric charge of one sign as a result of differential incorporation of ions, and the liquid-like layer of the growing crystal acquires charge of the same magnitude but opposite sign, principally in the regions where the linear rate of growth of the ice crystal lattice is greatest. When growth ceases, the charge separation collapses due to recombination effects.

Manifestation of the effect of electric multipoles was first realized in the T-shaped aggregates known to be produced under appropriate conditions (Odencrantz et al., 1968; Magono and Tazawa, 1972). Other manifestations of the effect of electric multipole include

enhanced aerosol scavenging by growing ice crystals (Pitter and Finnegan, 1986).

The multiplication of ice in the cloud chamber parallels a phenomenon known in solution crystallization as crystal breeding, or false grain, whereupon colloidal suspensions of high concentrations of growing crystals (i.e., sugar) initiate spontaneous nucleation of new, smaller crystals (Van Hooke, 1961). The mechanism responsible for crystal breeding is unknown, but electrostatic effects are suspected.

6. CONCLUSIONS

We interpret the aircraft data to substantiate our laboratory experiments which indicate ice multiplication occurring under appropriate growth conditions in a manner analogous to crystal breeding or false grain reported in the crystallization literature. An important component in this mechanism is the presence of soluble salts in the cloud water which provide strong freezing potentials. This result, if substantiated, provides a method for modifying clouds which are too warm to treat with silver iodide, and additionally provides a long-lasting, self-perpetuating mechanism for propagating ice.

A link between crystal breeding from solution crystallization and ice multiplication in atmospheric clouds has been postulated, with laboratory and field evidence in support of an effect caused by the presence of soluble salts which result in greater potential differences across growing interfaces of ice. This postulate of a new ice multiplication mechanism requires additional study before it can be established as fact, but our preliminary results are encouraging in this respect.

These results need to be substantiated by further experimentation before the technique is operationally used for weather modification. Potential benefits of the use of ammonium carbonate include (1) ease of dispensing -- the experiment utilized existing silver iodide generator equipment with slight modifications; (2) inexpensive; (3) absence of silver; (4) environmentally safe (ammonium carbonate is a fertilizer); (5) ease of handling (non-toxic); (6) effective at -4 C; and (7) long-lasting, self-perpetuating effect.

7. ACKNOWLEDGEMENTS

The authors thank the following for assistance in the experiment in North Dakota during June, 1987: Lynn Rose, Director, North Dakota Weather Modification Program, the Dr. C. Tony Grainger of the University of North Dakota for providing the cloud physics data from the Citation, and Don Griffith and George Wilkerson of North American Weather Consultants for providing the sulfur hexafluoride tracer data. Funding for this experiment was provided by the National Oceanic and Atmospheric Administration (NOAA) as part of the Federal-State cooperative program (Roger Reinking, Program Manager).

8. REFERENCES

Biswas, K.R., and A.S. Dennis, 1971: Formation of a rain shower by salt seeding. **J. Appl. Meteorol., 10,** 780-784.

Biswas, K.R., and A.S. Dennis, 1972: Calculations related to formation of a rain shower by salt seeding. **J. Appl. Meteorol., 11,** 755-760.

Blanchard, D.C, 1972: Comments on "Formation of a rain shower by salt seeding." **J. Appl. Meteorol., 11,** 556-557.

Dennis, A.S., P.L. Smith, Jr., B.L. Davis, H.D. Orville, R.A. Schleusener, G.N. Johnson, J.H. Hirsch, D.E. Cain, and A. Koscielski, 1974: Cloud seeding to enhance summer rainfall in the northern plains. Report 74-10, prepared for Division of Atmospheric Water Resources Management, Bureau of Reclamation, by the Institute of Atmospheric Sciences, South Dakota School of Mines and Technology.

Finnegan, W.G., and R.L. Pitter, 1986: Study of the initial aggregation of ice crystals. **Preprints**, Conference on Cloud Physics, Snowmass, CO, C110-C112.

Gertler, A.W., and R.L. Steele, 1980: Experimental verification of the linear relationship between IR extinction and the liquid water content of clouds. **J. Appl. Meteor., 19,** 1314-1317.

Gross, G.W., 1968: Some effects of trace inorganics on the ice/water system. **Trace Inorganics in Water.** Advances in Chemistry Series, 73. American Chemical Society, Washington, D.C., 27-97.

Havens, A.V., 1972: Comments on "Formation of a rain shower by salt seeding." **J. Appl. Meteorol., 11,** 557.

Magono, C., and S. Tazawa, 1972: Aggregation phenomena of ice crystals. **J. Meteorol. Soc. Japan, 50,** 489-495.

Odencrantz, F.K., W.S. McEwan, P. St. Armand, and W.G. Finnegan, 1968: A mechanism for multiplication of atmospheric ice crystals: Apparent charge distribution on laboratory crystals. **Science, 169,** 1345-1346.

Petrushin, A.G., 1983: Extinction and scattering of infrared radiation by polydisperse systems of ice plates and cylinders. **Izv., Atmos. Oceanic Phys., 19**, 197-201.

Pitter, R.L., and W.G. Finnegan, 1986: Effect of the size distribution of falling snow on aerosol particle scavenging. **Preprints**, Conference on Cloud Physics, Snowmass, CO, C71-C74.

Rangno, A.L., and P.V. Hobbs, 1983: Production of ice particles in clouds due to aircraft penetrations. **J. Clim. Appl. Meteorol., 22**, 214-232.

Schock, M.R., 1968: Analysis of a randomized salt seeding experiment on cumulus clouds. M.S. Thesis, Department of Meteorology, South Dakota School of Mines and Technology.

Steele, R.L., A.W. Gertler, U. Katz, and D. Lamb, 1981: Cloud chamber studies of dark transformations of sulfur dioxide in cloud droplets. **Atmos. Environ., 15**, 2341-2342.

Van Hooke, A., 1961: **Crystallization Theory and Practice.** Reinhold Publ. Co., New York.

Vonnegut, B., 1948: Production of ice crystals by the adiabatic expansion of gas. **J. Appl. Phys., 19**, 959.

Workman, E.J., and S.E. Reynolds, 1950: Electrical phenomena occurring during the freezing of dilute aqueous solutions and their possible relationship to thunderstorm electricity. **Physical Review, 78**, 254-259.

USE OF UNIQUE FIELD FACILITIES TO SIMULATE EFFECTS OF ENHANCED RAINFALL ON CROP PRODUCTION

Stanley A. Changnon and Steven E. Hollinger
Climate and Meteorology Section
Illinois State Water Survey
Champaign, Illinois 61820

1. INTRODUCTION

The major goal of the weather modification research in Illinois has been to develop a technology in rainfall enhancement that would result in increased Illinois crop yields and a reduction in the year-to-year variations of crop yield (Changnon, 1986). Much of what has been assessed about the value of added water on crop yields in Illinois has come from the use of crop yield-weather models based on historical records of yields and past weather conditions (Garcia et al., 1987). The actual rainfall amounts have been used as inputs to regression type models and the predicted yields with the effects of additional rainfall compared to those yields estimated with natural rainfall. The model results point to the importance of summer weather conditions, particularly the July and August rainfall. However, the basis of their computation and the related assumptions leave the prediction of yield increases apt to be obtained too uncertain. Thus, actual field experiments are needed to evaluate and quantify the effects of differing amounts of additional rainfall on crop yields.

In the spring of 1987, recently constructed "rain shelters" became available in which field experiments of rain effects on crops could be conducted. Some shelters were designed to be moved over the test plot area during a rain event to exclude natural rain. When there was no precipitation falling, the shelters could be moved off the plots so the plants experienced the same weather as other crops in the region. An overhead sprinkler irrigation system was installed in the shelters so the time, amount, and quality of water applied to each plot could be controlled. This system allowed for the establishment of an experimental design to begin to test the validity of the crop-weather model results in an actual field situation. This paper addresses the 1987 field experiment, the facility, the rain models used, and the yield results.

2. EXPERIMENTAL METHOD

A multi-year field experiment was established in the spring of 1987 to determine the effects of augmentation of natural rainfall through rain increases on crop yields. Two shelters, one movable and the other stationary, were used in the 1987 experiment. The stationary shelter was left open so that natural (1987) rainfall could reach the crop and soil, and was fitted with a suspended overhead sprinkler irrigation system that allowed the application of additional water on each plot. The sprinkler nozzles were raised as the crop grew so that the database between the sprinklers and the top of the crop was 1.2 m. The plots in the stationary open shelter were treated with predetermined amounts of water added to the actual 1987 daily rainfall.

The water treatments in the movable shelter were designed to test the effects of added rain during a typical dry summer, a typical average rainfall summer, and a typical wet summer. The 1987 experiment will be replicated in 1988 and other growing seasons. The 1987 water additions began 1 June and ended on 31 August.

Corn (a Mo17 x B73 Cross) and soybeans (a Williams variety) were planted in the stationary (open) and mobile (covered) shelters on 28 May 1987. Prior to planting the corn, 341 kg ha^{-1} of nitrogen, 94 kg ha^{-1} of potassium, and 94 kg ha^{-1} of phosphorus were applied. The corn was planted in a 0.76 m spaced rows at a population of 64,220 plants ha^{-1}. The soybeans were planted with the same row spacing as the corn with a plant density of 430,000 plants ha^{-1}. The plots are both situated on a Drummer silty clay loam soil (fine-silty mixed mesic Typic Haplaquolls), a naturally poorly drained soil that had been artificially drained. These conditions are typical of those found through much of Illinois. The plots are located in east central Illinois on the University of Illinois Agricultural Experiment Farms at Urbana. The shelters were provided by the University of Illinois Agronomy Department.

3. FACILITIES

3.1 Stationary Shelter

The stationary shelter was an aluminum framework supporting a series of controllable nozzles, each centered over a 3x3 meter plot. The amount of water going to each of 6 plots could be individually controlled.

Ten different rainfall treatments were replicated three times. The ten treatments, consisted of additional water applied to various plots after each rain event. The water was totally deionized, and then ions added to make the water match that local rainwater. The additional rain increments were applied in the morning after determining the previous day's rainfall at 0700. Figure 1 shows a map of the field plots and the ten treatments.

S - 1	S - 7	S - 6	C - 1	C - 4	C - 1
S - 3	S - 7	S - 4	C - 9	C - 5	C - 8
S - 10	S - 4	S - 3	C - 1	C - 3	C - 7
S - 5	S - 2	S - 5	C - 3	C - 7	C - 9
S - 3	S - 6	S - 1	C - 2	C - 2	C - 10
S - 10	S - 7	S - 6	C - 9	C - 5	C - 5
S - 9	S - 2	S - 8	C - 3	C - 2	C - 7
S - 1	S - 9	S - 10	C - 4	C - 10	C - 4
S - 2	S - 4	S - 9	C - 6	C - 6	C - 10
S - 5	S - 8	S - 8	C - 8	C - 6	C - 8

1 = Natural Rainfall for 1987
2 = Increase all daily rains 10%
3 = Increase all daily rains 25%
4 = Increase all daily rains 40%
5 = Increase all daily rains of 0.254 cm to 2.54 cm by 10%
6 = Increase all daily rains of 0.254 cm to 2.54 cm by 25%
7= Increase all daily rains of 0.254 cm to 2.54 cm by 40%
8 = Increase all daily rains above 2.54 cm by 10%
9 = Increase all daily rains above 2.54 cm by 40%
10 = Increase all daily rains less than 0.254 cm by 40%

a. Test plots for the stationary (uncovered) experiments

C - 5	C - 2	C - 2
C - 2	C - 6	S - 1
C - 1	C - 5	C - 5
C - 3	C - 3	C - 4
C - 4	C - 1	C - 6
C - 6	C - 4	C - 3
S - 6	S - 3	S - 2
S - 1	S - 5	S - 5
S - 5	S -6	S - 4
S - 3	S - 2	S - 6
S - 2	S - 1	S - 1
S - 4	S - 4	S - 3

1 = Normal Rainfall
2 = Normal Rainfall plus 25%
3 = Typical Dry Year
4 = Typical Dry Year plus 25%
5 = Typical Wet Year
6 = Typical Wet Year plus 25%

b. Test plots for the mobile (covered) experiments

Figure 1. Patterns of field plots.

3.2 Mobile Shelter Experiment

The mobile shelter consisted of an aluminum frame covered by plastic with a suspended sprinkler system. The shelter was mounted on a track and moved on or off the test plots by a motor triggered by an automatic rain switch. By this means, all natural rainfall was excluded from the plots. The area covered was 10 by 40 meters and contained 36 test plots (each 3x3 m), each with individually controlled sprinkler nozzles centered over the plot. Figure 1 is a diagram of the plots in the shelter. Figure 2 presents photographs of the nozzles and the soybean planted portions of the shelter. The experiments conducted here studied the effects of altered rain level, applied to represent the effects of a typical average summer, a typical wet summer, and a typical dry summer, on crop yields. The typical average, wet, and dry summer were based on historical climate values from Urbana, Illinois. Water applications were conducted at times specified in the models developed using historical precipitation data. The water applications to simulate added rainfall due to weather modification were 25% more than the daily amount designated in the models.

4. SUMMER RAINFALL MODELS

The typical summer seasons were designed using the long-term (1888-1986) average values of rainfall for June, July and August; the statistical distribution of rain days for each month; and the temporal distribution of rain days and rain amounts for each month. The results of this climatic design became "summer (Jun-Aug) rain models" for (1) an "average" summer, (2) a typical "wet" summer, and (3) a typical "dry" summer. Each summer type was defined using the data for the 18 wettest summers, the 18 driest summers, and the 18 summers having rain values nearest the 99-year average at Urbana. The monthly values selected for composing the wet, the near average, and the dry summers were based on the probability distributions of monthly rain values (Changnon, 1959).

The frequency distributions of rain days during each type of summer were determined by analysis of the monthly frequencies in the 1888-1986 Urbana climate record. The resulting average frequencies of rain days for the wet, average, and dry summers are presented in Table 1.

4.1 Average Summer Model Calculations.

The daily rain day distributions for 0.254 mm (0.01 inch) increments were the basis for calculating the actual amounts for the average summer conditions. As shown in table 1, an "average summer" in Urbana has 26 days of $\geq$0.254 mm of rain. The frequency distributions show that 40% of these days, or 10

Covered shelter with soybean plots

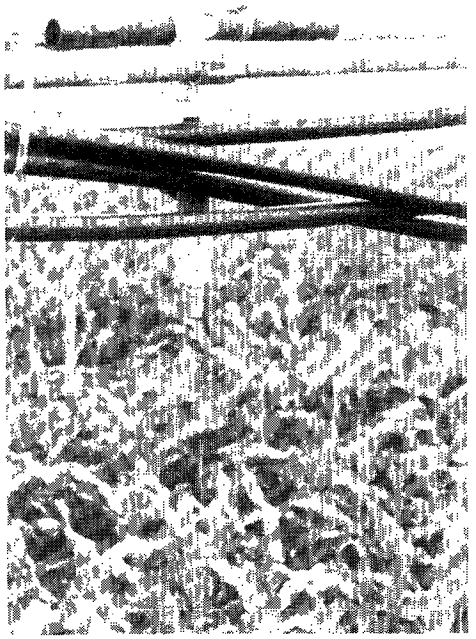

Nozzle used to apply water to 3x3 meter test plots in both shelters

Figure 2. Field facilities.

Table 1. Rain day frequencies for Urbana, Illinois, 1901-1985

Summer Month	Days with Rainfall ≥0.254 mm Wet	Avg	Dry	≥6.35 mm Wet	Avg	Dry	≥12.7 mm Wet	Avg	Dry	≥22.8 mm Wet	Avg	Dry
June	12	10	10	7	5	4	5	3	2	2	1	1
July	10	8	7	5	4	3	3	2	1	2	1	0
August	10	8	7	4	3	2	3	2	1	1	1	1
TOTALS	32	26	24	16	12	9	11	7	4	5	3	2

rain days, were composed of values between 0.254 (0.01 inch) and 2.54 mm (0.1 inch). In this latter category, ten evenly distributed values were selected for insertion in the "average" summer rain model, with values ranging from 0.254 up to 2.54 mm.

These ten values were then distributed amongst the three summer months according to the magnitude of the 0.254 mm values (table 1), such that 4 rain days in this category were assigned to June, 3 to July, and 3 to August.

The amounts assigned within each month were decided based on the magnitude of the average monthly rainfall amounts. That is, the June average is 101.6 mm which is 36% of the summer total of 279.4 mm; the July average was 86.36 mm which is 31%; and the August average was 91.44 mm which is 33%. The sum of the 10 values was 15.24 mm, and application of the June percentage (36) to this resulted in 5.588 mm. Four rainfall values from the 10 were selected so that their sum approximated 5.588 mm. The values selected were 0.508, 0.762, 1.778, and 2.54 mm. This process was then repeated for the days in July and August.

A similar approach was used for determining and assigning heavier rainfalls for each of the 2.54 mm rain day categories (and the average summer). The 2.794 to 5.08 mm daily rain events represented 13% of all rain days, and three rain days were assigned to this category for the summer (1 in June, 1 in July, and 1 in August). Three days (1 each month) were also assigned to the 5.334 to 7.6 mm category.

Each of the 2.54-mm categories from 7.62 mm up through 22.8 mm averaged one rain day during the summer. The rain amount chosen and assigned to each of the rain categories was in the middle of the range (i.e., 8.8 mm for the 7.8 to 10.1 mm range). The six largest values were distributed with 2 assigned in June, 2 in July, and 2 in August. The distribution was such that each month received approximately 33 mm of total rainfall from these days. The final moderately heavy rain day values selected were 15.4 and 17.7 mm for June; 8.8 and 22.8 mm for July; and 12.4 and 21.5 mm for August.

The average summer also has three rain days with ≥22.8 mm, and these were assigned one to each

month. Their magnitude in each month was established by summing all the other daily values already assigned, and subtracting those totals from the monthly average total. For example, in June, the 9 daily rain values less than 22.8 mm already selected totaled 58.2 mm. The difference between this value and the monthly mean of 101.6 mm for June is 43.4 mm; therefore, the greater than '22.8 mm' value used for June was 43.4 mm.

All rain days thus selected for each month were then distributed at dates using available climatic information. Feyerherm et al. (1966) showed that 50% of all summer rain days in central Illinois are followed by another rain day, but that the likelihood of 3 days of rain in a sequence is extremely small, less than 6%. Therefore, half of the summer rain days were "coupled" so that there would be two rain days in a row. For example, half of the rain days in June (6 of the 10) were used to form 3 pairs of rain days. Furthermore, each pair formed consisted of a relatively high and a moderately low rain value since past Urbana rain data (1951-70) revealed that 91% of such paired daily values differed by 50% or more.

The final temporal distribution of rain days throughout each month was based on 85-year amounts of rain per date and on probabilities of dry periods (Changnon, 1959). These provided information as to which dates of each month were apt to be in the wet or dry periods. The "wetter" summer periods included 8-15 June, 23-28 June, 2-5 July, and 10-19 August. The daily rain amounts selected were concentrated in these 'more likely' rain periods. For example, there are 10 days with 0.254 mm or more rain in June in an "average summer"; and, seven of these days were distributed within the two June 'wetter' periods. Two of the 8 July rain days were put in the 2-5 July period, and 4 of the 8 measurable rain days in August were distributed within the 9-day period of 10 to 18 August. The remaining rain days in each month were then randomly distributed amongst the other parts of each month, but such that no rainless period persisted for more than 7 days (an event with a low probability, <7%, for summer).

4.2 Wet and Dry Summer Rain Models

The rain-day distributions (by calendar dates) for the dry and wet summers were much the same as that set for the average summer. The magnitudes of rainfall on a rain day were adjusted for the wet and dry summers to match monthly averages, but not the rain dates; however, certain rain days identified in the average summer were deleted in the dry summer, and some days were added in the wet summer to conform to the values shown in table 1.

The amount of rain assigned to each rain day was determined by: 1) using the average monthly rainfall in wet and dry summers; and 2) using the rain day frequencies (table 1) to guide adjustments of the average summer daily values already selected. The mean June, July, and August rainfalls in the wet and dry summers were obtained from frequency curves (Changnon, 1959). These showed that the 20% frequency level (the wettest 18 years), a dry June had 70% of the June average rainfall, and a 20%-level wet June had 137% of the average rainfall.

The average of the rain day frequencies for the four rainfall levels shown in table 1 were used to determine the daily rainfall values. For example, table 1 shows that a July in a typical dry summer has one less rain day at the 0.254 mm level than the average. Therefore, one rain day already selected for the average July had to be deleted.

The rain-day level frequencies in table 1 reveal that the one day with $\geq$25.4 mm (1 inch) of rain in the average July does not occur in a dry July; hence the value of 39.878 mm rainfall assigned to 5 July in the average summer was reduced to 20.320 mm. In a like manner, the amounts of daily rainfall in the dry summer were adjusted downward to conform to match the average statistical distributions, and so that their sums matched the dry summer monthly values.

The rainfall values for months in wet summers were constructed from the average values in a similar fashion. The goal was to ensure that the adjusted values equaled the daily frequencies for the wet summer months shown in table 1, and that their totals matched the monthly totals for the wet summer. Many of the adjustments of average daily rainfall were to the heavier daily rainfall amounts, particularly those greater than 12.7 mm per day.

Finally, the rate of rainfall, the time of day that the rainfall occurred, and the duration of the rainfall event had to be specified. The control system for applying water prohibited variations of rain rates during a "rain period." Thus, the water application on a day with 8.128 mm rainfall had to be applied at a fixed rate. Further, the duration of the rain event had to be long enough to apply the specified amount of rain. In the case of the very heavy rain events in the covered shelter, and to prevent the "rain" from running off a plot onto an adjacent plot receiving less rainfall, it was necessary to divide the event into several smaller events on the same day.

The time of day of the 'rain event' was determined from an analysis of the diurnal distribution of summer rains (Huff, 1971). In general, this showed that between the hours of 0900 LST and 1400, each hour received 3% of the rain; between 1400 and 2000 each hour receives approximately 4%; and between 2000 and 0900 each hour receives about 5% of the total rain. This reflects the nocturnal maximum and morning minimum of Illinois.

Since we did not have the personnel to distribute water at all times of the day, a schedule involving three different times of application distributed across a sequence of six rain days was used to emulate nature. The prescribed water amount was applied in the hours between 1500 and 2000, and beginning at 1500, on the first and third 'rain day' of the 6-day sequence (which began on 1 June). On the second, fourth, and fifth 'rain days' of the sequence, the prescribed water values were applied between 0600 and 1500. After the initial sequence was done, it was repeated on the next 6 rain days, and continued through the summer. This scheme put 50% of the rain time in the nocturnal maximum, 33% in the late afternoon (lesser peak), and 17% in the mid-day minimum, a distribution that fit the local climatology.

5. FIELD RESULTS FOR 1987

Crop yields were determined by harvesting the center two rows of each plot. For corn, the ears were weighed, adjusting the weight to 15.5% moisture, and then calculating the yield. The yield components of the harvested soybean crop that were recorded are: (1) number of plants harvested; (2) number of pods per plant; (3) number of pods with at least one seed greater than 5 mm in diameter; (4) number of seeds per plant; and (5) the average weight of each seed. The yield was determined on a weight and moisture adjustment.

Treatments (added rainfall) in the shelters were started on schedule. The corn and soybean crop had just emerged by 1 June. During the vegetative stage of growth (June), the weather was unusually hot and dry. Differences in heights of the plants in the different treatments were easily observed and series of photographs were taken at several intervals.

Problems Developed. On 30 July a once in 100-year rainfall (114.3 mm) occurred in a 4-hour period. At the time of the storm, the movable shelter was over the plots (as scheduled) and no rain fell on the plots. However, due to the excessive rainfall rate and the level lay of the land, the plots were exposed to added surface runoff for approximately 3 hours. The soil moisture profiles of all plots were measured and found to be recharged. (At the time of this storm the corn was silking and the soybeans were beginning to flower.) Thus, during the critical corn growth stage of flowering, the "dry summer" plots were recovering from any stress they had been exposed to. Soil moisture measurements after the storm allowed estimation of the "water application" received by the flood, and this value was used to halt planned daily water applications scheduled for 4 days in the 30 July to 9 August period. During this interval, all water was excluded from the movable shelter.

The stationary (open shelter) experienced severe lodging problems at the end of July, which were caused by several factors. These included the 337 kg ha^{-1} of nitrogen, in addition to the residual nitrogen from three prior years of soybeans on these plots, plus the late May planting date and reduced light intensity caused by partial shading of the crop by the infrastructure of the stationary shelter. These caused the corn plants to grow taller than normal without additional thickening of the stem resulting in a weaker plant. Consequently, some plants were blown over by storm downdrafts at the end of July and this limited the corn results. The soybean plots in the stationary shelter did not experience any problems, and the results from these open plots are usable.

Relevant to the 1987 yield outcomes were the other (uncontrolled) weather conditions in 1987. The spring season (Mar-May) was unseasonably warm and dry providing some early moisture stress conditions in June. June itself had above normal (+3°F) temperatures and was relatively dry until late in the month when rain produced an above normal total. July and August had near normal temperatures and both had above normal rainfall. The 3-month (Jun-Aug) total experienced in the open shelter plots was 17.84 inches (45.2 cm) which is 6.9 inches or 162% above normal, truly a very wet summer.

The soybean and corn yields in the covered shelter plots, and the soybean yields from the open shelter are summarized in table 2. Each rainfall treatment was made on 3 randomly selected plots, and the yield values shown are the averages of the 3 plots with comparable treatment. Also shown in table 2 is the total rain (water) applied in the 3 summer months (Jun-Aug) to the covered plots, and to the open shelter plots.

Table 2. The soybean and corn yields from the experimental plots and their associated rainfall (water) applications.

	Covered Plots		
Rainfall Treatment	Rainfall, mm	Soybean Yield, bu/acre	Corn Yield, bu/acre
Dry summer	160.00	43.7	79.3
Dry +25%	200.66	45.4	76.2
Average summer	278.56	48.0	70.6
Average +25%	345.44	47.9	87.6
Wet summer	381.08	44.9	106.1
Wet +25%	474.98	47.3	98.7

	Open Plots - Soybeans	
Rainfall Treatment	Rainfall, mm	Yield, bu/acre
Actual Rain	452.1	32.7
Actual +10%	497.8	26.1
Actual +25%	566.4	30.7
Actual +40%	635.0	23.7
All daily rains of 0.1 to 1.0 inch, up by 10%	469.9	32.1
All daily rains of 0.1 to 1.0 inch, up by 25%	495.3	27.6
All daily rains of 0.1 to 1.0 inch, up by 40%	520.7	27.1
All daily rains >1.0 inch, up by 10%	480.1	29.6
All daily rains >1.0 inch, up by 40%	561.3	26.6
All daily rains ≤0.1 inch, up by 40%	459.7	34.4

The values of yields and rainfall levels are compared on table 3. The results are largely as expected. The results for soybeans in the covered plots show that 25% rain increases in typical wet and dry summers produced crop yield increases but with a minor decrease (-0.1 bu/acre) in average to average +25% for no apparent reason. The corn results are also partly anomalous. Past weather-crop research (Huff and Changnon, 1972) indicated that a wet summer made wetter by 25% would produce a crop yield decrease, and as shown in table 3, it did, by 7.4 bu/acre. The oddest result is the decrease in corn yields from a dry to dry +25% rain condition. Examination of the plot yield values provided a possible explanation for these two anomalous outcomes.

The unusual outcome in the covered plots include a decrease in bean yields from normal rainfall to normal +25%, were a result of 1 of 3 plots having an unusual yield value. In the "average year" for soybeans, the 3 plots yield values were 44.6, 44.7 and 54.8. The latter value was the single highest plot value and >4 bu/acre higher than any other plot, suggesting an incorrect or unrepresentative value. If the average rain value were the average of the two others, 44.7 bu/acre, the shift in bean yields in table 3 from normal rain to normal +25% would be +2.2 bu/acre, a reasonable figure.

Similarly, the corn yield decrease from dry rain to dry +25% (table 3) was odd. The dry summer +25% rain value for corn yields in table 2 appears too low and the 3 plot yield values were 97.9, 71.6, and 59.1 (the lowest of all plot values). If this low outlier considered erroneous were eliminated, the average for dry +25% would be 84.7 bu/acre. Then the shift in corn yields in table 3 from the dry rain level to the dry +25% level would be reasonable, +5.4 bu/acre, not a decrease of 3.1 bu/acre.

The values of the covered shelter plots are shown in Figure 3. The soybean and corn values both show: (1) highest yields in the mid-rainfall (near average) range of 300 to 400 mm; (2) slightly lesser yields with heavier summer amounts, >400 mm; and (3) the lowest yields with the lowest rain values. Given that these value are also dependent on the other weather conditions in 1987 (normal temperatures), the covered plots results indicate that the optimum rainfall for beans was about 300 mm (11.8") but was about 375 mm (~15") for corn. (Note that the average rain is 278 mm.)

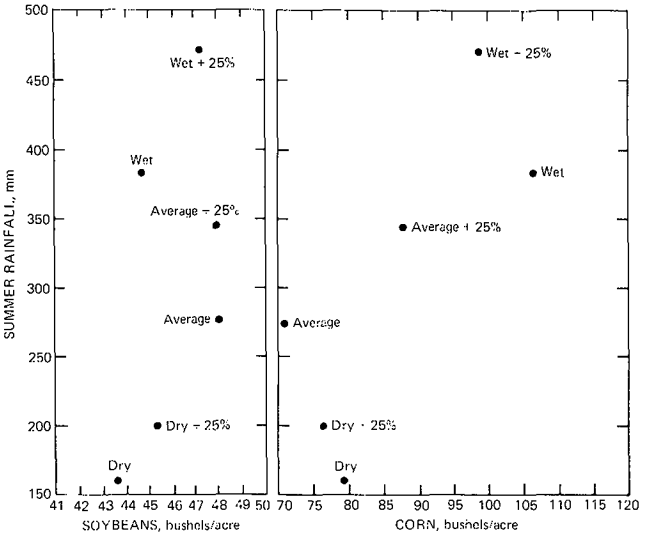

Figure 3. Summer rainfall and crop yields in covered plots, 1987

Table 3. Comparison of yield shifts between treatments in both plot areas.

Covered Plots	Shift in Soybeans (bu/acre)	% of base	Shift in Corn (bu/acre)	% of base
Dry Summer to Dry + 25%	+1.7	+3.9	-3.1	-3.9
Normal Summer to Normal +25%	-0.1	-0.2	+17.0	-24.0
Wet Summer to Wet +25%	+2.4	+5.3	-7.4	-7.0

Open Plots:	Shifts in soybean yields, bu/acre	% of base
Actual rain to +10%	-6.6	-20.2
Actual rain to +25%	-2.0	-6.1
Actual rain to +40%	-9.0	-27.5
Actual rain versus increases in raindays in 2.54 to 25.4 mm range		
Actual rain increased by 10%	-0.6	-1.8
Actual rain increased by 25%	-5.1	-15.6
Actual rain increased by 40%	-5.6	-17.1
Actual rain versus increases of all >25.4 mm rains		
Actual rain increased by 10%	-3.1	-9.5
Actual rain increased by 40%	-6.1	-27.8
Actual rain versus increases of all <.254 mm rains		
Actual rain increased by 40%	+1.7	+6.3

Corn yield outcomes were somewhat odd. The lowest yield came with the average rainfall; with slightly higher yields with dry summer rainfall levels (dry and dry +25%). Results may have been affected by the type of summer temperatures.

The results for the uncovered plots were limited to soybeans since wind damage to the corn plots (described above) affected the yields. The soybean-yield rain values for the 10 treatments selected are shown in table 2, and relevant yield comparisons are shown in table 3. The plot of summer rain against the soybean yields (Fig. 4) reveals that the actual summer rain experienced in 1987 was the best for beans and that all but one of the rain additions to simulate weather modification, decreased bean yields. Only the 40% increase to the days with <0.254 mm (0.1 inch), which included only 7 days in June-August, indicated a slight increase in yield. The results (Fig. 4) reveal that too much rain was damaging to bean yields. Apparently (given the 1987 temperatures and sunshine), the optimum rainfall for beans was in the 350 to 300 mm range, as revealed by the results of the covered plots (Fig. 3).

Further tests of the simulated increases in 1988 under different temperature and sunshine conditions should allow more definitive interpretations of the rain-yield relations. The 1987 outcomes will also be compared with predictions from weather-yield regression models to help calibrate the models. The results for 1987 indicate, in general, that rainfall increases of 10 to 40% will increase yields of corn and soybeans if the actual rainfall is in the below to near average range. The increases will be relatively small, 4 to 20%, of that expected, or generally 3 to 6 bu/acre.

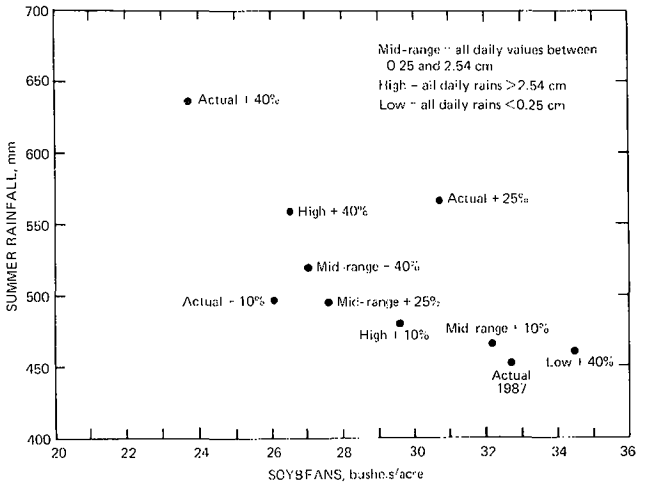

Figure 4. Summer rainfall and soybean yields in uncovered plots, 1987

Acknowledgements. This research has been partly supported on two grants from NOAA: NA 86RAH06051 and NA 87RAH06051. The considerable assistance of Wayne Banwart and Eugene Ziegler of the University of Illinois, Agronomy Department, in managing the test plots is gratefully acknowledged.

6. REFERENCES

Changnon, S.A., 1959: Summary of the Weather Conditions at Champaign-Urbana, Illinois. Bulletin 47, Ill. State Water Survey, Urbana, 95 pp.

Changnon, S.A., 1963: Precipitation in a 550-square-mile area of Southern Illinois. Trans. Ill. Acad. Sciences, 56: 164-187.

Changnon, S.A., 1986: Illinois Weather Modification Project: PACE. Preprints, Tenth Conference on Planned and Inadvertent Weather Modification, Amer. Meteorol. Soc., Boston, 315-319.

Feyerherm, A.M., Bark, D., and W. Burrows, 1966: Probabilities of Sequences of Wet and Dry Days in Illinois. Kansas Technical Bulletin 139K, Kansas State University, Manhattan, KS, 55 pp.

Garcia, P., Offutt, S., Pinar, M., and S. Changnon, 1987: Corn Yield Behavior: Effects of Technological Advance in Weather Conditions. J. Clim. and Appl. Meteorol., 26:713-721.

Huff, F.A., 1971: Distribution of Hourly Precipitation in Illinois. Circular 105, Ill. State Water Survey, Urbana, 23 pp.

Huff, F.A. and S.A. Changnon, 1972: Evaluation of Potential Effects of Weather Modification on Agriculture in Illinois. J. Appl. Meteorol., 11:376-384.

EFFECTS OF ADDED SUMMER RAINFALL ON THE HYDROLOGIC CYCLE OF MIDWESTERN WATERSHEDS

H. Vernon Knapp, Ali Durgunoglu, and Stanley A. Changnon
Illinois State Water Survey
Champaign, IL 61820

ABSTRACT: The effects of added summer rainfall on agricultural areas in Illinois and the Midwest were investigated by using a quasi-distributed-parameter watershed model. Increases in summer convective rainfall during July-August were simulated and used in the model to describe the changes in soil moisture, crop water use, shallow ground water, and streamflow conditions which could potentially result from precipitation augmentation practices. Two periods, representing very dry and very wet conditions, were used in the simulations with 10% to 25% precipitation increases. Results suggest that the greatest proportion of additional summer rainfall eventually percolates into ground water, and that less than 25% percent of the precipitation increase is used by the crops. Simulated increases in summer rainfall offer limited utility in reducing crop water stress because the rainfall events do not always coincide with the period of greatest crop water need. Methods, such as irrigation, which provide additional water at a specified time and amount can produce significant benefits to the plants.

1. INTRODUCTION

In order to understand the impacts of precipitation augmentation on agricultural productivity and freshwater resources, it is necessary to evaluate these changes on soil infiltration and moisture, shallow ground-water movement, and streamflow. The moisture brought by increases in rainfall (or other sources such as irrigation) could potentially be distributed into one of four hydrologic processes: 1) runoff into a stream, 2) seepage into ground water, 3) evaporation into the atmosphere, and 4) abstraction from the soil into the plant for eventual transpiration into the atmosphere. Only the last of these processes is of primary benefit to the plant.

A quasi-distributed-parameter model was developed to simulate soil moisture and baseflow conditions for agricultural areas in Illinois and the Midwest. A model labeled the PACE Watershed MODEL (PWM) was designed and developed over two years with components sensitive to water movement processes. This provided the potential for evaluating paths for increased amounts of rainfall, and thus offer some possible answers as to the usability of potential augmentation (Durgunoglu *et al.*, 1987). The PWM was calibrated for the Kaskaskia Ditch watershed (at Bondville in central Illinois) by using soil moisture and streamflow records for the period of 1981–1985. The model was validated by using streamflow records for two additional periods, 1951–1954 and 1972–1975. These two periods embrace significantly dry and wet periods of record for the watershed.

This paper describes simulation studies performed for evaluating the hydrologic effects of precipitation augmentation for a watershed in central Illinois and special simulation studies performed for analyzing the effects of using early season rain augmentation and irrigation on crop stress reduction. Several levels of precipitation increase are evaluated to determine the overall benefit to agriculture in terms of crop water status. Results describe changes in soil moisture, crop water use, shallow ground water, and streamflow conditions over periods of years selected to present both wet and dry climatic conditions in the watershed. Included is a brief analysis of the characteristics in crop water supply needed to improve the crop condition.

2. PRECIPITATION AUGMENTATION SIMULATIONS

Precipitation augmentation was simulated for two historical periods, 1951–1954 and 1972–1975. These periods were selected as examples of a very dry and very wet set of years, in central Illinois, respectively. The model was tested with the actual daily rainfall in these eight years, and then precipitation was increased in the months of July and August for days on which rainfall had been recorded. By limiting the rainfall increases to days which historically had experienced precipitation, the original distribution of rain-producing storms is maintained. Further, no evidence exists to suggest that the total number of days with rain in Midwestern convective rain conditions could be increased (Changnon and Semonin, 1975; Changnon and Hsu, 1981).

Four levels of precipitation increase were analyzed:

1. All rain-producing clouds are seeded, causing a 10% increase in all July-August rainfall;
2. All rain-producing clouds are seeded, causing a 25% increase in all July-August rainfall;
3. All rain-producing clouds are seeded (July-August), but causing a 25% increase only for storms which otherwise would have daily precipitation totals in the range of 0.1 to 1.0 inches; and
4. Only half of the rain-producing clouds are seeded (July-August), causing a 25% increase in rainfall for those storm events.

The range of selected increases (10 to 25%) in daily rain events is in agreement with levels used in other regions with convective rainfall regime (Weather Modification Advisory Board, 1978). The selection of increases only in 0.1- to 1.0-inch daily rain was used to match levels believed most useful to agricultural production and soil preservation (Changnon, 1981). The test of increases on 50% of the days was to measure the effect of intermittent modification.

The additional rainfall associated with each of the levels of augmentation will either 1) run off into the stream during the rainfall event, 2) evaporate from the surface or shallow layers of soil, 3) infiltrate into the soil and later be used by

plants for transpiration, or 4) remain in the soil and eventually percolate down to the ground-water table. The processes simulated are listed as follows:

P = Total Precipitation

ET = Total Evapotranspiration

TR = Total Transpiration

SM_{min} = Minimum Available Soil Moisture for the Year

ΔSM = Change in the Soil Moisture for the Year

Seep = Total Deep Percolation from Soil Moisture Component

QR = Total Surface Runoff from Soil Moisture Component

Σ(Seep + QR) = Weighted Total of (Seep + QR) for All Soil Types

Q_{est} = Total Streamflow Estimate from Ground Water Component

Q_{obs} = Total Observed Streamflow

For each of the simulated levels of precipitation augmentation, a summary was developed describing the distribution of the additional precipitation among the various hydrologic processes (Durgunoglu *et al.*, 1988). Examples of these are provided in tables 1 and 2 for two years of simulation, and for both Flanagan and Drummer soils, the two soils in the watershed and typical of prairie soils of the Corn Belt. Also included in these tables are the simulated values of total streamflow for the entire watershed (the Kaskaskia Ditch).

The increase in precipitation was distributed among four variables, as described in the equation:

$$\Delta P = \Delta ET + \Delta Seep + \Delta QR + \Delta(\Delta SM) \quad (1)$$

where Δ represents the amount of change in the variables, as defined earlier, from conditions with no augmentation. The variable of greatest concern in tables 1 and 2 is TR, the total transpiration for the year. Any increases in TR represent increased crop water use, which signifies a reduction in crop water stress. All values of transpiration are included in the total evapotranspiration value (ET). The change in the minimum soil moisture, SM_{min}, is also significant in that it represents the extent of soil moisture depletion during the growing season. The change in soil moisture for the year, ΔSM, will ordinarily be greater under augmented conditions, but may fluctuate from year to year since this term depends on conditions during the preceding year.

In the summary of total flows for the watershed, the term Σ (Seep + QR) is the weighted total of seepage and runoff for the entire watershed. Over a long period of time, this term will be equal to the estimated runoff of the watershed, Q_{est}. However, because of the effect of ground-water storage, these two terms will be slightly different for any one year. For example, during the drought years (1952–1954, see table 1) the estimated discharge is higher than Σ (Seep + QR) because of the contribution of ground-water storage to the stream.

The simulated conditions suggest that during the wetter years (1972–1975, see table 2), a great percentage of the additional rainfall will run off during storms or percolate down into ground water. For example, in 1973 the estimated increase in rainfall for the largest level of augmentation (25% for all rainfall) is 3.06 inches (table 2). Of this amount, the simulation for the Flanagan soil estimates that a total of 2.97 inches will either run off during the storm events (1.20 inches) or percolate into ground water (1.77 inches). The simulated increase in total streamflow for the watershed in 1973 is 2.86 inches. Because storm runoff is greater, potential increases in the severity of flood events should be a consideration when seeding clouds under wet-soil conditions. Virtually none of the precipitation increase is used by the crops (variable TR), and it is possible that excessively high levels of soil moisture could have a detrimental effect by inhibiting crop growth. Research has shown that overly wet summer conditions in Illinois decrease corn and soybean yields (Huff and Changnon, 1972).

For the dryer years of 1951–1954, the simulated increases in precipitation appear to be more evenly used among the various hydrologic processes. During these years, the average annual increase in summer precipitation (given a 25% level of augmentation) is 1.58 inches. However, the maximum increase in crop transpiration during any of these years is only 0.36 inches for Flanagan soil and 0.21 inches for Drummer soil, both in 1952 (table 1). A majority of the increases in precipitation appear to stay in the soil, unused by the plants, eventually to enter the ground water through percolation (the "Seep" variable).

The average distribution of the additional precipitation into the various hydrologic processes in the dry years is presented in table 3. As noted, most of the additional water eventually percolates into ground water. Little of the precipitation increase tends to be used by the crop. This is likely a result of 1) the limited amount of additional rainfall occurring during any one storm, and 2) the distribution of rainfall-producing storms within these dry years. This relationship between distribution of storms and crop water use is further examined in the following section.

3. OTHER SIMULATION TESTS

In order to study and better understand the apparently limited effect of precipitation increases on the amount of simulated crop transpiration, two other types of water increases were simulated in the model. The first case examined a scenario where precipitation augmentation is initiated earlier in the year (during the month of June) in order to increase the general soil-moisture level of the soil. The second case examined the effects of large water applications, potentially available through irrigation, on simulated crop water use. The soil-moisture component was used to simulate these cases for Flanagan soils for the three driest years (1953, 1954, and 1983). Calculations were done for the 8 test years (1951–54, 1972–75) and for 5 recent years.

A crop stress index was defined for use in describing the effect of soil moisture and crop water use on crop development. The crop stress value for any one day is defined as the fractional amount of potential crop growth that is suppressed because of the lack of moisture available to the plant. If, on any one day, the crop is under severe stress and no crop growth occurs, a unit value of crop stress is recorded. Severe crop stress is assumed to occur whenever actual transpiration (as limited by soil moisture) is less than 50% of the potential transpiration (Saxton *et al.*, 1984). Partial stress is assumed to

Table 1. Summary of Water Volumes Used in the Hydrologic Processes and Precipitation Augmentation for 1952, a Dry Year.

FLANAGAN SOIL (1952)					
	Simulation Condition				
Process	0	1	2	3	4
P	33.86 (0.00)	34.35 (0.49)	35.07 (1.21)	34.70 (0.84)	34.28 (0.42)
ET	27.19 (0.00)	27.44 (0.25)	27.73 (0.54)	27.63 (0.44)	27.41 (0.22)
TR	15.54 (0.00)	15.70 (0.16)	15.90 (0.36)	15.86 (0.32)	15.70 (0.16)
SM_{min}	12.94 (0.00)	13.20 (0.26)	13.59 (0.65)	13.36 (0.42)	13.15 (0.21)
ΔSM	-2.83 (0.00)	-2.62 (0.21)	-2.33 (0.50)	-2.50 (0.33)	-2.67 (0.16)
Seep	8.41 (0.00)	8.42 (0.01)	8.47 (0.06)	8.44 (0.03)	8.42 (0.01)
QR	1.07 (0.00)	1.09 (0.02)	1.18 (0.11)	1.11 (0.04)	1.09 (0.02)
Seep + QR	9.48 (0.00)	9.51 (0.03)	9.65 (0.17)	9.55 (0.07)	9.51 (0.03)

DRUMMER SOIL (1952)					
	Simulation Condition				
Process	0	1	2	3	4
P	33.86 (0.00)	34.35 (0.49)	35.07 (1.21)	34.70 (0.84)	34.28 (0.42)
ET	25.22 (0.00)	25.34 (0.12)	25.46 (0.24)	25.44 (0.22)	25.34 (0.12)
TR	15.59 (0.00)	15.69 (0.10)	15.80 (0.21)	15.78 (0.19)	15.70 (0.11)
SM_{min}	11.36 (0.00)	11.58 (0.22)	11.91 (0.55)	11.72 (0.36)	11.55 (0.19)
ΔSM	-0.01 (0.00)	0.02 (0.03)	0.02 (0.03)	0.02 (0.03)	0.02 (0.03)
Seep	6.90 (0.00)	7.16 (0.26)	7.63 (0.73)	7.38 (0.48)	7.12 (0.22)
QR	1.67 (0.00)	1.74 (0.07)	1.88 (0.21)	1.77 (0.10)	1.72 (0.05)
Seep + QR	8.57 (0.00)	8.90 (0.33)	9.51 (0.94)	9.15 (0.58)	8.84 (0.27)

TOTAL FLOWS AT BONDVILLE (1952)					
	Simulation Condition				
Process	0	1	2	3	4
Σ(Seep + QR)	9.04 (0.00)	9.22 (0.18)	9.58 (0.54)	9.36 (0.32)	9.19 (0.15)
Q_{est}	12.24 (0.00)	12.57 (0.33)	12.85 (0.61)	12.63 (0.39)	12.50 (0.26)
Q_{obs}	10.65 (0.00)				

Condition:

0 = No cloud seeding is done (natural condition);

1 = All rain-producing clouds are seeded during July-August, causing a 10% increase in all rainfall;

2 = All rain-producing clouds are seeded during July-August, causing a 25% increase in all rainfall;

3 = All rain-producing clouds are seeded during July-August, causing a 25% increase, but only for storms which otherwise would have daily precipitation totals in the range of 0.1 to 1.0 inches;

4 = Only half of the rain-producing clouds are seeded during July-August, causing a 25% increase in rainfall for those storm events.

Numbers in parentheses indicate increase from condition 0.

All values are in inches.

Table 2. Summary of Water Volumes Used in the Hydrologic Processes and Precipitation Augmentation for 1973, a Wet Year.

FLANAGAN SOIL (1973)					
	Simulation Condition				
Process	0	1	2	3	4
P	49.20 (0.00)	50.43 (1.23)	52.26 (3.06)	50.52 (1.32)	49.86 (0.66)
ET	28.74 (0.00)	28.79 (0.05)	28.85 (0.11)	28.84 (0.10)	28.80 (0.06)
TR	15.52 (0.00)	15.55 (0.03)	15.59 (0.07)	15.59 (0.07)	15.56 (0.04)
SM_{min}	16.62 (0.00)	16.68 (0.06)	16.78 (0.16)	16.78 (0.16)	16.70 (0.08)
ΔSM	0.00 (0.00)	0.00 (0.00)	0.00 (0.00)	0.00 (0.00)	0.00 (0.00)
Seep	17.02 (0.00)	17.77 (0.75)	18.79 (1.77)	18.09 (1.07)	17.56 (0.54)
QR	3.40 (0.00)	3.84 (0.44)	4.60 (1.20)	3.56 (0.16)	3.47 (0.07)
Seep + QR	20.42 (0.00)	21.61 (1.19)	23.39 (2.97)	21.65 (1.23)	21.03 (0.61)

DRUMMER SOIL (1973)					
	Simulation Condition				
Process	0	1	2	3	4
P	49.20 (0.00)	50.43 (1.23)	52.26 (3.06)	50.52 (1.32)	49.86 (0.66)
ET	26.77 (0.00)	26.80 (0.03)	26.85 (0.08)	26.85 (0.08)	26.81 (0.04)
TR	15.78 (0.00)	15.80 (0.02)	15.83 (0.05)	15.83 (0.05)	15.80 (0.02)
SM_{min}	13.40 (0.00)	13.46 (0.06)	13.55 (0.15)	13.55 (0.15)	13.48 (0.08)
ΔSM	0.06 (0.00)	0.06 (0.00)	0.06 (0.00)	0.06 (0.00)	0.06 (0.00)
Seep	17.75 (0.00)	18.43 (0.68)	19.36 (1.61)	18.74 (0.99)	18.25 (0.50)
QR	4.52 (0.00)	5.03 (0.51)	5.88 (1.36)	4.77 (0.25)	4.65 (0.13)
Seep + QR	22.27 (0.00)	23.46 (1.19)	25.24 (2.97)	23.51 (1.24)	22.90 (0.63)

TOTAL FLOWS AT BONDVILLE (1973)					
	Simulation Condition				
Process	0	1	2	3	4
Σ(Seep + QR)	21.31 (0.00)	22.50 (1.19)	24.28 (2.97)	22.54 (1.23)	22.07 (0.76)
Q_{est}	21.18 (0.00)	22.30 (1.12)	24.04 (2.86)	22.32 (1.14)	21.73 (0.55)
Q_{obs}	21.56 (0.00)				

Condition:

0 = No cloud seeding is done (natural condition);

1 = All rain-producing clouds are seeded during July-August, causing a 10% increase in all rainfall;

2 = All rain-producing clouds are seeded during July-August, causing a 25% increase in all rainfall;

3 = All rain-producing clouds are seeded during July-August, causing a 25% increase, but only for storms which otherwise would have daily precipitation totals in the range of 0.1 to 1.0 inches;

4 = Only half of the rain-producing clouds are seeded during July-August, causing a 25% increase in rainfall for those storm events.

Numbers in parentheses indicate increase from condition 0.

All values are in inches.

Table 3. Average Distribution of Additional Precipitation to the Various Hydrologic Processes during Dry Years (1951–1954).

Hydrologic Process	Flanagan Soil	Drummer Soil
Soil Evaporation	6%	2%
Crop Water Use	23%	15%
Surface Runoff	16%	15%
Percolation	55%	68%

occur when the actual transpiration rate is between 50% and 80% of the potential rate. The total crop stress index is the cumulative number of crop stress values for the growing season.

Table 4 provides values of the crop stress index estimated by the soil moisture component, and the average yield for corn crops in Champaign County, Illinois (obtained from the Illinois Department of Agriculture), for the 13 years simulated by the model. Although the period of 1950s demonstrate little relationship between crop stress and crop yield, there exists a strong relationship between these variables in the 1970s and 1980s. The crop stress index appears to be an adequate tool for evaluating the effect of soil moisture on crop yield.

Table 4. Comparison between the Crop Stress Index and Average Corn Yield for Simulated Years.

Year	Crop Stress	Average Yield (Bushels/Year)
81	0.00	137
82	0.01	147
83	18.42	89
84	4.66	128
85	0.00	154
72	0.00	129
73	0.98	123
74	5.06	98
75	0.00	136
51	0.00	58
52	0.61	62
53	9.18	61
54	11.14	63

3.1 Simulation of June Augmentation

It was thought that by increasing rainfall in June as well as in July and August the soil moisture might be increased prior to the dry periods which cause the most severe stress conditions for the crops. Examination of table 5, however, indicates that the additional June rainfall did little to increase the amount of crop water use in these 3 dry summers. Even with the 2.29 inches of additional rainfall simulated for June 1983 (in addition to July-August augmentation), transpiration for that year is increased by only 0.13 inches from the July-August augmentation condition. An examination of the rainfall record for the summer of 1983 indicates that a 28-day period occurred (between July 5 and August 3) in which the precipitation was only 0.30 inches. During this period there were only two days with rainfall. Assuming the highest level of precipitation augmentation simulated in this study, only 0.075 inches of additional rainfall would occur during these two days. The model shows this to have been of negligible value. This period also experienced several weeks having extremely high evapotranspiration demand.

The difference between the potential and actual transpiration simulated for this period in 1983 is shown in figure 1a. Similar periods of high evapotranspirative demand and little rainfall can be seen in other dry years simulated (see figures 2a and 3a). The differences between the bottom line (unaugmented transpiration) and the middle line (transpiration with augmentation) indicate that increased rainfall does little to increase the crop water use, which would in turn decrease crop stress. Therefore, regardless of the soil moisture conditions at the beginning of these periods, significant crop stress would be expected because of lack of rainfall.

The above example indicates that simulated augmentation conditions were unable to substantially reduce crop stress because of the lack of rain-producing storm events. A conclusion from this example is that in order to achieve considerable benefit during dry years, augmentation efforts will need to produce significant amounts of rainfall (for example, near 0.5 inches) from conditions where little rainfall would otherwise be expected. This conclusion may be further supported by the results of the other simulation test in which larger amounts of water were brought to plants in otherwise dry conditions by irrigation.

3.2 Simulation of Heavy Water Applications

Two cases of heavy water applications were simulated for the Flanagan soil: one in which a total of 3 inches of irrigation water was applied (1 inch applied 3 times during the year), and the other where 4 inches of water was applied (1 inch applied 4 times). The presumption in both cases is that water supplies are available to provide these amounts via irrigation. The applications of water were triggered when the soil moisture in the top 12 inches of the soil column fell below a threshold level. For the case involving a total of 3 inches of application, a lower level of soil moisture was tolerated before application.

A summary of the distribution of these heavy applications to the various hydrologic processes within the soil is given in table 5. The lowest increase in crop transpiration for any one year of simulation was 1.38 inches in 1954. This value can be obtained by subtracting the TR value with no augmentation (15.19 inches) from the TR value with irrigation (16.57 inches). On average over these three years, 64% of the water added during irrigation is used for crop water use (see table 6). The values in table 6 can be compared with those in table 3 to detect the major differences in the distribution of water between likely precipitation augmentation and heavier applications from irrigation. Without considerations for cost differences or availability of water, irrigation is more efficient in supplying moisture to the crops because the water is supplied at the time when the plants need it most. The irrigation events are primarily needed only during those extended periods which ordinarily would have little, if any, rainfall.

The effect of heavier water applications from irrigation events in improving the crop transpiration conditions is illustrated in figures 1b, 2b, and 3b. For all three years, the irrigation water reduces the differential between the potential transpiration and actual transpiration to less than half of the origi-

Table 5. Summary of Water Volumes Used in the Hydrologic Processes of the Soil Moisture Component: Precipitation Augmentation and Irrigation Simulations for Flanagan Soil (All values are in inches).

Year	Process	No Augmentation	Heavy Applications (3 Inches)	Heavy Applications (4 Inches)	25% Augmentation (July-August)	25% Augmentation (June-August)
1953	P	26.09	29.09	30.09	27.22	27.95
	ET	24.33	26.46	27.21	24.70	24.87
	TR	15.90	17.55	17.59	16.25	16.25
	SM_{min}	12.28	13.43	13.80	12.49	12.49
	ΔSM	-2.11	-1.27	-1.04	-2.43	-2.43
	Seep	2.86	2.90	2.91	3.78	4.28
	QR	0.99	0.99	0.99	1.15	1.20
	Crop Stress Index	9.18	0.00	0.00	6.96	6.96
1954	P	29.70	32.70	33.70	31.60	32.28
	ET	25.92	27.72	27.72	26.26	26.46
	TR	15.19	16.57	16.57	15.39	15.51
	SM_{min}	14.15	15.23	15.23	15.02	15.22
	ΔSM	3.63	3.51	3.28	4.03	4.24
	Seep	-0.37	0.82	1.05	0.12	0.81
	QR	0.52	0.63	0.64	0.59	0.76
	Crop Stress Index	11.14	3.81	3.81	9.66	9.22
1983	P	50.26	53.26	54.26	51.77	54.06
	ET	30.21	32.70	33.52	30.74	30.90
	TR	18.18	20.74	21.56	18.66	18.79
	SM_{min}	12.40	12.83	12.96	12.63	13.14
	ΔSM	0.06	0.06	0.06	0.06	0.06
	Seep	14.29	14.63	14.76	14.86	15.58
	QR	5.65	5.82	5.87	6.05	7.46
	Crop Stress Index	18.42	3.82	1.72	14.82	14.25

Table 6. Average Distribution of Large Water Applications to the Various Hydrologic Processes during Dry Years (1951–1954).

Hydrologic Process	Flanagan Soil
Soil Evaporation	8%
Crop Water Use	64%
Surface Runoff	3%
Percolation	25%

nal differential. Because stress conditions affect the growth rate of crops, the potential transpiration rate can actually be increased by supplying the crops with sufficient moisture earlier in the year. This occurs in 1954 (Figure 3b), when at the end of the growing season potential transpiration is greater and the corn crop is more developed. In the same manner, a well-developed crop is more susceptible to crop stress during dry conditions simply because its transpirative demand is greater.

The reduction in the crop stress index resulting from irrigation is provided in table 5. Irrigation reduces the crop stress to zero in 1953, and the indexes for 1954 and 1983 are reduced to 35% and 21% of the original values, respectively. The improvement in stress conditions resulting from large water applications from irrigation help substantiate the view that, in order to the most good, precipitation augmentation would need to create rainfall within otherwise dry or marginal periods.

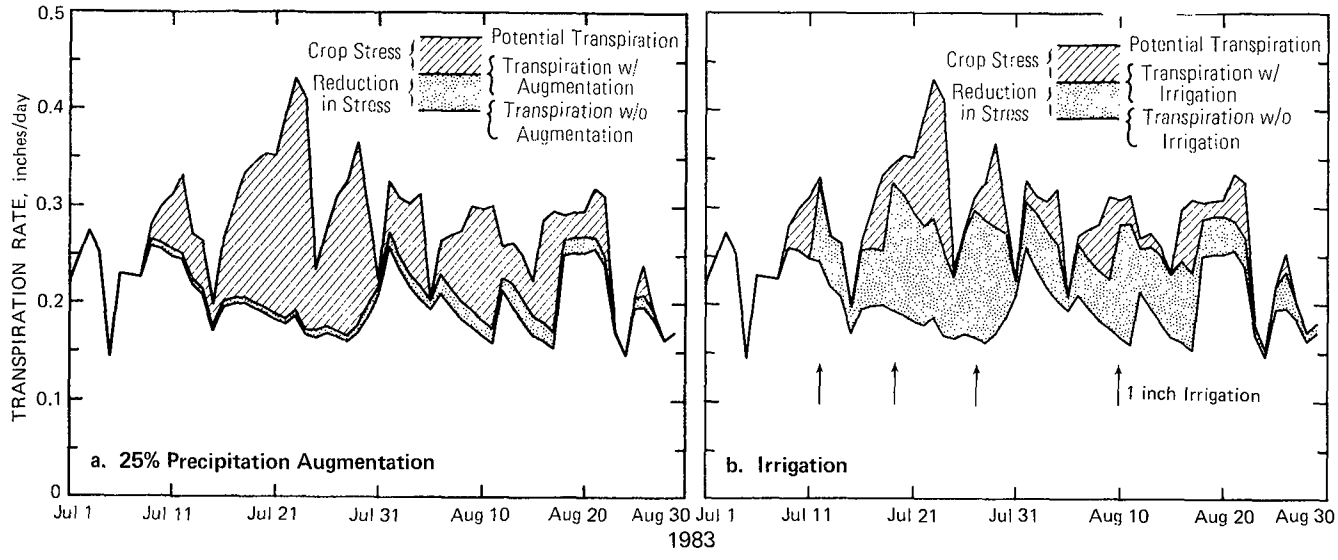

Figure 1. Change in the transpiration rate in 1983 due to a) precipitation augmentation, and b) irrigation (1-inch applications are noted as arrows).

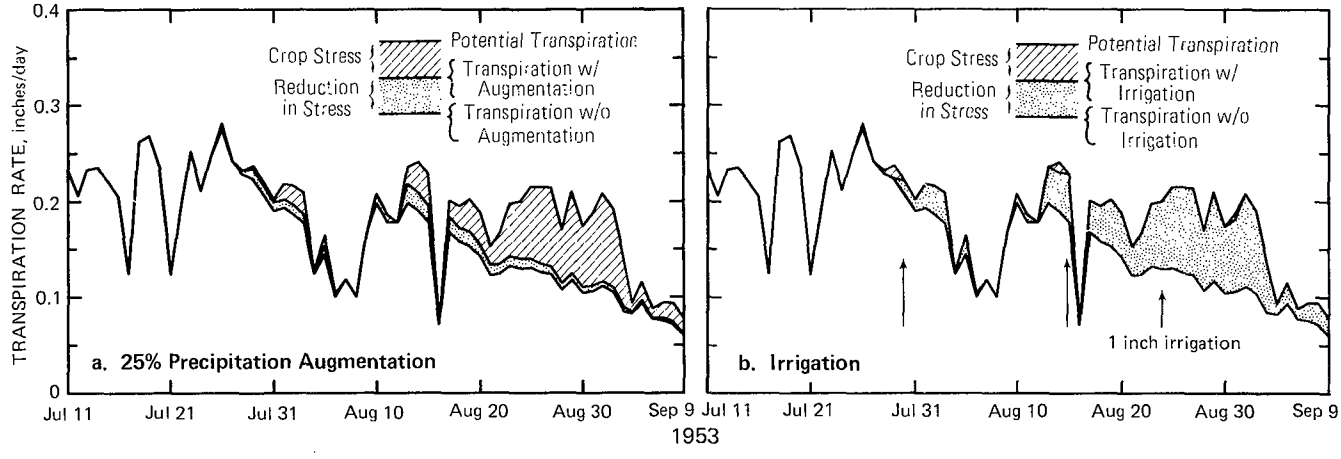

Figure 2. Change in the transpiration rate in 1953 due to a) precipitation augmentation, and b) irrigation.

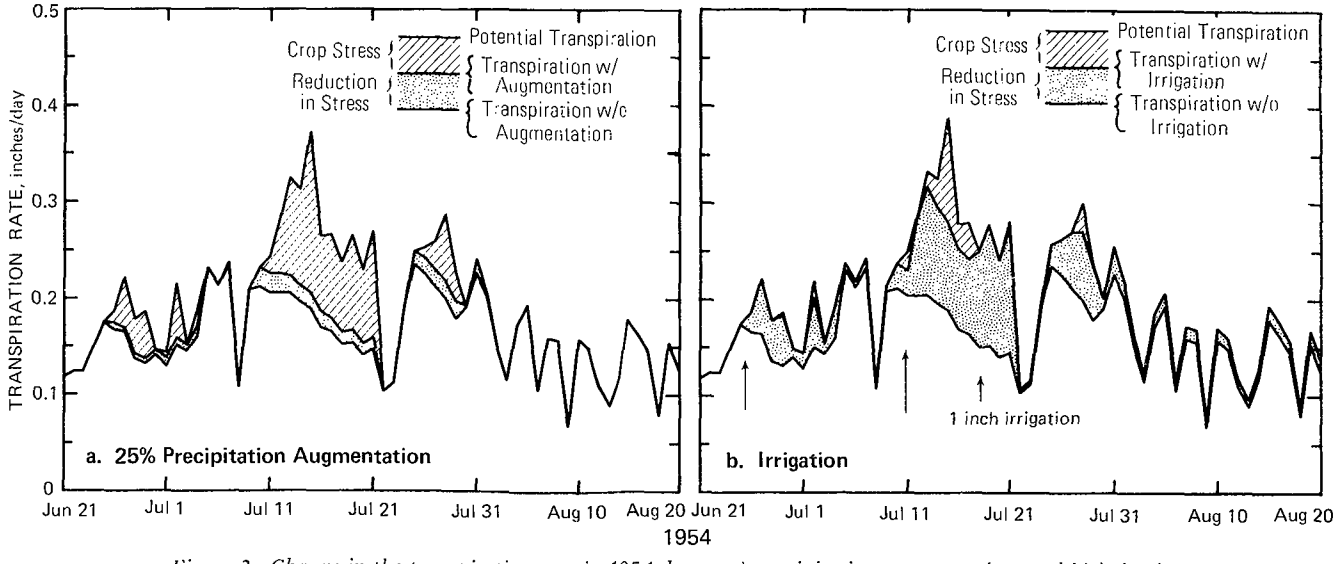

Figure 3. Change in the transpiration rate in 1954 due to a) precipitation augmentation, and b) irrigation.

4. SUMMARY AND CONCLUSIONS

The PACE Watershed Model (PWM) was designed and developed to simulate soil moisture and baseflow conditions for agricultural areas in Illinois and the Midwest. The model was applied to a watershed in central Illinois for two periods, 1951–1954 and 1972–1975. These two periods embrace significant dry and wet periods of record for the watershed. The model represents the hydrologic processes of soil moisture, evapotranspiration, percolation, baseflow, and streamflow. Those were simulated for these two 4-year periods to develop base conditions for examining the effects of precipitation augmentation on soil moisture, crop water use, and streamflow conditions in the basin.

Four levels of increased precipitation were simulated for the watershed, ranging from 10% up to a 25% increase in all precipitation during the months of July and August. All modeled simulations indicated that a great percentage of potential precipitation increase will add to ground water due to increased percolation, and eventually supplement the baseflow. However, only a small percentage of the increased precipitation would be used by the crops. The amounts of increased crop water use resulting from augmentation appear to be insufficient to have significant effects on the total crop water stress conditions or associated crop growth. This insufficiency is mainly due to the temporal distribution of precipitation which does not generate sufficient rain during typically short (one to three week) periods of crop water stress.

Two alternative conditions were examined in an attempt to explain the minimal effectiveness of the precipitation increases to meet crop demands. The first condition involved increasing the summer soil moisture levels by augmenting rainfall earlier in the summer (June). This condition provided little benefit to the crop water status. The second alternative tested was a simulation of heavy water applications (1-inch) by irrigation, and activated based on the soil moisture levels. These simulated conditions caused a significant increase in total crop water use and a reduction in total crop stress. These findings are in agreement with earlier less firm findings that indicated that rainfall increases, to be of reasonable value to crop production in the Midwest, would need to be substantial and greater than an average increase of 25% (Changnon, 1981).

Crop water stress conditions in midwestern prairie soils are produced by long periods of little rainfall. For this reason the temporal distribution of the rainfall is as great a concern as is the total amount of precipitation. Methods, such as irrigation, which can provide additional water to crops at any time and amount during these dry spells obviously produce a maximum benefit to the plant. If precipitation augmentation is to be of greatest utility to the improvement of midwestern agricultural conditions, significant rainfall amounts (for example, ≥0.5 inch) are needed during those periods when little or no rainfall would otherwise occur.

The METROMEX findings based on an outcome of substantial (30 to 70%) increases in certain heavy summer rain events, and subsequent measurable crop yield increase reveal that agricultural benefits can occur from just enhancement of existing rain conditions if they are sufficiently large (Changnon, 1977). The impact of increased (10 to 25%) precipitation on general water resources is found to be beneficial, unless it is done during very wet periods. The results have indicated that additional precipitation can actually increase baseflows, and thus improve water quality during dry periods without significantly increasing surface runoff.

Acknowledgements. This research was conducted as part of the Precipitation Augmentation for Crops Experiment. Parts of the research were supported under NOAA grants 86RAH06051 and 87RAH06051.

5. REFERENCES

Changnon, S.A. and R.G. Semonin. 1975. METROMEX: Lessons for Precipitation Enhancement in the Midwest. J. Wea. Mod., 7, 77-87.

Changnon, S.A. 1977. Impacts of Urban-Modified Precipitation on Man's Activities. J. Wea. Mod., 9, 8-18.

Changnon, S.A. 1981. Hydroclimatological, Meteorological, and Agricultural Constraints on Precipitation Enhancement. Extended Abstracts, Eighth Conference

Changnon, S.A. and C.-F. Hsu. 1981. Evaluation of Illinois Weather Modification Projects of 1976-1980. Circular 148, Illinois State Water Survey, Champaign, 31 pp.

Durgunoglu, A., H.V. Knapp, and S.A. Changnon, Jr. 1987. PACE Watershed Model (PWM): Volume 1, Model Development. Illinois State Water Survey Contract Report 437, Champaign, 90 pp.

Durgunoglu, A., H.V. Knapp, and S.A. Changnon, Jr. 1988. PACE Watershed Model (PWM): Volume 2, Weather Modification Simulations. Illinois State Water Survey Contract Report 439, Champaign, 55 pp.

Huff, F.A. and S.A. Changnon. 1972. Evaluation of Potential Effects of Weather Modification on Agriculture. J. Appl. Meteorol., 11, 376-384.

Saxton, K.E., P.F. Brooks, R. Richmond, and J.S. Romberger. 1984. Users Manual for SPAW--A Soil-Plant-Air-Water Model. USDA-SEA-AR, Unpublished Manual.

Weather Modification Advisory Board. 1978. The Management of Weather Resources. Vol., Dept. of Commerce, NOAA, Washington, DC, 229 pp.

A PRELIMINARY NUMERICAL EXPERIMENT IN SIMULATING THE DISPERSION OF SF_6

Fred J. Kopp
Institute of Atmospheric Sciences
South Dakota School of Mines and Technology
Rapid City, South Dakota 57701-3995

Abstract. A numerical simulation of an SF_6 tracer experiment conducted on July 19, 1985, in North Dakota has been made. Both SF_6 and AgI seeding are simulated in the model, although not concurrently. Only one seeding agent is simulated in a particular run of the model. The numerical experiments show that the SF_6 and AgI will disperse in a similar fashion initially but, as the AgI is activated inside the cloud, there will be some differences. The development of detectable ice and precipitation as a result of AgI seeding will likely diverge somewhat from the SF_6 dispersion.

1. INTRODUCTION

The efficacy of the dispersal of seeding materials in clouds that are to be treated has been under question for some time (Stith et al., 1986). Researchers have dispersed seeding materials into the updrafts below cloud base to minimize the possibility that the seeding materials are carried off away from the target clouds. This raises the question of how much the seeding material is dispersed while being carried through the cloud. If the seeding material remains in a small volume, the seeding effects will affect only a small portion of the cloud leaving the greater portion of the cloud untreated, which is not the desired result. The seeding material is not easy to detect. In the case of CO_2, the seeding material is found in the atmosphere, in large quantities naturally, so detection of CO_2 gas is not evidence of seeding material. Warburton and Maher (1985) collected rainfall and analyzed the water for silver. Most of the seeded days resulted in the detection of silver, but so did some of the non-seeded days. While the results suggest that the seeding material does get into the precipitation, the questions posed on the dispersion of the seeding material in the cloud are not answered.

Stith et al. (1986) report on using sulfur hexafluoride (SF_6) as a tracer. This gas is not found in the atmosphere naturally and can be detected in very small amounts (parts per trillion). The experiment releases the SF_6 tracer into the cloud in the same manner as AgI is released. An instrumented aircraft is then used to detect the SF_6, allowing the movement of the gas to be traced with time. These experiments are expected to answer some of the questions raised in the above discussion with the following assumptions. The expectation is that the AgI seeding material nuclei will behave in much the same way until activation of the AgI. Sulfur hexafluoride is not washed out by the water droplets in the cloud, so the gas will outlast the AgI. Consequently, detection of the movement of SF_6 will only mimic the movement of the AgI for a limited time.

Numerical model experiments are being conducted to test the extent to which the SF_6 will simulate the AgI transport. The model assumes that the two materials will be transported in the same way, but that the AgI will be an active seeding agent and will therefore interact with the cloud. Essentially, the SF_6 is an inactive AgI agent in the modeling. The simulation will show the extent to which the SF_6 and the AgI disassociate from each other. Also the location of the ice and precipitation particles relative to the two seeding agents will be simulated.

2. CLOUD MODEL

The model (Orville and Kopp, 1977) was modified to simulate the movement of SF_6 on a grid with 100 meter spacing. Essentially, the seeding field in the model was modified to behave like the silver iodide but with no interaction apart from being advected by the winds. This modification permitted SF_6 to be simulated in addition to AgI and CO_2. Only one seeding agent was allowed in any single simulation, so the combined effects of seeding with two agents was not possible. An assumption was made that the AgI seeding effects produce a very small dynamic effect. In this case, the dynamic effects were small.

Also, the AgI was not followed in the model after the AgI nuclei were simulated to become active. Following activation, the activated AgI was removed leaving inactivated AgI. In nature, of course, the AgI would be present in the cloud ice crystals formed by the activated AgI nuclei. The model does not distinguish between natural ice and "seeded" ice. In theory, one can distinguish between a natural ice crystal and one produced by AgI by examining the crystals for AgI. In practice, finding silver in seeded precipitation has been ambiguous (Warburton and Maher, 1985).

The two dimensionality of the model constrains the simulation of the three-dimensional problem. Certainly, the seeding materials were dispersed in three dimensions in the experiments, but this cannot be simulated in the model. Nonetheless, the two-dimensional results can give insights that may help interpret the observations.

3. INITIALIZATION OF MODEL

Several simulations were made with the aircraft sounding taken July 19, 1985, near

Dickinson. This sounding was very dry with a mixing ratio of 6-7 gm kg^{-1} of water vapor in the boundary layer. There was also a very strong inversion between 650 and 700 hPa. Little convective activity would be expected from the sounding even with convergence or orographic lifting. Some moisture may have been advected in at some level to have produced the observed clouds. In any case, the model was given a bubble of moisture to enhance cloud formation. None of these simulations produced a particularly satisfactory cloud, however, primarily because the cloud tops were too low. For the results presented here, the Dickinson sounding was used in modified form. This sounding was taken in the morning at 1000 MDT and, while even drier, the upper level inversion was weaker. In the lower levels, the dew points were modified by using a descending aircraft sounding. This increased the mixing ratio to 7 gm kg^{-1} rather than the 5 or so that the Dickinson sounding indicated. A heat and moisture bubble was added in the lower layers of the model. The temperature was highest near the surface, decreasing above while the moisture was greatest in the center such that the maximum mixing ratio was about 1 km above the surface. The bubble had a maximum temperature excess of 3°C at the bottom, and mixing ratio excess of 8 gm kg^{-1} at the center, and decreased outward. The total mixing ratio in the bubble was 15 gm kg^{-1} at one point with a larger area of 10 to 12 gm kg^{-1} which was supersaturated. This resulted in instant cloud formation with a low cloud base.

At 9 min in the simulation, seeding material was introduced. Two seeding simulations were run. First, SF_6 seeding was simulated. The SF_6 was released in the middle of the cloud at a rate of 16 gm km^{-1}. The release was at 3.8 km MSL in an updraft, and the in-cloud temperature was near 0°C. A flight trajectory perpendicular to the plane of the model was assumed, so the seeding material was initially distributed in a circle.

Silver iodide seeding was also simulated in the exact position as the SF_6 so the AgI would follow the same trajectory until the effects of the AgI seeding affected the airflow. The same seeding rate was also used, although this was probably lower than the rate actually used in the field experiment.

4. RESULTS OF THE SIMULATIONS

The initial cloud base was at 1 km AGL, or about 1.8 km MSL, due to the bubble of excess moisture used to start the model. Within 10 min, the cloud base rose to 2.8 km MSL (Fig. 1), still

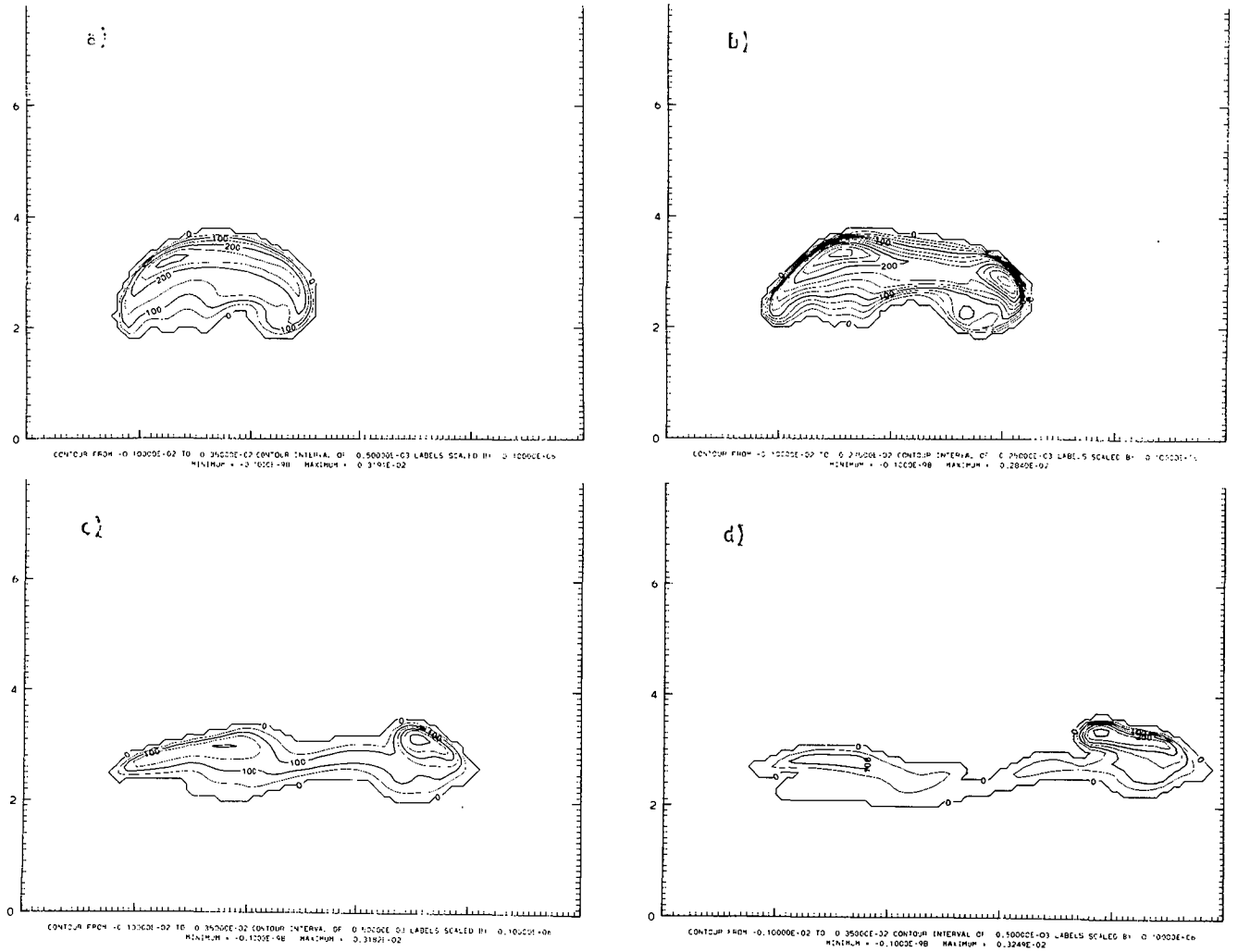

Fig. 1: Cloud water from SF_6 case but applicable to all cases: (a) At 9 min when seeding is done; (b) at 12 min. Note that the cloud is breaking apart. (c) 15 min; and (d) 18 min. In (c) and (d), the breakup of the cloud into two pieces is completed. Contours in gm gm^{-1}. See text for discussion.

somewhat lower than observed. The cloud base remained at approximately this level for the next few minutes. Cloud tops were about 4.8 km MSL, 9 min into the simulation and remained at this level for several minutes. By 18 min into the simulation, the cloud top fell to about 4.2 km MSL, and then fell gradually until the clouds dissipated at 34 min. The cloud on the right at 15 min (Fig. 1c) was formed by splitting away from the original cloud. Signs of the cloud splitting were evident at 12 min in Fig. 1b. As the initial thermal rose, the center cooled while the edges of the bubble retained a warm spot. A gravity wave formed and carried the right-hand part of the original cloud with it. The left-hand portion of the cloud probably was a gravity wave moving upstream that was held in place by the mean flow. The vertical motions at 12 min were broken into two main updraft regions located under the two centers of maximum cloud water in Fig. 1b. A downdraft developed, reaching to the surface between the left and right updrafts. This downdraft extended through the central part of the cloud in Fig. 1c and was responsible for the descending cloud top. By 18 min (Fig. 1d), the cloud was in essentially two parts, the split effectively completed by the downdraft.

4.1 Sulphur Hexafluoride Case

The SF_6 case was identical to the non-treated case, except that SF_6 was traced. Initially, the SF_6 cloud of gas was about 0.5 km per side with the core about half that size (Fig. 2a). After 3 min, the core concentration dropped by an order of magnitude and the cloud of gas had spread out into an elliptical shape 2 km wide by 1 km deep (Fig. 2). The expansion in the area covered was consistent with the decrease in maximum mixing ratio. As shown in Fig. 3, the concentration of SF_6 decayed exponentially with time. Also shown in Fig. 3 are the observed SF_6 concentrations for this case. The observations are trending downward also. In the first minute, the decrease was very sharp due to numerical spreading as the initial concentration was confined to a few grid points. The total mass of SF_6 remained constant in the grid within a few tenths of a percent so that the decrease in the maximum concentration was a result of an increase in the size of the SF_6 cloud (Fig. 2). Initially, the central maximum was carried upward and downwind. After 3 min, little of the SF_6 was left in the initial position and very little, if any, was transported upwind, as shown by the contours. Any upwind transport would have been due to diffusion. Six minutes after seeding, the center of the SF_6 cloud was lower than the initial cloud, although the top of the SF_6 extended as high as the original release. The SF_6 was being transported downward and to the right with the winds. No traces greater than 2 ppt of SF_6 were left at the initial release point. The cloud of tracer gas remained in a single cloud and was not split in two. In the next few minutes, the SF_6 continued to move with the airflow which carried the gas downward and downwind. At 21 and 24 min, the contour interval changed as the concentration of the SF_6 decreased to a few ppt so the enlargement of the gas cloud was somewhat exaggerated. The 200 contour at 21 and 24 min compares with the 25 contour (not labeled) at 18 min because the scaling on the labels changed by an order of magnitude. At 18 min (and before), the 50 contour label was 5 ppt, while in the last two plots, 200 was 2 ppt.

In the simulated time period from 15 to 21 min, the SF_6 gas cloud moved out of the water cloud that was seeded. The water cloud was dissipating, particularly in the downdraft, but the cloud's position was somewhat stationary, anchored to the initial updraft region where the bubble was introduced. After 18 min, the cloud dissipates and moves with the airflow.

4.2 Silver Iodide Case

The initial distribution of AgI was identical to the SF_6. This was done to make the comparison as easy as possible. The AgI was not conserved since it was active and interacted with the cloud microphysical process to produce ice crystals. Three minutes after seeding (Fig. 4a), there was a big difference between the SF_6 cloud and the AgI smoke cloud. Their positions were very similar, but the top of the AgI cloud appeared to be cut off with the contours becoming closely packed. The maximum mixing ratio was nearly an order of magnitude less than the SF_6 at this time. The freezing level was at the top of the AgI cloud, so the missing AgI was activated in the below freezing environment and was removed from the seeding agent field. Cloud ice (Fig. 5a) was growing at this time above the AgI cloud. At 15 min in the simulation, the AgI was more evenly dispersed, but the SF_6 extended to higher levels in the cloud. The AgI was carried by the airflow in much the same way as the SF_6. Compared at 18 and 21 min, the SF_6 and AgI fields continued to show similar patterns, with the basic difference, the expected absence of the AgI at below freezing temperatures.

Cloud ice (Fig. 5) appeared in the upper region of the seeded area of the cloud where the AgI field contours were cut off at 12 min. The cloud ice does not extend as high as the SF_6, the growth being concentrated near the initial AgI seeding location. The snow field (Fig. 6) was growing in the region of the cloud ice at 12 min and above. Much of the cloud ice appears to have been swept out in the uppermost regions by the snow, which was more extensive than the cloud ice at 12 min. At 15 min, the cloud ice field had two distinct growth areas, one in each cloud. The SF_6 and AgI contours (Figs. 2c and 4b) show that the AgI would have seeded them both. The snow was carried along with the the airflow as the SF_6 was, but at 15 min, the snow field was lagging behind the SF_6. This was also the case at 18 min, where the snow field was beginning to show unmistakable signs of melting when falling through the freezing level. The tightly packed contours were an indication of a sink in the production of snow. Figure 7 showed that the rain was forming from melted snow at 12 min as the snow field fell or was carried below the freezing level. The rain envelope followed the SF_6 outline in the lower levels until about 21 min when the rain began to fall below the level of SF_6.

5. CONCLUSIONS

The SF_6 and AgI did follow the same trajectories after release in the model. This was to be expected in the model since both substances are treated the same numerically. There were differences in the spread of the two fields, however. The differences were due to the AgI nuclei activating and forming ice crystals. Activated AgI

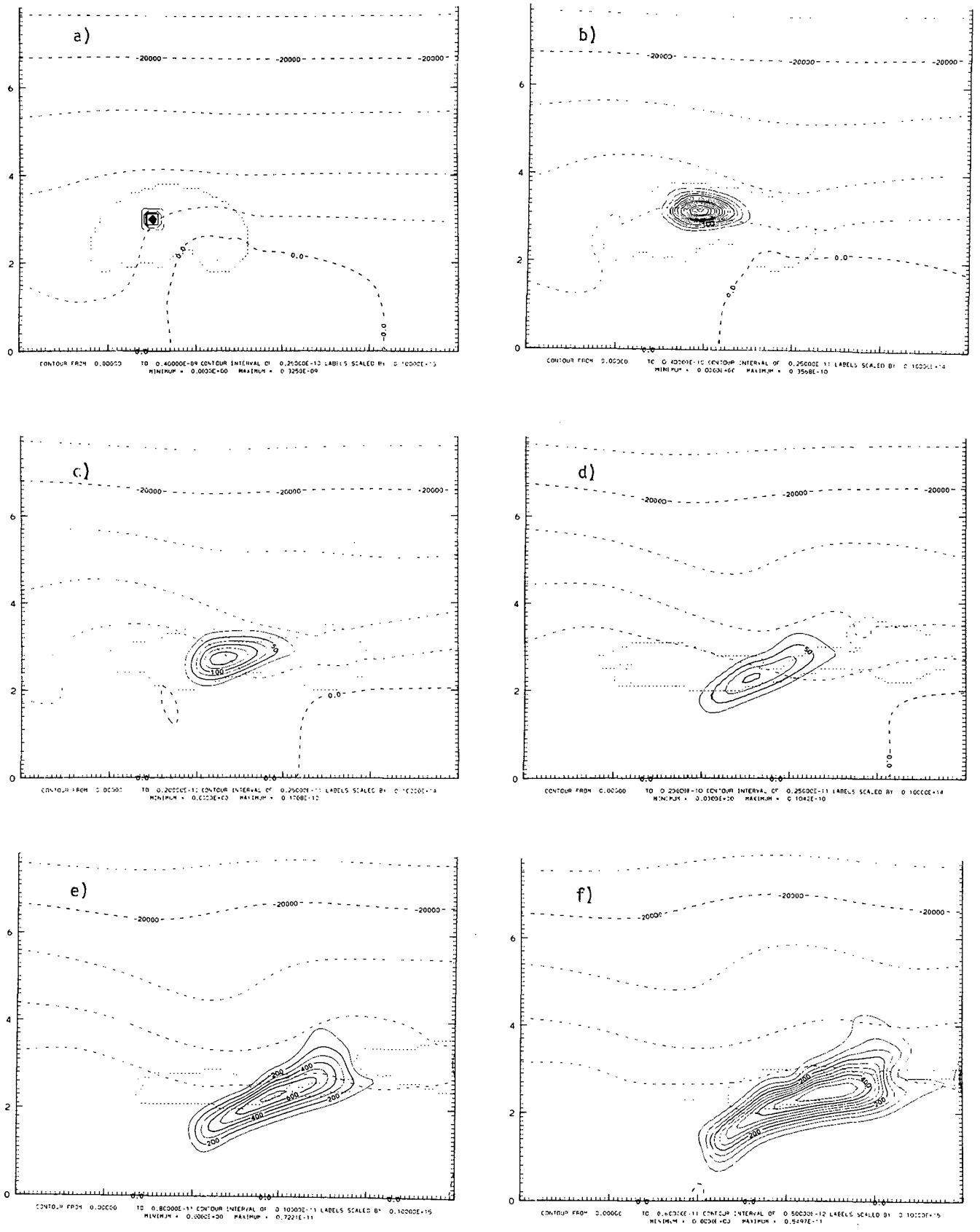

Fig. 2: Sulfur hexafluoride contours at (a) 9 min, through (f) at 24 min, with 3-min intervals. The initial distribution of SF_6 is shown in (a). In (b) through (d), the contour interval is constant at 2.5 ppt mixing ratio, changing in (e) to 1; and (f) to 0.5. The airflow carries the SF_6 along, spreading it out. See text for discussion.

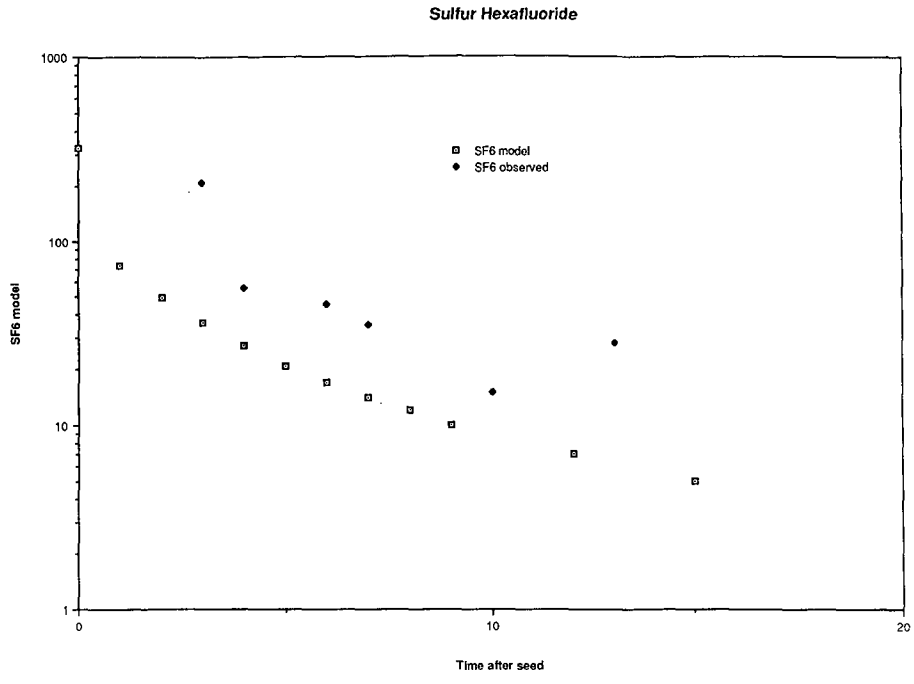

Fig. 3: Sulfur hexafluoride decay with time. The y-axis shows the maximum mixing ratio in gm per trillion gm of air. Time, on the x-axis, is in minutes from the beginning of the simulation. The results from the modeling are shown along with the observations made.

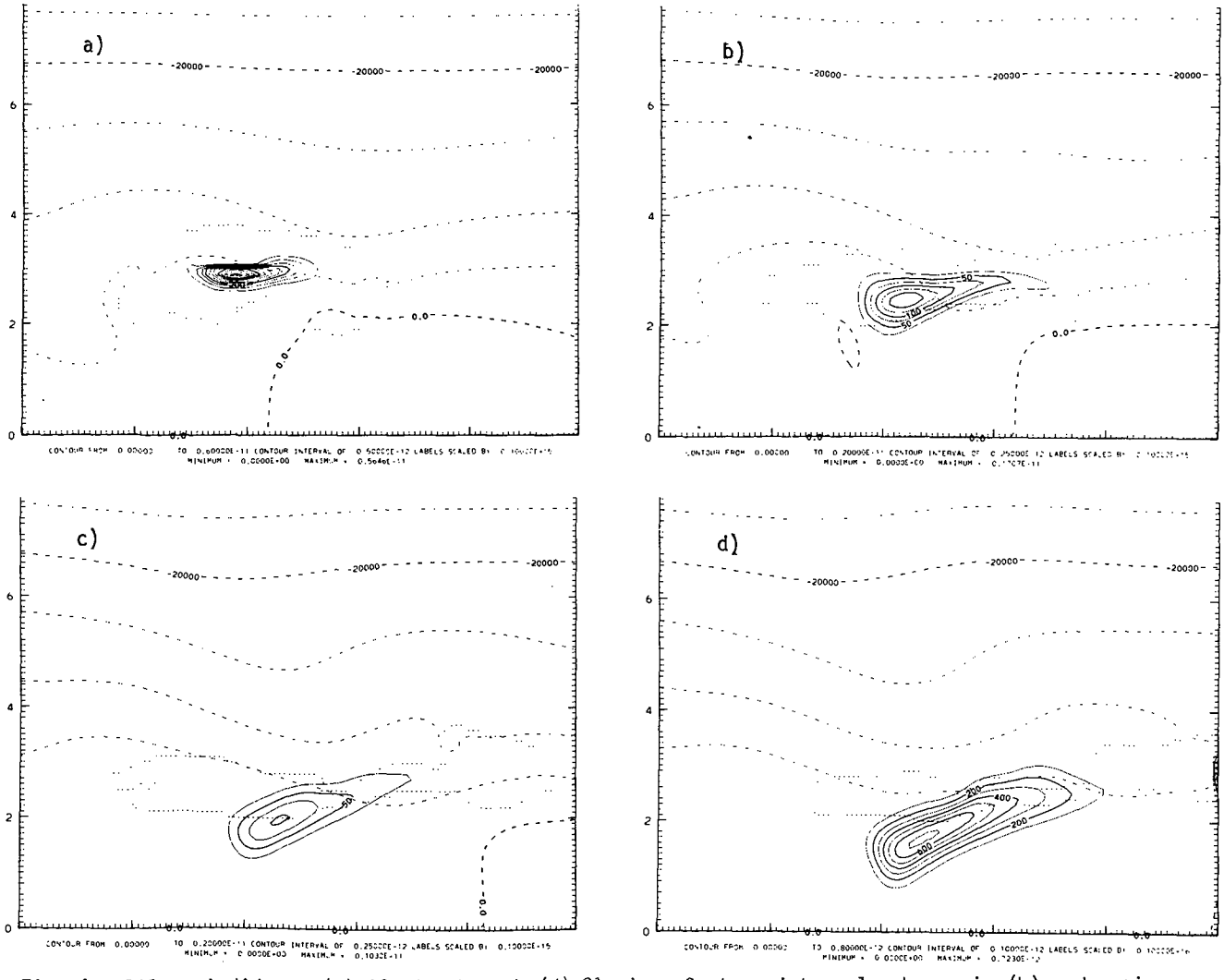

Fig. 4: Silver iodide at (a) 12 min through (d) 21 min. Contour intervals change in (b) and again in (d).

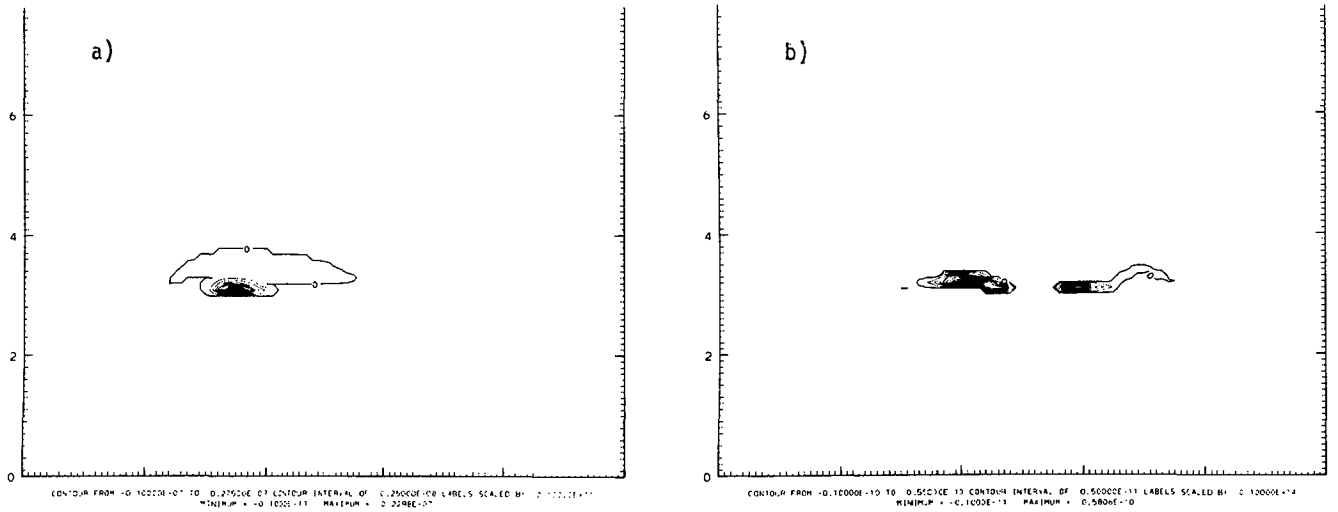

Fig. 5: Cloud ice in silver iodide case at 3-min intervals from 12 min in (a) to 15 min in (b). The mixing ratio is very small with the contour interval in (a) 2.5 ppb and 5 ppt in (b).

nuclei were removed from the AgI seeding field since they were no longer available for seeding.

One important result was that the precipitation can be displaced from the seeding field, as shown in Figs. 4b and 6b. Even though the snow was being carried along, there was growth in the snow contents. As the SF_6 was carried along, however, there was no growth. Consequently, the SF_6 tends to decay as it spreads while the snow grows. This displacement was not large and, in general, the precipitation seems to develop in the downwind half of the SF_6 field. The implications of this would be that SF_6 could be sampled while the expected precipitation particles may not be there, or that the precipitation might be detected while the SF_6 could be below the threshold for detection.

The other important result was that the concentration, as predicted by the model, indicated that the concentration of SF_6 falls off rapidly after release and would be one to two orders of magnitude less than the initial concentration as measured by detectors a few seconds after release.

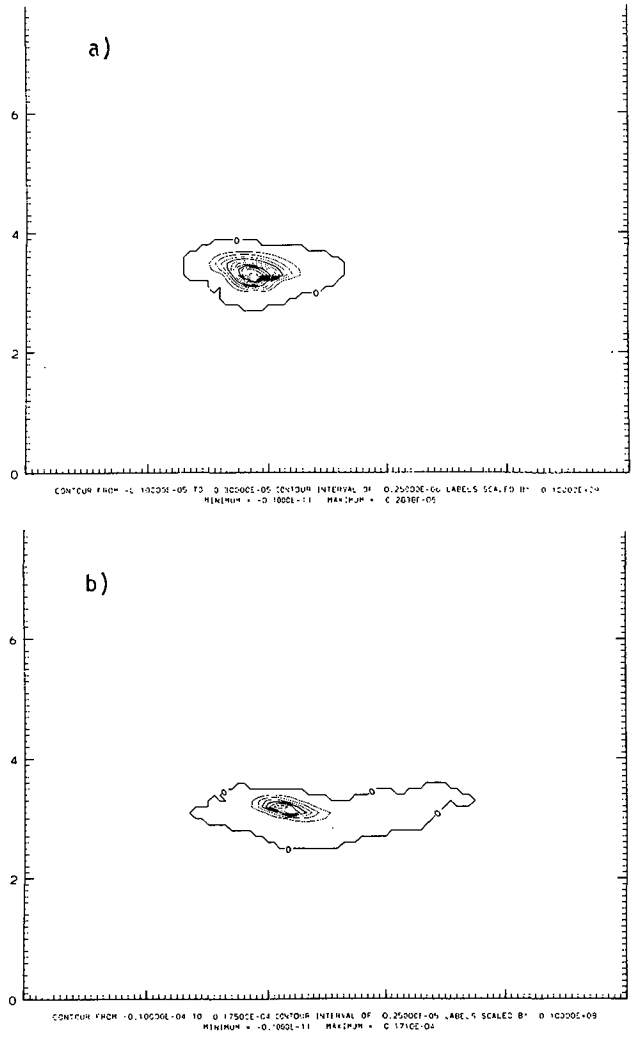

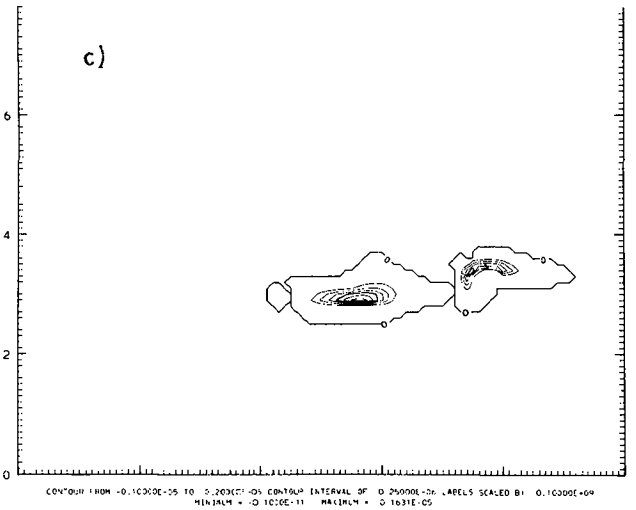

Fig. 6: Snow field from silver iodide case shown at (a) 12 min through (c) 18 min. The mixing ratio maximum and minimum are given in gm per gm air. The largest is a few hundredths of a gm kg^{-1}.

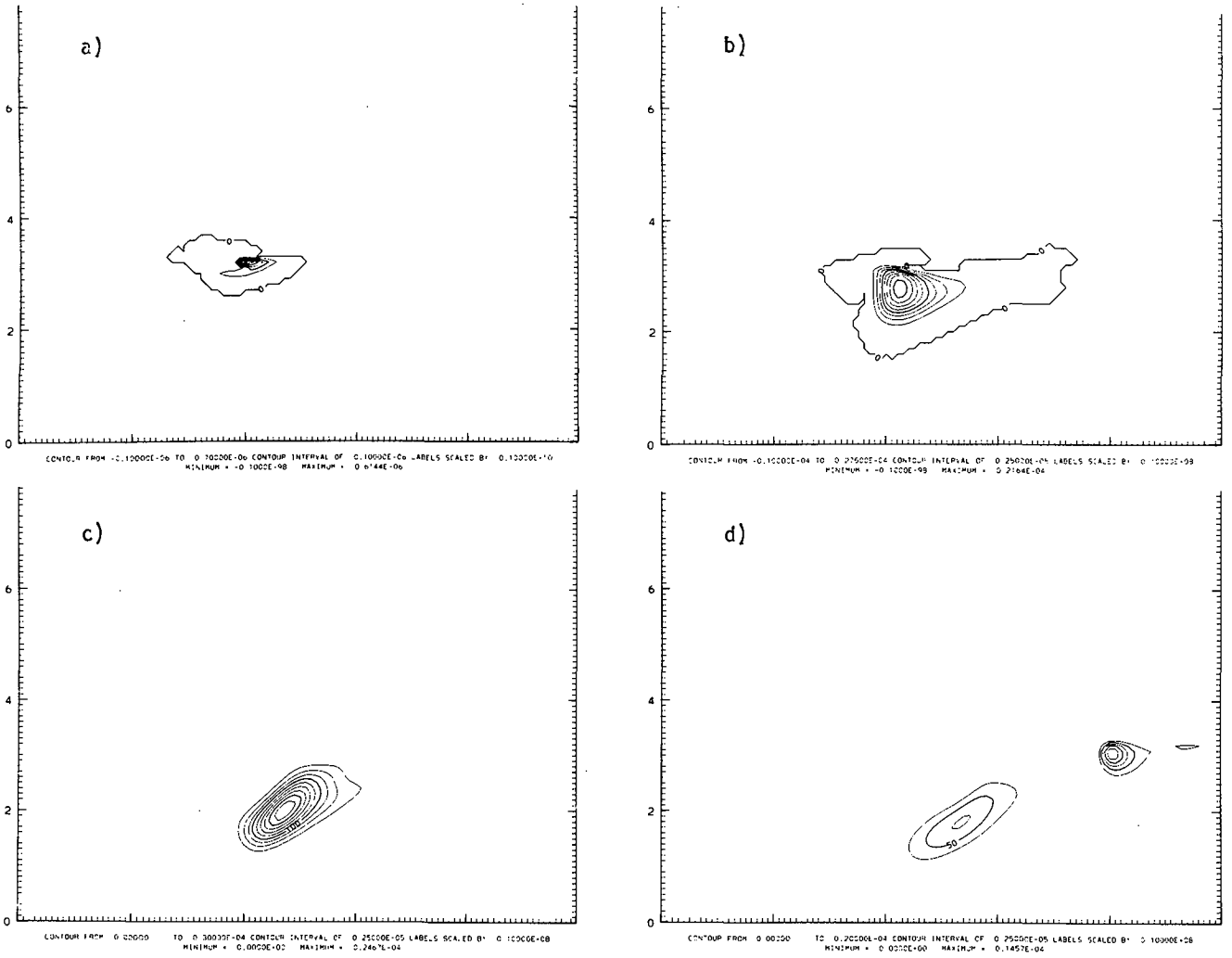

Fig. 7: Rainwater in the silver iodide case from (a) 12 min to (d) 21 min. The mixing ratio maximum and minimum are given in gm per gm air. They are very small, being a few hundredths of a gm kg^{-1}.

Observations (Stith et al., 1986) confirm these results. The observations tended to give a higher concentration, suggesting that the model may have too much diffusion or the initial conditions may have been different.

Acknowledgments. This work was supported by the North Dakota Atmospheric Resource Board under Contract No. ARB-IAS-87-1 and the National Science Foundation under Grant No. ATM-8516940. The computer simulations were done at the computing facilities of the Scientific Computing Division of the National Center for Atmospheric Research sponsored by the National Science Foundation.

Thanks also go to Mrs. Joie Robinson for preparation of the manuscript.

6. REFERENCES

Orville, H. D., and F. J. Kopp, 1977. Numerical simulation of the life history of a hailstorm. J. Atmos. Sci. 34:1596-1618. [Reply: J. Atmos. Sci., 35:10 (1978), 1554-1555.]

Stith, J. L., D. A. Griffith, R. L. Rose, J. Flueck, J. R. Miller and P. L. Smith, 1986. Aircraft observations of transport and diffusion in cumulus clouds. J. Climate Appl. Meteor., 25:1959-1970.

Warburton, J. A., and C. T. Maher, 1985. The detection of silver in rainwater: analysis of precipitation collected from cloud-seeding experiments. J. Climate Appl. Meteor. 4:560-564.

THE JUNE 1972 BLACK HILLS FLOOD AND THE LAW *

Ray Jay Davis
J. Reuben Clark Law School
Brigham Young University
Provo, Utah 84602

Abstract. An effort to increase rainfall by seeding clouds near Rapid City, South Dakota on June 9, 1972, was followed hours later by a flash flood that caused loss of life and property damage. A state inquiry concluded that weather conditions beyond human control brought about the flood. A lawsuit filed against the federal government was dropped after a court ruled that the case did not qualify as a class action. Nonetheless the flood interfaced with flood hazard mitigation law, weather modification regulation, legal liability, and governmental immunity.

1 INTRODUCTION

Everyone involved in weather modification should be aware of the Black Hills Flood of evening and night June 9, 1972. Because some clouds in Black Hills area had been seeded earlier that day as part of a precipitation enhancement experiment, state officials were concerned over possible public perception that the seeding had caused the flood. If a causal connection had been proven in court, the last decade and a half of weather modification history would have been different. It never was shown that the seeding contributed to the flood. Nevertheless weather modification legal developments have interacted with the events of June 9, 1972. Consequently it is useful to examine the legal ramifications of the Black Hills Flood.

Some flash floods are very destructive. The Black Hills Flood was (Boone, 1972). Two hundred thirty-eight persons died; property loss estimates exceeded $150 million. In addition to local and state funds, $48 million was provided by the federal Department of Housing and Urban Development for clean up and flood hazard mitigation (Swanson, 1987). During the recovery 152 commercial structures were relocated and 1,200 residential units were moved (Barnett, 1987).

The Institute of Atmospheric Sciences of the South Dakota School of Mines and Technology at Rapid City had conducted two seeding flights over the plains east of the Black Hills area on the day of the storm. The flights were part of an experimental sodium chloride seeding project, funded through a contract from the Bureau of Reclamation. A state-sponsored investigation of the flood concluded that some of the seeding material may have been caught up into the storm, but that the seeding had not contributed to the flood. The report stated that the "flood was caused by meteorological conditions beyond the control of man." It concluded that had there been no weather modification activities, "the damage would have been the same." (St.-Amand et al., 1973).

In addition to the state investigation of the Black Hills Flood, the National Oceanic and Atmospheric Administration sent a survey team to the area. The focus of the NOAA report was upon observation of storm development, flood warnings, and dissemination of flood hazard information (House, 1972). Weather modification was not mentioned. There also was a study of the meteorology of the flood done by the South Dakota School of Mines (Dennis et al., 1973).

From these inquiries, subsequent events such as the Big Thompson Flood, and legal developments during the years that have elapsed since the Black Hills Flood, several legal ramifications of floods following cloud seeding activities have appeared. Among the legal interfaces between the flood of Rapid City and the law are: (1) flood hazard mitigation law, (2) weather modification regulation, (3) legal liability, and (4) governmental immunity from liability.

* A version of this paper was presented at the 11th Conference on Weather Modification, Am. Met. Soc., Edmonton, Alberta, Oct. 7,1987.

2 FLOOD HAZARD MITIGATION

Current law and practice of flood hazard mitigation have been affected by the Black Hills Flood. It is preferable to undertake mitigation measures before loss of lives and property by flooding, or to do so after a modest flood which sounds an alarm. However the community's will to do something to mitigate future dangers is at a peak only for a short time after a disaster. Rapid City was at risk after June 9, 1972 and it was clear that something should be done to break the cycle of building, flood loss, rebuilding, more flood loss, etc. In view of recurrent past floods, future floods could be expected. But they could be made less destructive. Disaster gave the city an opportunity to do something constructive. Rapid City's leaders and citizens did so (Rahn, 1975, 1984). Other areas subject to flash flood hazards have a positive example of what they too can do.

Two avenues might be pursued to reduce flood damage: (1) minimize flooding through impoundments, levees, vegetation management, etc.; and (2) mitigate flood losses through relocation and flood-proofing. The first techniques were not available for Rapid City. There was and is a dam at Pactola upstream from Rapid City, but the deluge of June 9, 1972 fell between the dam and the city. The Army Corps of Engineers had refused to build a closer dam at Dark Canyon because the cost-benefit ratio was not high enough. That left the city with the flood hazard mitigation option as its only course of action (Barnett, 1987).

Rapid City now has a belt of parkland four blocks wide and five miles long along the creek. The approach has been to get people out of the flood plain by clearing residences and moving businesses to higher ground. Two high-cost businesses were not moved, but were flood-proofed; a shopping center and the neighborhood around it were protected by a dike. The idea was to do as much as possible with available funding, not to achieve the perfect solution (Burnett, 1987). Rapid City has become a model for other communities which wish to protect their residents from flash floods. The relocation took a joint city-state-federal effort, and thus it came under the aegis of local, state, and federal laws.

The legal tools used by the city included flood plain zoning to keep people from rebuilding in the affected areas, buying properties in the floodway, and tightened building code flood proofing requirements. These actions were accomplished by enacting city ordinances. The property purchases, although they generally went smoothly, led to litigation which was taken twice to the South Dakota Supreme Court. In the so-called Boland Cases, that court ruled that property owners in the flood zone had rights to notice and to a hearing before their homes were demolished, and to fair compensation for the taking (Deering, 1987).

The bulk of the funding for the relocation came from the federal government. Such large sums are not available now, but the National Flood Insurance program currently provides subsidized flood insurance to property owners in communities which have adopted flood plain zoning that qualifies under federal standards (Gore, 1987; Baram & Miyares, 1982). Rapid City and thousands of other cities and towns throughout the country qualify. By keeping encroachment from flood prone areas, they are mitigating losses from future floods. Building in the flood plain no longer is happening in Rapid City.

3 WEATHER MODIFICATION REGULATION

Weather modification activities are regulated through state statutes which require cloud seeders to keep records of their activities, to make periodic reports to some administrative agency, to obtain professional licenses for project supervisors, and to be issued operational permits which indicate the target and control areas, set forth operational plans, and generally inform regulators about the projects (Davis, 1970). The critical need is restrict weather modification activities to sensible projects carried out by qualified persons in a professional manner. Good regulation effected under a strong statute and enforced by competent professionals cannot of itself insure that cloud seeding will be risk free, but it can reduce dangers. Hence the state investigation recommended improvement of South Dakota's regulatory system by clarification of the distinction between professional licenses and operational permits (St.-Amand et al., 1973). The legislature made the necessary change.

The Black Hills Flood influenced introduction of a new version of state weather control statutes. Earlier enacted laws, including South Dakota's did not require operational plans to include seeding suspension criteria. The draftsmen of the Illinois law had Rapid City in mind when they wrote that statute (Ackermann et al., 1976). It began a generation of state laws which not only required permits and licenses, but also demanded that weather modifiers set forth suspension criteria in their operational plans providing for automatic shut down in the face of known impending severe weather events (Council of State Governments, 1977).

There are two difficulties with seeding suspension criteria. First, they do not prevent seeding when

conditions leading to a storm are not forecast. The 1972 program in the Black Hills area had suspension criteria relating to soil moisture and rainfall conditions. The weather situation on the evening of June 9, 1972 was very different than the one presented at the morning weather briefing. Perhaps no set of criteria would have picked up on the remarkable confluence of events that led to such a change.

A second type of difficulty with seeding suspension rules is with the criteria themselves. They may allow seeding in meteorological situations in which either there will be an appearance of impropriety or even actual seeding-caused losses; or they may be so tough they will shut off seeding whenever there is a reasonable chance of successful treatment. A law demanding that the regulatory authorities avoid either extreme puts them in a delicate position. North Dakota, for example, drafted suspension criteria as part of its regulations. Later, regulators found it necessary to adjust the criteria so the public interest still was protected, but sound seeding projects could occur (Changnon et al., 1986).

4 LEGAL LIABILITY

Plaintiffs who have sought money damages from weather modifiers and their sponsors through judicial action have been unsuccessful. A basic reason for their failure has been complainants' inability to prove that their losses were caused by the weather modification activities. The same difficulty over establishing what would have happened but for the seeding and hence the ability to claim credit for precipitation or runoff that followed cloud treatment also has acted to protect the seeder from liability for harms which have taken place after his intervention (Davis & St.-Amand, 1975). The causal connection between seeding and something which happens later is hard to establish on statistical or empirical grounds.

To prove that their losses were caused by seeding, plaintiffs must establish through evidence that seeding materials were released which penetrated the clouds at such a place and time and in such a concentration as to change the storm behavior. In the Rapid City case, the state investigators assumed that salt could have been swept into the clouds. Additionally, a plaintiff would have to prove that, once in place, the seeding materials did in fact bring about a change. Calculations by the investigators concluded that the type of seeding material used, under these conditions, would not have intensified the storm (St.-Amand et al., 1973).

Expert testimony is necessary to establish causation. The Los Angeles basin floods of 1978 had a weather modification aspect. There had been seeding. Expert testimony was taken in depositions on the claim that cloud seeding played a role in bringing about the floods (Davis & St.-Amand, 1982). In June 1987, the Supreme Court of the United States decided in First English Evangelical Lutheran Church v. Los Angeles County, one of the cases arising from the flood, that if interim flood plain zoning by the county had the effect of banning use of the property and constituted a "taking" or confiscation of the property by the county, the Due Process Clause of the Federal Constitution would require the government to pay damages for such inverse condemnation (Kusler, 1987a). Chief Justice Rehnquist, in the first reference to cloud seeding by the high court, noted that the church also had made a claim that the flood was caused by cloud seeding sponsored by the county. He stated that the cloud seeding issue was a state matter which could be developed in state proceedings, and that its presence in the case did not prevent the Supreme Court from ruling on the "taking" issue.

The California trial court in the Lutheran Church Case had dismissed the cloud seeding claim because there had been an effort to found it upon a theory of strict liability in tort. It is necessary for claimants not only to prove in court that the conduct of the defendant cloud seeders caused them harm, but also that such conduct fit within some liability theory. Because of the tremendous potential for harm, some flood cases have been fit within the theory of strict liability (Kusler, 1987b; Kusler & Platt, 1982). By extension, cases involving cloud seeding-induced floods would be founded upon the strict liability concept. The California court, however, did not accept the argument.

Water resources development, especially in arid and semi-arid country, usually is regarded both as natural and necessary. Hence there is authority for the proposition that flood losses associated with such development should give rise to liability only when the defendant developer has been guilty of negligence (Little, 1984; Fairchild, 1979). Since there is no printed report of the California court opinion, it is not possible to be certain why it rejected strict liability. An educated guess would be that trial court's decision was a vote in favor of carefully formulated and conducted weather modification. Only when cloud seeders are negligent by falling below the standards of professional conduct will they be liable for damages arising from their activities.

During the years since the Black Hills Flood liability law development has changed direction. The 1970s were a

time of expanding notions of liability. The 1980s have brought a new look at this area of law with the so-called "tort reform" movement. Governmental entities, professional groups, and insurers have banded together using their political muscle in state legislatures to alter in their favor substantive and procedural rules of tort law and the law of damages. The legal climate is better for defendants than previously. The message for cloud seeders and their sponsors is welcome: now and in the future they may be less likely to be targets of liability litigation (Davis, 1987).

5 IMMUNITY FROM LIABILITY

There were several candidates for defendants in liability litigation arising from the 1972 Black Hills Flood. First, there were the individuals--the pilot of the aircraft from which the salt was dispensed, the scientists at the School of Mines, and the Bureau of Reclamation officials who were involved with the federal research contract with the School of Mines. Considering the millions of dollars in property loss and the loss of 238 lives, none of individuals was a very attractive target for plaintiffs. Even with insurance, (most of them probably did not have personal liability insurance covering this sort of thing) there would not have been deep enough a pocket even to begin paying for the losses.

The state would have been a more attractive target. With its taxing capacity it could have raised a significant sum to pay damages; but South Dakota in 1972 retained sovereign immunity. It could not then have been found liable for harm caused by employees of one of its agencies--the South Dakota School of Mines and Technology (Keeton et al., 1984). During the decade and a half that has passed, the South Dakota situation has changed only to the extent that now the state and its agencies can be found liable only if they have purchased liability insurance (Marshall, 1983; Miner, 1981). Also, of course, if seeding activities could be fit within the concept of a "taking," then there would be liability under the notion of inverse condemnation (Deering, 1987).

The impracticality of suing individuals, and the immunity of the state, left the families of flood victims with only the option of suing the United States of America. That, too, had its problems, difficulties, which in the end, left the families without any remedy. Like the states, the government of the United States has immunity, except to the extent it has waived it. The Federal Tort Claims Act and its various amendments set forth that waiver, and the procedures that must be followed. Those procedures begin with filing an administrative claim with the responsible department, in this case the Department of the Interior which is the parent of the Bureau of Reclamation (Berman, 1985). Four claims were filed on behalf of the families of named flood victims, and a claim additionally was filed to represent other injured persons by a class action. The Department of the Interior rejected the claims. A variety of grounds could have been given: an assertion that the Bureau of Reclamation merely had financial oversight over spending contract funds and hence no federal activity or employee was involved; a claim that the seeding had not caused the flood; and the argument that the Federal Torts Claims Act did not allow predicating liability on a strict liability theory. No negligence was shown in this case.

When the claims were rejected by the Department of the Interior, they then were filed in federal court as Lunsford v. United States (Changnon et al., 1977). The South Dakota District Court ruled that the case was not proper for a class action because the named parties could not represent the entire class of flood victims. An interim appeal was taken to the Court of Appeals at St. Louis which ruled for the government stating that because the plaintiffs had not sought a definite sum on behalf of the unnamed members of the class and because their complaint did not show authority to represent the other victims, the case could be pursued only on behalf of the individuals named as plaintiffs. This created a problem of funding the trial. Lawyers and expert witnesses cost money. For example, it was estimated that litigation costs ran at least $300,000 in the Yuba City weather modification trial in the 1950s (Mann, 1968). Costs of Rapid City two decades later could have been higher. It is easier to raise money to pay litigation costs from a large group than from a few people. The Court of Appeals in Lunsford also ruled that there was not as yet an adequate record in the case to determine the applicability of federal flood control legislation which immunizes the federal government for actions undertaken as a part of such a project. In any event, the plaintiffs did not elect to continue the case, and federal immunity won the day.

6 CONCLUSIONS

The Black Hills Flood of 1972 was an important event in the legal history of weather modification. It influenced flood hazard mitigation; it gave emphasis to the need for legislatively and administratively mandated suspension criteria; it touched upon the liability issue; and it showed the continuing viability in at least one jurisdiction of the sovereign immunity defense.

7 REFERENCES

Ackermann, William, Stanley Changnon & Ray Davis, 1974. The Weather Modification Law for Illinois, Bull. Am. Meteo. Soc., 55, 745.

Baram, Michael & J.R. Miyares, 1982. Managing Flood Risk: Technical Uncertainty in the National Flood Insurance Program, Colum. J. Envir. Law., 7, 129.

Barnett, Don, 1987. The Rapid City Experience. Flash Flood Mitigation Symposium, FEMA, Rapid City, SD.

Berman, George, 1985. Federal Tort Claims at the Agency Level: The FTCA Administrative Process, Case Western Reserve Law Rev., 35, 509.

Boone, 1972. The Rapid City Flood . . . June 9, 1972. Boone, Lubbock, TX. Changnon, Stanley, Howard Bluestein, Ray Davis and Harold Orville, 1986. Review and Recommendations on the Use of Safeguards in the North Dakota Weather Modification Program. Report to the ND Wea. Mod. Bd., Bismarck, ND. 11 pp.

Changnon, Stanley, Ray Davis, Barbara Farhar, J.E. Haas, J.L. Ivens, Martin Jones, Donald Klein, Dean Mann, Griffith Morgan, Steven Sonka,Earl Swanson, C.R. Taylor and Jon Van Blokland, 1977. Hail Suppression: Impacts and Issues. Ill. State Water Survey, Urbana, IL, p. 157.

Council of State Governments, 1977. Weather Modification Control Act, 1978 Suggested State Legislation. Council of State Governments, Lexington, KY, p. 20.

Davis, Ray, 1970. State Regulation of Weather Modification, Ariz. Law Rev., 14, 659. _____, 1987. Weather Modification Regulation for the Twenty-First Century, Conf. on Irrigation Systems for the 21st Century, ASCE, NY.

Davis, Ray & Pierre St.-Amand, 1982. Expert Witnesses in Weather Modification Legal Proceedings. J. Wea. Mod., 14, 78. _____, 1975. Proof of Legal Causation in Weather Modification Litigation: Reinbold v. Sumner Farmers, Inc. and Irving P. Krick, Inc., J. Wea. Mod., 7, 127.

Deering, Harold, 1987. Reducing the Risk of Floodplain Management Decisions Under South Dakota Law. Flash Flood Mitigation Symposium, FEMA, Rapid City, SD.

Dennis, A.S., R.A. Schleusener, J.H. Hirsch & A. Koscielski, 1973. Meteorology of the Black Hills Flood of 9 June 1972. 8th Conf. on Severe Local Storms, AMS, Boston, MA.

Fairchild, Janet, 1979. Liability for Overflow of Water Confined or Diverted for Public Water Power Purposes, American Law Reports Third, 91, 1065, Bancroft-Whitney, San Francisco, CA.

Gore, Douglas, 1987. The National Flood Insurance Program 1976-1986. 10th Conf. on Natural Hazards Res. & Applications, NHRAIC, Boulder, CO.

House, D.C., 1972. Black Hills Flood of June 9, 1972. Report NOAA NDSR 72-1, U.S. Dept. of Commerce, Rockville, MD, 20 pp.

Keeton, W. Page, Dan Dobbs, Robert Keeton & David Owen, 1984. Prosser & Keeton on Torts §131, West Pub., St. Paul, MN.

Kusler, Jon, 1987a. The "Taking Issue" and First Evangelical Lutheran Church vs. Los Angeles County. Flash Flood Symposium, FEMA, Rapid City, SD. _____, 1987b. Liability as a Dilemma for Local Managers. Flash Flood Mitigation Symposium, FEMA, Rapid City, SD.

Kusler, Jon & R. Platt, 1982. Law of Floodplains & Wetlands, p. 3-6, Fed. Emergency Manag. Agency, Washington, DC.

Little, John, 1984. Allocations of Risk Before and After the Flood--Who Picks Up the Pieces?, Rocky Mtn. Min. Law Inst., 30, 18-1.

Mann, Dean, 1986. The Yuba City Flood: A Case Study of Weather Modification Litigation, Bull. Am. Met. Soc., 49, 690.

Marshall, Mark, 1981. Sovereign Immunity and the South Dakota Plaintiff: A Practical Approach, SD Law Rev., 26, 300.

Miner, Celia, 1983. An Analysis of South Dakota's Sovereign Immunity Law: Governmental v. Official Immunity, SD Law Rev., 28, 315.

Rahn, Perry, 1984. Flood-Plain Management Program in Rapid City, South Dakota, Bull. Am. Geological Soc., 95, 85. _____, 1975. Lessons Learned from the June 9, 1972 Flood in Rapid City, South Dakota, Bull. Assn. Engr. Geologist, 12, 83.

St.-Amand, Pierre, Ray Davis & Robert Elliott, 1973, Report on Rapid City

Flood of June 9, 1972, J. Wea. Mod., 5, 318.

Swanson, Leonard, 1987. Mitigation and Recovery after Disaster Case Study; Rapid City, South Dakota. Flash Flood Mitigation Symposium, FEMA, Rapid City, SD.